22 August 2012 Project No. 09-1373-1004

Dr. Rick Schryer
Fortune Minerals Limited
148 Fullarton Street
Suite 1600
London, ON, N6A 5P3

RESPONSES TO NATURAL RESOURCES CANADA TECHNICAL REPORT RECOMMENDATIONS FOR THE NICO PROJECT

Dear Sir,

On 19 June 2012, Fortune Minerals Limited (Fortune) received a request for the Mackenzie Valley Environmental Impact Review Board (MVEIRB) to submit responses to the recommendations made by Parties in their Technical Reports for the NICO Project. Fortune responded the request; however, as the submission of Natural Resources Canada (NRCan) Technical Report was delivered after the deadline and due to the nature of the questions (many requests were highly technical and specific); Fortune and Golder Associates Ltd. (Golder) indicated a meeting with NRCan would be preferred to address their recommendations.

A conference call took place on 26 July 2012, between NRCan, Fortune, and Golder to provide further clarification to the technical recommendations outlined in NRCan's "Technical Submission for the Environmental Assessment of Fortune's Proposed NICO Mine Project", submitted to the MVEIRB on 22 June 2012. The following participants were on the conference call:

NRCan	**Fortune**
Christine Rivard	Rick Schryer
Fons Schellekens	
Aruna Dixit	**Golder**
Rob Johnstone	Ken Bocking
Veronica Mossop	Devin Hannan
John King	Lasha Young

The information below provides written clarification to the technical recommendations which could not be completely addressed on the 26 July 2012 conference call. During this conference call, NRCan agreed that a letter containing supplemental discussion would be an appropriate forum to address these concerns. This document addresses the points which required a written response.

Recommendation 1

NRCan recommends that the Proponent consider, during final detailed design, the potential localized uranium anomalies near Borrow Source 1. NRCan is willing to working collaboration with the Proponent.

Response:

Fortune will carry out geochemical characterization testing on all potential borrow areas before using any of the materials. Fortune will not use Borrow Sources with elevated concentrations of uranium or other contaminants.

Recommendation 2

NRCan recommends that the Proponent provide:

a) *Explanation in which projects, where and how the runoff coefficients and infiltration coefficients for CDF, perimeter dyke and till cover shown in Table 3.III.3-4 were determined*

Response:

The runoff coefficients and infiltration coefficients presented are based on field data and our experience on similar projects. The runoff coefficient for the natural soil, for instance, was calculated from watersheds in the area where flows were monitored. Section 11.2.2.2.2 of the Developer's Assessment Report (DAR) provided the mean discharge rates per unit area from several drainage areas around the NICO Project area. The runoff coefficients of these drainage areas were calculated using the long-term average mean annual precipitation of 343.5 millimetres (mm) (equivalent to 0.0109 cubic metres per second per square kilometre [m3/s/km^2]) as shown in Table 1. The measured runoff coefficients vary between 0.30 to 0.48. The upper bound of this range was used for the water balance calculations.

Table 1: Annual Runoff Coefficients for Local Watersheds

Watershed Area	Mean Discharge Per Unit Area ($m^3/s/km^2$)	Mean Precipitation Per Unit Area ($m^3/s/km^2$)	Annual Run-off Coefficient
Lou Lake Drainage	0.0045	0.0109	0.41
Burke Lake Drainage	0.0040	0.0109	0.37
Indin River	0.0052	0.0109	0.48
Emile River	0.0033	0.0109	0.30

$m^3/s/km^2$ = cubic metre per second per square kilometre

The runoff coefficients used in water balance calculations are summarized in Table 3.2-4 in the DAR. The average of the monthly runoff coefficients for natural ground is shown as 0.48. This is at the high end of the range shown in Table 1. It should however be noted that the coefficients used in the DAR are before lake evaporation, while those in Table 1 are based on stream flows which are net of lake evaporation. In summary, the coefficients used in the DAR agree with coefficients calculated from monitored watersheds for purposes of the initial design.

b) Clarification how recharge rates of 10 mm/y in lowlands and 30 mm/y in highlands were estimated;

Response:

A recharge value estimate of 50 mm/yr was derived in Annex G of the DAR. However, as explained in Annex G, this estimate is considered high. As such, 50 mm/yr was considered an initial upper bound on recharge input for the preliminary model, with an understanding that lower recharge rates were likely acceptable.

Observations of downward gradient trends in the upland groundwater levels and groundwater levels at or near surface in lowland areas provided the conceptual basis for setting recharge values higher in the upland areas versus the lowland areas.

The recharge rates in the upland and lowland areas were then fine-tuned and finalized throughout model calibration. The model was calibrated through a "trial-and-error" process by varying the recharge and hydraulic conductivity of the hydrostratigraphic units within the model until simulated groundwater elevations, flow directions and stream discharge adequately agreed with observed conditions. Calibration targets included average static water levels measured at 82 NICO wells and low flow measurements at 10 surface water stations. It was found that the recharge rates utilized in the model generally resulted in a adequate match to observed heads. Furthermore, the simulated baseflows were below or within the measured low-flows at the gauges (DAR Figure 11.I-16). As baseflow separation was not possible at these gauges (mainly due to interference from beaver dams), a modelled flow below or between the measured low-flow range was considered a reasonable match.

c) Explanation how the specific yield values in Table 11.I.4-3 were determined

Response:

As described in Section 11.I.4.6.3 of the DAR, the specific yield of the overburden material was determined from literature values. The specific yield of the bedrock material was set equal to the porosity of the bedrock as had been determined from packer testing data and analysis of rock characteristics using the "Osnes Extraction from Fixed-Interval-Length Effective Transmissivities" (OxFilet) method. The OxFilet method is a stochastic approach to determine equivalent porosity, based on in-situ hydraulic conductivity (packer) testing data and the properties of the fractures intercepted in the borehole. The method is described in detail in a paper by Dershowitz (1995), provided in Appendix I. Slides from a PowerPoint presentation of the application of the OxFilet method to the NICO data are also included in Appendix I.

In conversation during the conference call of 26 July 2012, NRCan hydrogeologist Christine Rivard commented that the specific yield of the fractured bedrock was lower than references that she is familiar with (which were in the range of 1%). Values determined for the NICO site using the OxFilet method are an order of magnitude lower than this.

Golder notes that the upper fractured rock is largely composed of rhyolite, a crystalline rock which is the extrusive equivalent of granite rock in which the connectivity of fractures controls ground water flow rather than the porosity of the rock itself, which can be considered to have no effective porosity. References confirm that a porosity of 0.2% to describe a fracture network in crystalline rock as porous media is not unprecedented. Golder notes that porosities of 0.3% (Davis 1969[1]) and 0% to 10% (Freeze and Cherry 1979[2]) have been documented for granite and crystalline rocks. It is also worth noting that the OxFilet

[1] Davis, S.N. 1969. Porosity and Permeability of Natural Materials. In Flow Through Porous Media. Ed. R.J.M. De Wiest. Academic Press, New York. pp. 53-89.

[2] Freeze, R.A. and J.A. Cherry. 1979. Groundwater. Prentice-Hall, Englewood Cliffs, New Jersey. 604 p.

method is based on in-situ measurements, and as such, it provides a superior estimate of porosity over general "textbook" values because it is site-specific. Specific yield values in rock are often close to or slightly less than the porosity value. As such, Golder's values of 0.2% porosity and specific yield in the upper bedrock are considered reasonable.

d) *Clarification what the right mean precipitation value is for the NICO site.*

Response

The average annual precipitation for the NICO site reported in Section 11.I.2.4 of the DAR was 281 mm/yr. Elsewhere in the report the average annual precipitation is reported as 343 mm/yr. The discrepancy is due to the fact that the raw data from the Environment Canada weather station provides an annual average precipitation of 281 mm/yr. However, this value was then corrected by Golder to compensate for precipitation gauge undercatch which resulted in a corrected average annual precipitation of 343 mm/yr. For consistency and improved accuracy the average annual precipitation of the NICO site should be considered to be 343 mm/yr. The undercatch corrected data is discussed in Section 4.0 of Annex G.

Recommendation 3

NRCan recommends that the Proponent provide:

a) *Explanation why the piezometric map was produced using the topography as an indicator of mean groundwater depth, while the correlation between topography and groundwater levels is very low;*

Response:

Golder respectfully disagrees that the correlation between groundwater depth and topography is "very low". On the contrary, the topography was found to be well correlated to groundwater depths. This correlation led to the interpolation of groundwater levels occurring 17 m below ground surface in upland areas (based on the average groundwater depth measured in the upland area where the mine is to be situated) and near ground surface in lowland areas.

This correlation is demonstrated in Figure 3-1, below. To help the reader please note the following:

- The water level at 97-51 conforms to the elevation of the decline portal. The drillhole trace passes within 20 m of the decline tunnel and its reading is interpreted to result from a fracture connection to the tunnel.

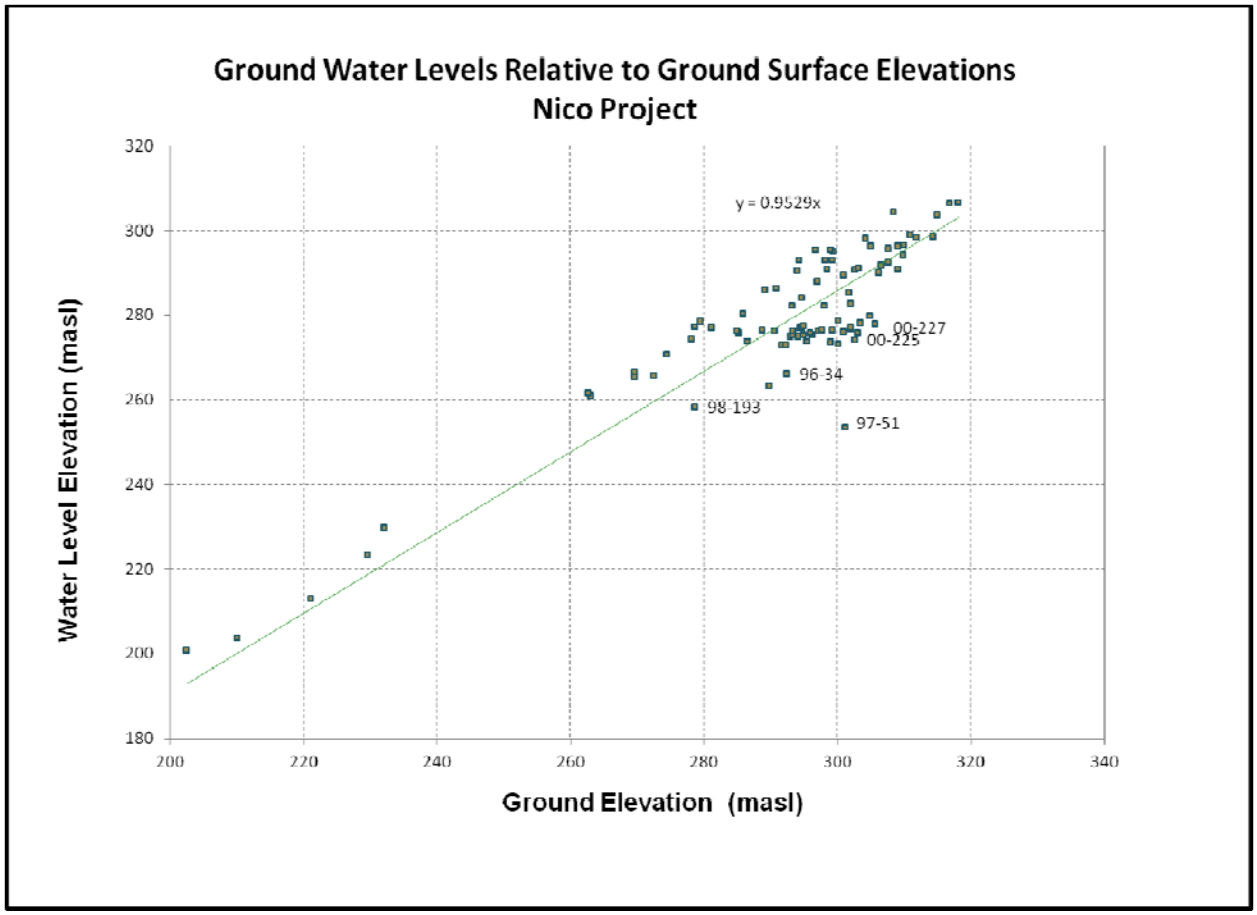

Figure 3-1: Ground Water Levels Relative to Ground Surface Elevations

b) Clarification how groundwater levels were estimated in lowlands, beyond streams

Response

As shown on Figure 11.I-6 of the DAR, groundwater levels were set equal to topographic elevations at lakes and streams in the lowland areas. Between these features and the upland groundwater levels the lowland groundwater levels were interpolated, as described in the following response, with the topographic surface acting as an upper bound on the groundwater levels.

c) Explanation which method of interpolation was used to create the piezometric map

Response

The inferred water table map shown in Figure 11.I-6 of the DAR was interpolated in Surfer 9.0 using the minimum curvature method at a grid spacing of 100 x 100 m.

d) Clarification if groundwater levels were measured during packer tests, and if vertical hydraulic gradients were estimated.

Response

Due to the low hydraulic conductivities of most of the rock intervals tested, no static groundwater levels could be obtained during packer tests and therefore no in-hole vertical gradients were estimated. Based on

the observed open hole and piezometer water levels compared to the relative depths of the open holes/piezometers it appears that there is a trend towards downward vertical gradients in the upland areas. This observation supports the conceptual groundwater model for the NICO site since the upland areas are presumed to be areas of groundwater recharge.

There is not enough data from the lowland areas to draw conclusions about vertical gradients in these areas.

Recommendation 4

NRCan recommends that the Proponent provide:

a) *A few (or at least one) cross-sections showing borehole logs with their depth, depth to bedrock and stratigraphy, as well as associated piezometric levels (at different depths if available) to better understand the hydrogeological context*

Response

Cross-sections showing three inclined geotechnical drillholes completed with single standpipe piezometer installations in the proposed pit area are shown on Figures 4A-1 to 4A-3. A geotechnical drillhole location plan is also included (Figure 4A-4) for reference.

Note: These cross-sections and location plan were previously provided to NRCan via the Information Request Responses provided to the Mackenzie Valley Review Board in December 2011 (See Response NRCan 1-4). They are also provided with this response for completeness.

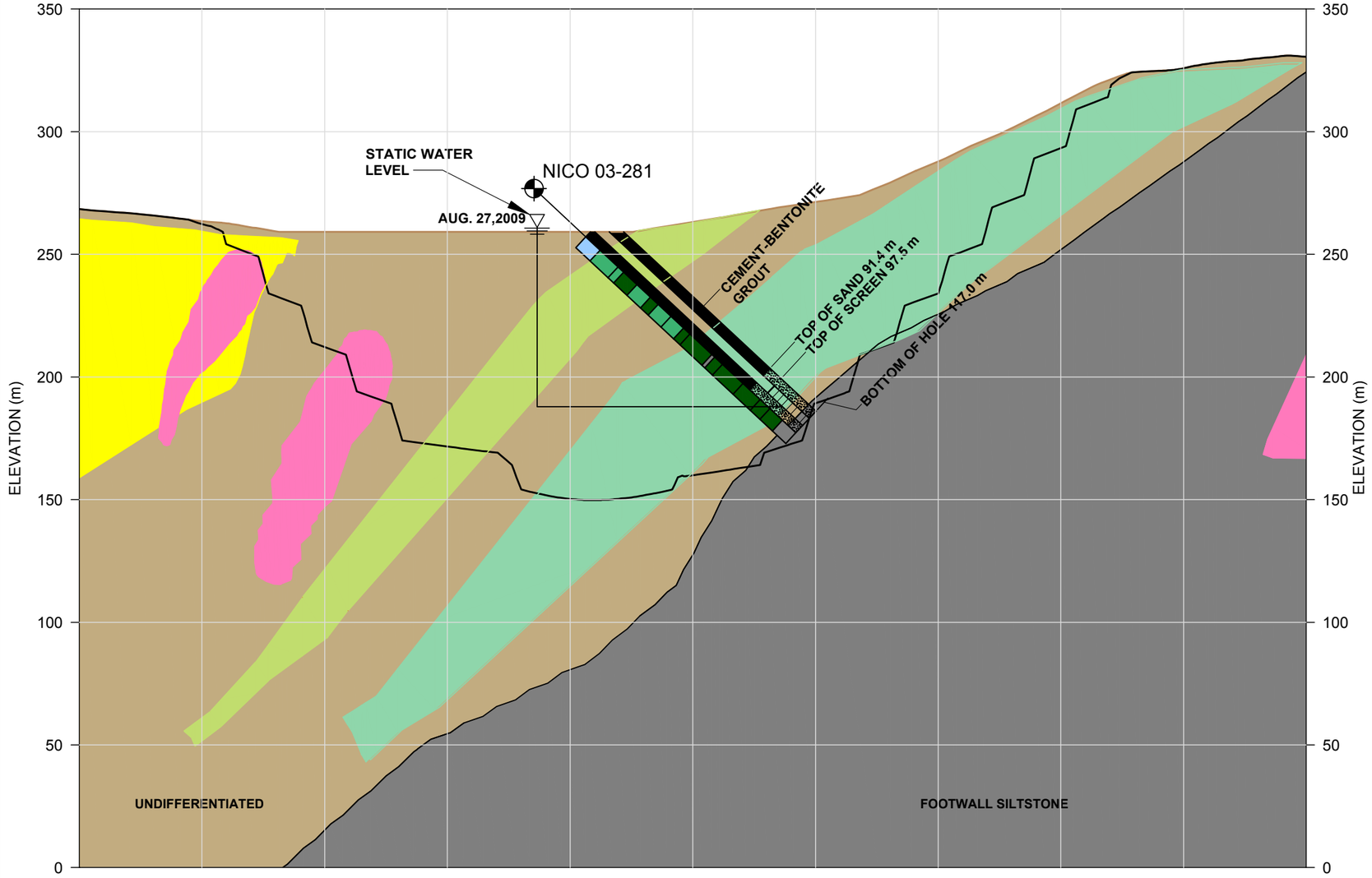

QUICK LOG TABLE NICO-03-281

FROM (m) *	TO (m) *	LITHOLOGY
0	7.92	Casing
7.92	17.95	BRS With/without mt
17.95	21.1	BRS With/without mt
21.1	28.48	BRS With mt
28.48	35.98	BRS With/without mt
35.98	40.32	BRS With mt
40.32	47.46	BRS With/without mt
47.46	54.44	BRS With/without mt
54.44	58.04	BRS With mt
58.04	70.29	BRS With mt
70.29	71.82	Siltstone
71.82	76.12	BRS With mt
76.12	87.61	BRS With mt
87.61	97.17	BRS With mt
97.17	102.57	BRS With mt
102.57	109.52	BRS With mt
109.52	117.04	Siltstone

* DOWNHOLE MEASUREMENTS

NOTES:

1. GEOLOGY, AND PIT SHELL INFORMATION WERE RECEIVED FROM GENE PURITCH INDEPENDANT MINE CONSULTANT (2009), AND FORTUNE MINERALS (JULY 2004).

SIMPLIFIED BEDROCK LITHOLOGY

I) IGNEOUS INTRUSIVES (DYKES)
- FELDSPAR - PORPHYRITIC
- QUARTZ - FELDSPAR

II) FABER LAKE GROUP VOLCANIC ROCKS
- K-SPAR ALTERED RHYOLITE

III) SNARE GROUP METASEDIMENTARY ROCKS (SUB-ARKOSIC WACKES, DOLOMITES, ARENITES AND SILTSTONES)
- UPPER ZONE
- MIDDLE ZONE
- LOWER ZONE
- UNDIFFERENTIATED
- FOOTWALL SILTSTONE

DETAILED DRILLHOLE LITHOLOGY
- CASING
- BRECCIA
- BRS WITH MT
- BRS WITH/WITHOUT MT
- FP/QFP
- RHYOLITE
- SILTSTONE
- SUBARKOSIC WACKE
- MAFIC DYKE

BOREHOLE LOCATION

N0.	NORTH (m)	EAST (m)	ELEV. (m)	AZIMUTH	DIP	DEPTH (m)
NICO 03-0281	7046896.38	512026.72	262.98	204.45°	-45°	117.04

40 0 40 80
SCALE 1:2000 METRES

Golder Associates
Mississauga, Ontario, Canada

SCALE	AS SHOWN
DATE	Aug. 17, 2012
DESIGN	CP
CAD	JFC
CHECK	LB
REVIEW	MR
FILE No.	0811180043IA4A-1.dwg
PROJECT No.	08-1118-0043 (3000)
REV.	A

TITLE: **BOREHOLE NICO 03-281 SECTION THROUGH OPEN PIT SHOWING GEOLOGY**

FORTUNE MINERALS LTD.
NICO PROJECT

FIGURE **4-A1**

PLOT DATE: _____
FILENAME: T:\Projects\2008\08-1118-0043 (FM, Yellowknife)\-IA-\0811180043IA4A-1.dwg

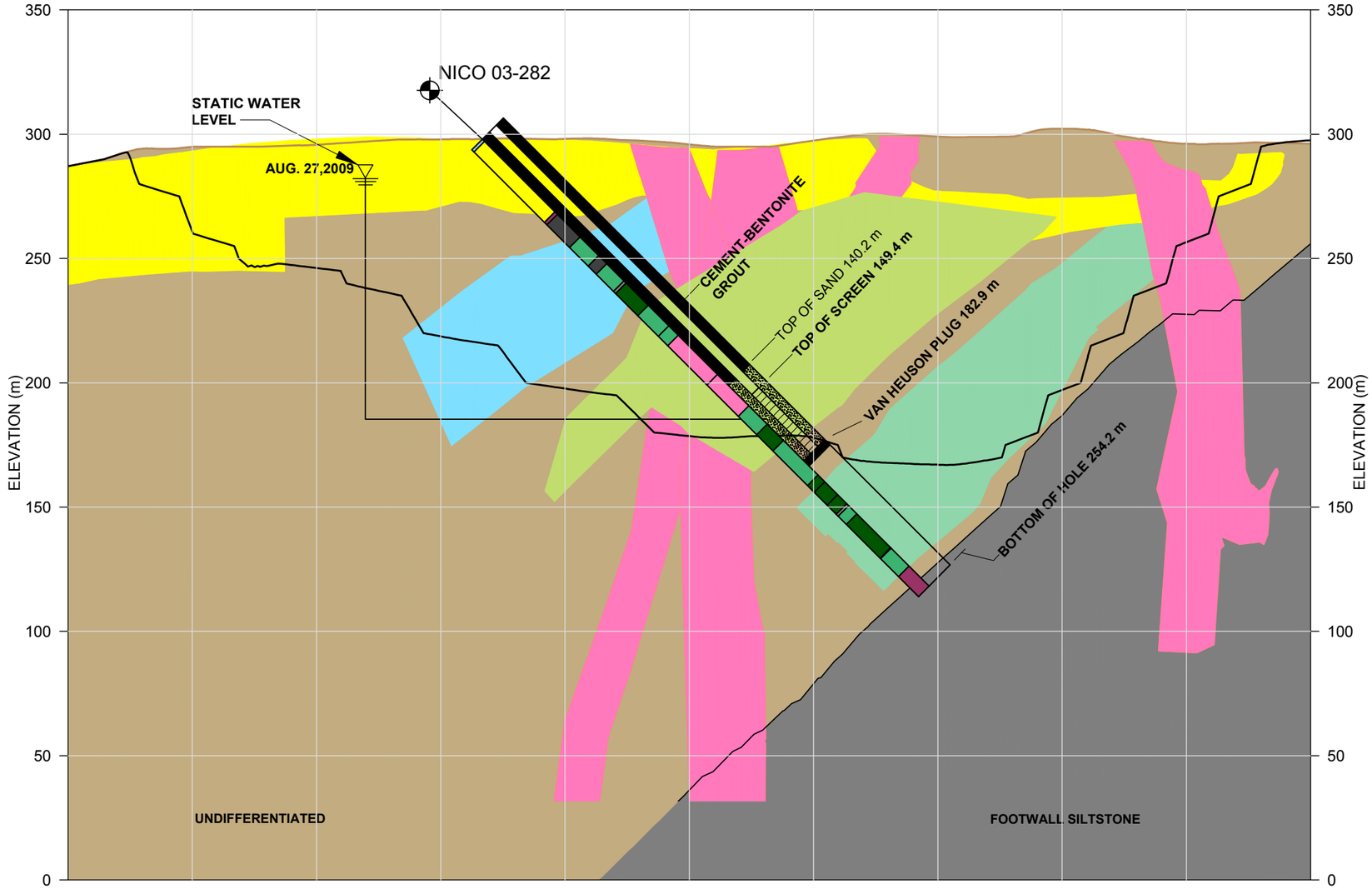

QUICK LOG TABLE NICO-03-282

FROM (m) *	TO (m) *	LITHOLOGY
0	1.22	Casing
1.22	41.3	Rhyolite
41.3	42.73	Breccia
42.73	55.65	Subarkosic Wacke
55.65	66.2	BRS With/without mt
66.2	70.8	Subarkosic Wacke
70.8	80.57	BRS With/without mt
80.57	81.8	Siltstone
81.8	94.47	BRS With mt
94.47	106.12	BRS With/without mt
106.12	111.5	BRS With/without mt
111.5	133.8	FP/QFP
133.8	151.69	FP/QFP
151.69	162.13	BRS With/without mt
162.13	171.33	BRS With mt
171.33	191.01	BRS With/without mt
191.01	194.89	BRS With mt
194.89	202.18	BRS With mt
202.18	207.34	BRS With mt
207.34	208.49	Siltstone
208.49	213.13	BRS With/without mt
220.13	232.31	BRS With mt
232.31	232.64	FP/QFP
232.64	242.86	BRS With/without mt
242.86	254.2	Breccia

* DOWNHOLE MEASUREMENTS

SIMPLIFIED BEDROCK LITHOLOGY

I) IGNEOUS INTRUSIVES (DYKES)
- FELDSPAR - PORPHYRITIC
- QUARTZ - FELDSPAR

II) FABER LAKE GROUP VOLCANIC ROCKS
- K-SPAR ALTERED RHYOLITE

III) SNARE GROUP METASEDIMENTARY ROCKS (SUB-ARKOSIC WACKES, DOLOMITES, ARENITES AND SILTSTONES)
- UPPER ZONE
- MIDDLE ZONE
- LOWER ZONE
- UNDIFFERENTIATED
- FOOTWALL SILTSTONE

DETAILED DRILLHOLE LITHOLOGY

- CASING
- BRECCIA
- BRS WITH MT
- BRS WITH/WITHOUT MT
- FP/QFP
- RHYOLITE
- SILTSTONE
- SUBARKOSIC WACKE
- MAFIC DYKE

NOTES:

1. GEOLOGY, AND PIT SHELL INFORMATION WERE RECEIVED FROM GENE PURITCH INDEPENDANT MINE CONSULTANT (2009), AND FORTUNE MINERALS (JULY 2004).

BOREHOLE LOCATION

N0.	NORTH (m)	EAST (m)	ELEV. (m)	AZIMUTH	DIP	DEPTH (m)
NICO 03-0282	7046666.92	512681.41	298.00	202.25°	-44.5°	254.20

40 0 40 80
SCALE 1:2000 METRES

Golder Associates
Mississauga, Ontario, Canada

SCALE	AS SHOWN
DATE	Aug. 17, 2012
DESIGN	CP
CAD	JFC
CHECK	LB
REVIEW	MR

FILE No. 0811180043IA4A-2.dwg
PROJECT No. 08-1118-0043 (3000) REV. A

TITLE **BOREHOLE NICO 03-282 SECTION THROUGH OPEN PIT SHOWING GEOLOGY**

FORTUNE MINERALS LTD.
NICO PROJECT

FIGURE **4-A2**

PLOT DATE: _____
FILENAME: T:\Projects\2008\08-1118-0043 (FM, Yellowknife)\-IA-\0811180043IA4A-2.dwg

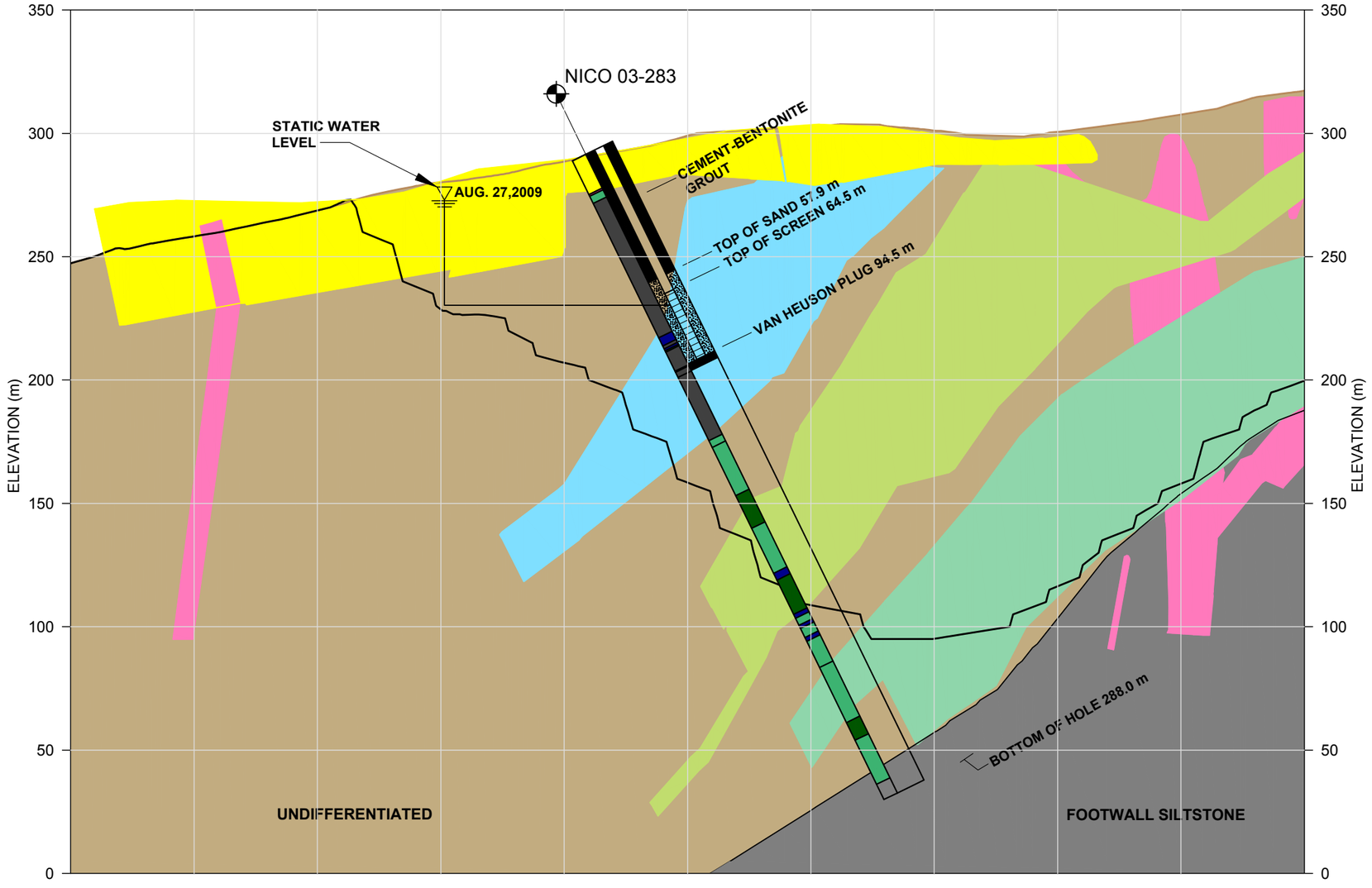

QUICK LOG TABLE NICO-03-283

FROM (m) *	TO (m) *	LITHOLOGY
0	15.2	Rhyolite
15.2	16.01	Breccia
16.01	19.23	BRS With/without mt
19.23	79.81	Subarkosic Wacke
79.81	83.49	Mafic Dyke
83.49	84.77	Subarkosic Wacke
84.77	85.67	Mafic Dyke
85.67	86.26	BRS With mt
86.26	94.9	Subarkosic Wacke
94.9	95.38	Mafic Dyke
95.38	97.63	Subarkosic Wacke
97.63	126.21	Subarkosic Wacke
126.21	129.26	BRS With/without mt
129.26	151.01	BRS With/without mt
151.01	165.74	BRS With mt
165.74	186.01	BRS With/without mt
186.01	189.12	Mafic Dyke
189.12	204.53	BRS With mt
204.53	206.31	Mafic Dyke
206.31	209.44	BRS With/without mt
209.44	210.89	Mafic Dyke
210.89	214.98	BRS With/without mt
214.98	216.7	Mafic Dyke
216.7	228.51	BRS With/without mt
228.51	253.34	BRS With/without mt
253.34	261.3	BRS With mt
261.3	281.23	BRS With/without mt
281.23	288.04	Siltstone

* DOWNHOLE MEASUREMENTS

NOTES:

1. GEOLOGY, AND PIT SHELL INFORMATION WERE RECEIVED FROM GENE PURITCH INDEPENDANT MINE CONSULTANT (2009), AND FORTUNE MINERALS (JULY 2004).

SIMPLIFIED BEDROCK LITHOLOGY

I) IGNEOUS INTRUSIVES (DYKES)
- FELDSPAR - PORPHYRITIC
- QUARTZ - FELDSPAR

II) FABER LAKE GROUP VOLCANIC ROCKS
- K-SPAR ALTERED RHYOLITE

III) SNARE GROUP METASEDIMENTARY ROCKS (SUB-ARKOSIC WACKES, DOLOMITES, ARENITES AND SILTSTONES)
- UPPER ZONE
- MIDDLE ZONE
- LOWER ZONE
- UNDIFFERENTIATED
- FOOTWALL SILTSTONE

DETAILED DRILLHOLE LITHOLOGY

- CASING
- BRECCIA
- BRS WITH MT
- BRS WITH/WITHOUT MT
- FP/QFP
- RHYOLITE
- SILTSTONE
- SUBARKOSIC WACKE
- MAFIC DYKE

BOREHOLE LOCATION

N0.	NORTH (m)	EAST (m)	ELEV. (m)	AZIMUTH	DIP	DEPTH (m)
NICO 03-0283	7046806.04	512518.70	291.49	210.70°	-64.50°	288.04

40 0 40 80
SCALE 1:2000 METRES

Golder Associates
Mississauga, Ontario, Canada

SCALE	AS SHOWN
DATE	Aug. 17, 2012
DESIGN	CP
CAD	JFC
CHECK	LB
REVIEW	MR

FILE No. 0811180043IA4A-3.dwg
PROJECT No. 08-1118-0043 (3000) REV. A

TITLE **BOREHOLE NICO 03-283 SECTION THROUGH OPEN PIT SHOWING GEOLOGY**

FORTUNE MINERALS LTD.
NICO PROJECT

FIGURE **4-A3**

PLOT DATE: _____
FILENAME: T:\Projects\2008\08-1118-0043 (FM, Yellowknife)\-IA-\0811180043IA4A-3.dwg

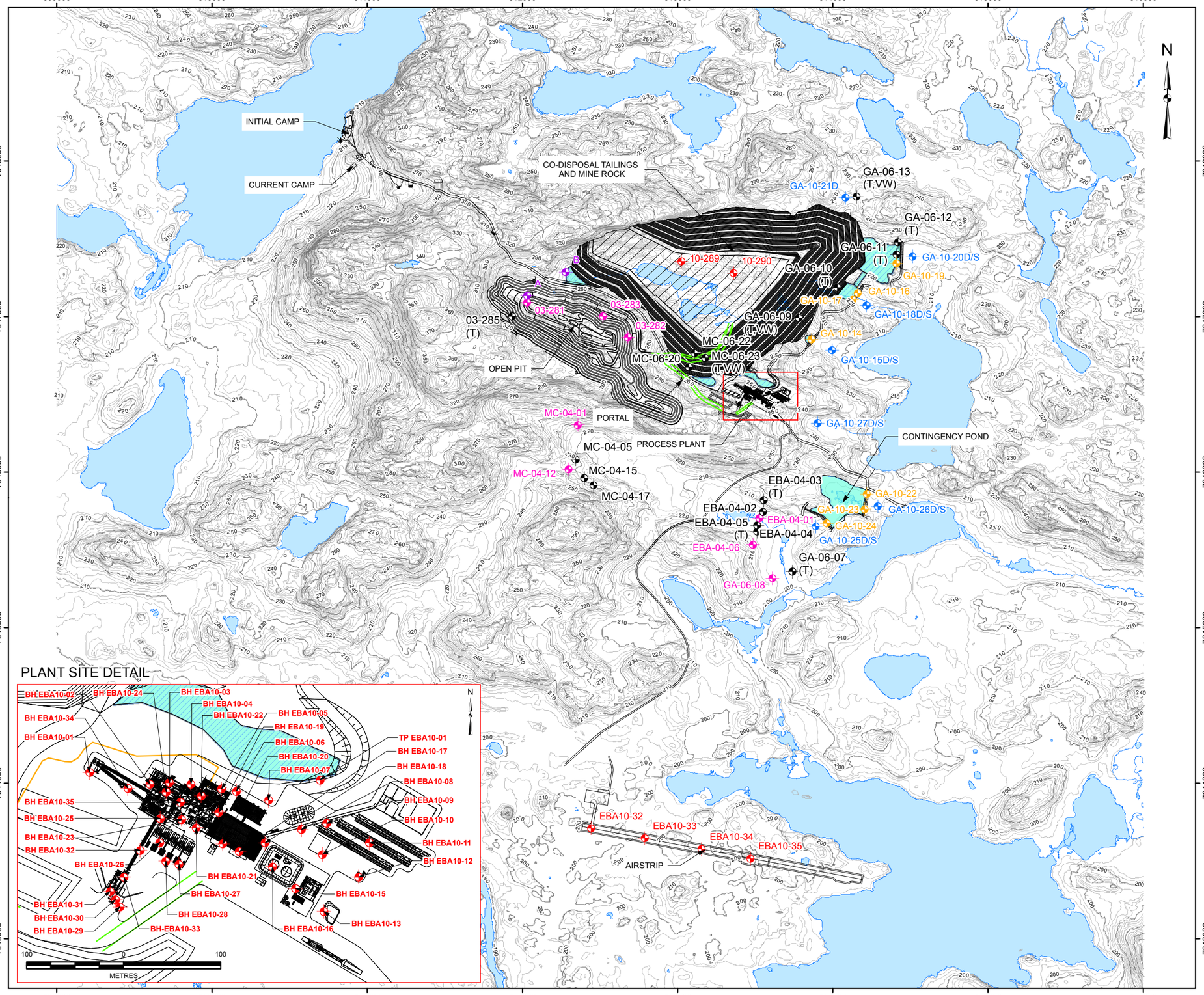

LEGEND

EXISITING LOCATIONS

- STAND PIPE
- OTHER
- THERMISTOR
- THERMISTOR VW PEZ

DRILLED LOCATIONS

- GEOTECHNICAL BOREHOLE
- MONITORING WELLS
- EBA AND FML BOREHOLE LOCATION
- WESTBAY SYSTEM MULTILEVEL GROUNDWATER MONITORING WELL

- HAUL ROAD
- SERVICE ROAD
- RIVER/STREAM
- TOPOGRAPHIC CONTOUR - *2 m INTERVAL*
- TOPOGRAPHIC CONTOUR - *10 m INTERVAL*
- INFRASTRUCTURE
- LANDFARM
- LAKE/POND
- SEEPAGE COLLECTION/ SURGE POND
- CONTINGENCY POND

NOTES

1. Plant site geotechincal holes not included on this figure.
2. D = Deep Monitoring Well
3. S = Shallow Monitoring Well
4. Pending Borehole Locations were not drilled March/April 2010 due to warm weather conditions and scheduling.
5. March/April 2010 Drilling locations were obtained using a handheld GPS device. Pending Nico Survey.

REFERENCE

-Topographic mapping obtained from Eagle Mapping, Fortune Minerals Limited, 2006 (File: Basemapping (FML, 20060718).dwg)

-Open Pit Configuration - Provided by P & E Mining Consultants Inc. (File: End_of_year2031.dxf Recieved August 26, 2010)

-Advaced Exploration Infrastructure - Provided by Aker Solutions (File: 0000g001D.dwg Recieved October 25, 2010)

-Projection: UTM Zone11 Datum: NAD 83

500 0 1,000

METRES

PROJECT

FORTUNE MINERALS LIMITED
NICO COBALT-GOLD-BISMUTH-COPPER PROJECT

TITLE

GEOTECHNICAL DRILLING LOCATIONS

Golder Associates
Mississauga, Ontario

FILENAME: DisturbanceAreas.mxd				
PROJECT NO. 10-1118-0046			SCALE AS SHOWN	REV. 0
DESIGN	SC	21 Oct. 2010		
GIS	SC	17 Aug. 2012		
CHECK	MR	17 Aug. 2012		
REVIEW	RS	17 Aug. 2012		

FIGURE: 4A-4

G:\Projects\2010\10-1118-0046_NicoFortuneMinerals\GIS\MXDs\Draft\Drilling\2010_Winter_Drilling_Locations.mxd

b) Clarifications how hydraulic conductivities (K) of the 1st, 5th, and 6th layers of the conceptual model (show in Figure 11.1-9) were selected

Response

Hydraulic conductivities of the 1st, 5th, and 6th (and indeed all model layers) were determined from the packer testing of the bedrock and grain size analysis of the overburden (see Section 11.I.2.5 of the DAR). This data was then fine tuned during model calibration to arrive at the final reported values.

The appropriateness of the hydraulic conductivity of the 1st layer is discussed in detail in the response to comment 4 e), below.

Upon further discussion with NRCan, it was Golder's understanding that a specific concern of NRCan's was linked to Figure 11.I-7 of the DAR, which shows a range of measured hydraulic conductivity values in rock corresponding to the model layers, and that perhaps the hydraulic conductivity decided upon for the 110 mbgs deeper layers (1E-9 m/s) may be underestimated based on the available hydraulic conductivity measurements corresponding to that depth range, particularly at 03-283 which shows a hydraulic conductivity of approximately 5E-8 m/s.

In response to this concern Golder notes that there are only three measurements solely confined to the 110 mbgs+ range (see Figure 4B-1, below). (For clarification: their values are 2E-10 m/s (03-283), 8E-10 m/s (03-282), and 5E-8 m/s (03-283), resulting in a geometric mean of 2E-9 m/s for this interval.) The higher value measured at 03-283 was interpreted as perhaps a local anomaly, as it would be unlikely that a fracture of this conductivity would be present and connected at a regional scale at this depth. In any event, the modelled bulk K falls within the range of measured values, is close to the geometric mean for this interval, and resulted in a satisfactory calibration. As such, Golder felt the value was appropriate.

It should be noted that thermistor readings and attempts to read water levels at standpipe piezometers in the vegetated wetlands (fens) of the Co-Disposal Facility (CDF) in the summer and fall of 2011 and 2012 indicate that the discontinuous permafrost layer appears to extend to all monitoring wells. All have remained frozen throughout the above-freezing months. Thermistor readings suggest the active layer is on the order of 4 m thick. In this context the overburden layers of the numerical model can be seen as conservative because the frozen ground is better represented as a no-flow layer rather than a low permeability layer, as it has been simulated.

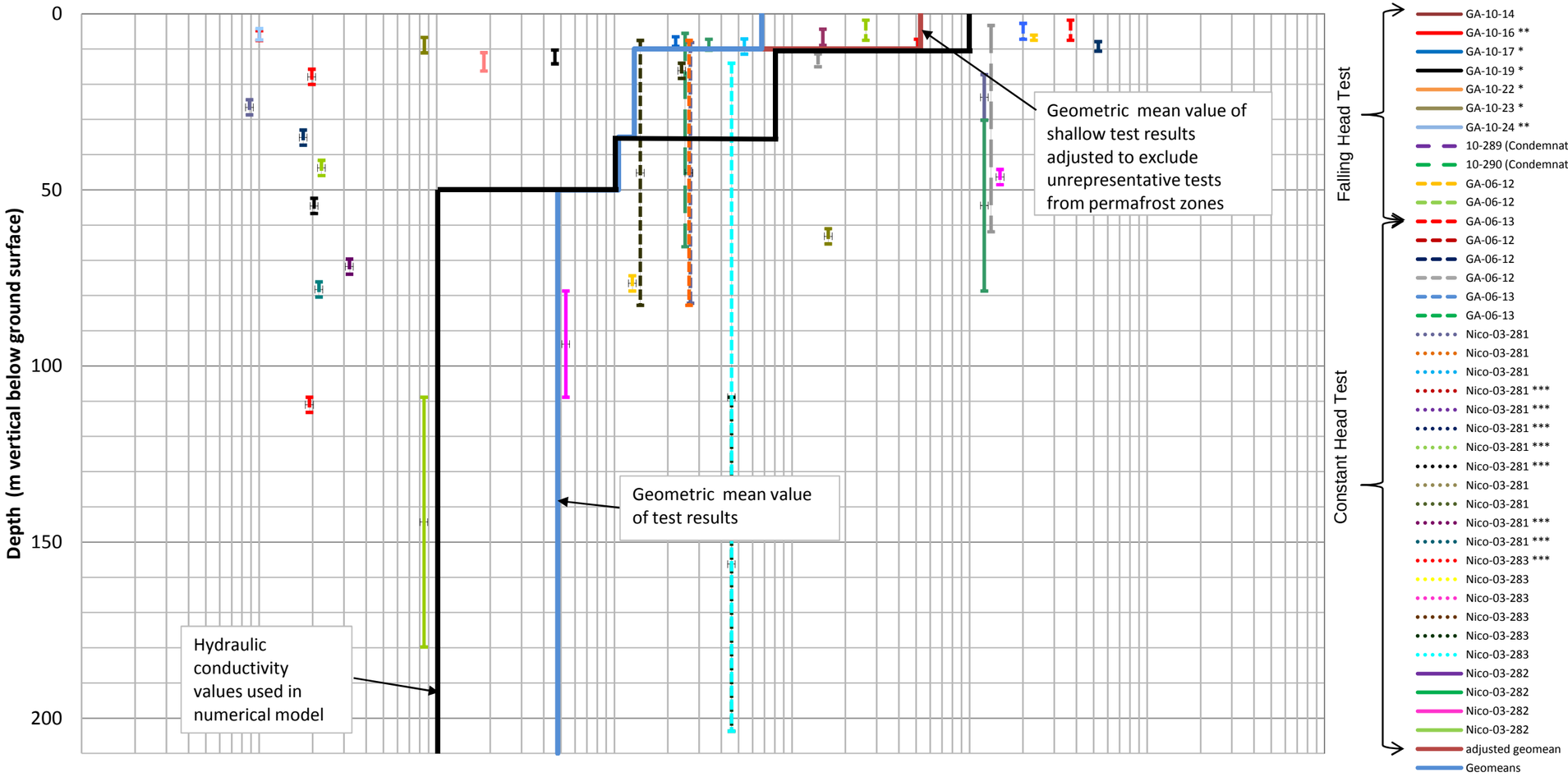

* The test interval may occur in frozen rock, and result may not be representative.

** The interval is either very tight rock or very tight rock and frozen. Result is not representative.

*** Value presented is an estimated Upper Bound on hydraulic conductivity.

Represents hydraulic conductivity applied in calibrated groundwater model.

Represents geometric mean of hydraulic conductivity tests at each depth interval

Represents adjusted geometric mean of hydraulic conductivity tests in 0 to 10 m depth interval

Golder Associates

Bedrock Hydraulic Conductivity Testing Results

PROJECT NO: 09-1373-1004		DATE:	August 2012
BY:	MB	CHECK:	MR

NICO Cobalt-Gold-Bismuth-Copper Project

FIGURE 4B-1

c) *Explanation if the K values were measured before or determined a posteriori during numerical modelling*

Response

As discussed in the previous response and in Section 11.I.5 or the DAR, the hydraulic conductivity ("K") values were initially determined from borehole packer testing in the bedrock and grain size analysis in the overburden. These initial values were then fine tuned in order to calibrate the model to observed conditions.

d) *Clarification if different combinations of K and recharge values were tried in groundwater flow model runs*

Response

Different combinations of hydraulic conductivity ("K") and recharge values were used in model runs as part of the calibration exercises (Section 11.I.5 or the DAR). Only the final values which resulted in the best calibrated model outputs were presented in the DAR.

e) *Explanation if the high value for layer 1 (10-6 m/s) was selected to be on the conservative side for infiltration*

Response:

The hydraulic conductivity of model layer 1 was not specifically selected to be on the conservative side for infiltration. The geometric mean value of the hydraulic conductivity tests centered within the layer 1 interval (depths from 0 up to 10 m) as shown on Figure 11.I-7 is calculated to be 6.8×10^{-8} m/s. This value is over an order of magnitude less than the layer 1 hydraulic conductivity used in the model (1×10^{-6} m/s). However it is important to note that several of the hydraulic conductivity tests conducted at these shallow depths occurred in boreholes where permafrost was observed in the overburden materials. This suggests that some of these tests may have been conducted in permafrost affected areas. In this case the results of the shallow hydraulic conductivity testing may have been unrepresentative due to ice blockage. If the hydraulic conductivity tests which were flagged as being likely unrepresentative are removed from the calculation then the geometric mean of the hydraulic conductivity testing in the layer 1 interval is 5.3×10^{-7} m/s which compares favourably with the value used in the groundwater model. An updated version of Figure 11.I-7 showing the geometric means and adjusted geometric means is provided in Figure 4B-1. Based on this analysis, the value used in the groundwater model for layer 1 is not considered to be unduly high and based on an interpretation of observed shallow bedrock conditions and the successful model calibration the hydraulic conductivity of 1×10^{-6} m/s for the upper bedrock is considered to be representative.

f) *Clarification if the modelled discharge (outflows) in different areas were compared in measured low flow values, and how the model was calibrated*

Response

As discussed in Section 11.I.5 of the DAR, the model was calibrated by varying the recharge and hydraulic conductivity values of the hydrostratigraphic units within the model until reasonable agreement was obtained between the model simulated values and the observed values of static groundwater levels in NICO wells, low flow measurements at stream flow gauges and the measured discharge rate through the portal opening to the flooded tunnel.

The modelled discharges were compared to the flow ranges measured at 10 flow monitoring stations as shown on Figure 11.I-16. Generally the simulated flow rates are at or below the low end of the measured range, as such, the model was deemed to be adequately calibrated to available flow measurements.

g) Explanation why not at least one pumping test was conducted, if a pumping test is planned, and if it is planned, when it will be conducted

Response

Due to the low hydraulic conductivities of the bedrock encountered on the NICO Project area no pumping test was conducted and no pumping tests are planned nor would they be useful. The low hydraulic conductivities would not permit a sustained, high volume pumping test such as would be required to provide useful data on the groundwater response on the scale of the NICO Project.

The filling of the decline was also used as a check on the reasonableness of measured in-situ and simulated hydraulic conductivity values.

The advanced exploration decline tunnel was driven approximately 1.7 km into the hillslope where the open pit and underworking will occur to collect a bulk sample for metallurgical testing. The decline was started in 2006 and completed in 2007. Dry working conditions were maintained with sumps and pumps. Tunnel discharge during dry or cold months was on the order of 4 m^3/day to 6 m^3/day. During freshet or storm events flows could increase by approximately an order of magnitude.

Water daylighted at the decline portal in 2009, approximately 2 years after the tunnel was closed, with meteoric water quality, rather than the groundwater quality of samples from monitoring wells 03-281, 03-282 and 03-283. This water quality confirmed the prediction that groundwater seepage would be very low relative to contributions from precipitation and snowmelt.

h) Clarification if the reason for this underestimated hydraulic heads could be a locally increased recharge

Response

To simplify the steady state calibration dataset at each well/borehole the measured water levels were averaged to provide a singular value. While this method does afford a straightforward approach it tends to mask the highly variable water levels that are observed at many of these locations in response to transient precipitation/melt events. Golder notes that water level increases of on the order of 25 m are observed in some wells on the hill where the open pit will occur in response to higher precipitation events. As the calibrated groundwater model is a steady state analysis, capturing these sporadic, transient events is not explicitly possible. As such there may be a tendency for simulated water levels to be underestimated in the context of comparing to an averaged calibration target that incorporates response to higher precipitation events. However, it was not the purpose of the modelling to simulate seasonal fluctuations. Similarly, the model the does not simulate winter months when ground water flow is reduced. The model simulated average non-winter conditions.

i) Justification to neglect runoff in this work, since the open pit floor will soon be situated at a lower elevation than a large part of the watershed

Response

Water inflows into the open pit from precipitation, runoff, or other non-groundwater seepage sources are addressed throughout the DAR, because water quality at closure is one of the NICO Project's key-line of inquiry.

The groundwater numerical model focused only on groundwater flow. Runoff to the pit (and other areas of the site) is addressed specifically in Section 3.III of the DAR Appendices. Furthermore, during active mining

operations the pit will be dewatered and any runoff to the pit will be removed and will not influence groundwater recharge rates.

Recommendation 5

NRCan recommends that the Proponent provide:

a) *Information on the expected K value of the thickened tailings*

Response

The expected permeability of the tailings is in the order of $1x10^{-8}$m/s. For example, a similar hydraulic conductivity was reported for the Kidd Creek thickened tailings in Timmins (Woyshner and St-Arnaud, 1994)[3].

b) *Information on the expected groundwater flow through the CDF, and from the CDF into the underlying material*

Response

It has been estimated that the soil cover that will be constructed over the surface of the CDF as part of the closure measures, will limit the infiltration of rain water into the CDF to about 15% of the mean annual precipitation (MAP). This is equivalent to about 50 mm per year, or 69,000 m^3 per year (over the 138 hectare footprint of the CDF). After the cover is in place, the CDF will slowly develop a state of flow equilibrium, such that the seepage flow out of the toes of the CDF will balance the rate of infiltration. Almost all of the water that infiltrates through the cover is expected to flow horizontally through the CDF and report to the Seepage Collection Ponds downstream of the CDF. Because of the stratified flow, very little of the infiltration will report to the groundwater flow system. The groundwater model (as shown in Table 11.I.2-2 of the DAR) predicts only an average baseflow of 252 m^3/day for the Nico Lake Creek (which includes watershed areas BL1 and BL2). These watershed areas occupy a total footprint of 18.5 km^2. The baseflow translates to 0.00016 $m^3/s/km^2$, which is only about 1.4% of the annual precipitation. The CDF is located within the BL2 watershed. This watershed is almost one third of the BL1 watershed. Therefore, the contribution of the groundwater discharge into the CDF is expected to be insignificant. .

Recommendation 6

NRCan recommends the following in order to identify sensitive areas along the road corridor and to support final route selection and road design to ensure environmental effects are minimized:

a) *Conduct detailed terrain analysis supported by geotechnical investigations to characterize terrain sensitivity along the proposed route and to identify areas of potential instability. The product associated with this analysis will be large scale route alignment sheets that include this detailed information;*

b) *Conduct thermal analysis and determined potential ground settlement for representative terrain types to support detailed road design including determination of the embankment height and other mitigation*

[3] Woyshner, M.R. and St-Arnaud, L.D., (1994). Hydrogeological evaluation and water Balance of a thickened tailings deposit near Timmins, ON, Canada. In Proceedings, Third International Conference on the Abatement of Acidic Drainage, Pittsburgh, PA, April 24-29, 1994

measures (such as drainage control). The analysis should consider changes in snow cover and drainage that may influence the ground thermal regime; and

c) *Include in the assessment of environmental impacts, consideration of longer tem effects associated with vegetation removal and changes in permafrost and drainage conditions along the road corridor.*

Response:
This was addressed during conference call on 26 July 2012, no further action required.

Recommendation 7

NRCan recommends the following with respect to environmental monitoring and management plans:

a) *Environmental monitoring and management plans include installation of instrumentation in addition to visual inspections to monitor changes to the ground thermal regime and ground movements especially in sensitive areas; and*

b) *Monitoring and mitigation/management plans be developed that define the criteria for the need for mitigation and selection of the appropriate mitigation technique.*

Response:
This was addressed during conference call on 26 July 2012, no further action required.

Recommendation 8

Recognizing the design of the CDF is at a preliminary design level, NRCan recommends the following for detailed and final design of the CDF:

a) *The Proponent conduct further geotechnical investigations within the footprint of the CDF to improve the characterization of foundation materials and to support the detailed design*

Response
There is sufficient geotechnical information along the perimeter of the CDF and the alignment of the Seepage Collection Pond dams for the current level of study. It is agreed that additional boreholes will need to be drilled within the CDF basin to better define the subsurface conditions prior to the detailed design of the facility.

b) *The Proponent refine the seepage and stability analysis for the CDF incorporating the new information from detailed geotechnical investigations. This will also include updated creep analysis and consideration of effects related to the possible presence of frozen and unfrozen layers within the pile such as porewater expulsion and elevated pore pressures*

Response
The slope stability and seepage analysis carried out will be updated once new geotechnical information is available. The geotechnical information gathered to date from the site does not support the presence of continuous ice lenses underlying the site and hence the previous design did not consider creep analysis. The need for such analysis will be determined by the outcome of the future investigation.

c) *The Proponent has committed to develop an effective CDF monitoring and management plan which includes installation of instrumentation (such as piezometers, slope inclinometers, settlement plates, thermistors). Plans should also include a definition of triggers (or critical values) that determine the need for implementation of mitigation and the criteria for selection of mitigation techniques.*

Response

An appropriate level of geotechnical instrumentation will be incorporated in the CDF to verify the proper performance of the facility. Details of the instrumentation system will be identified during detailed design. The system will include thermistor strings, settlement hubs, piezometers and inclinometers. An OMS manual will also be prepared for the facility prior to the commencement of operation which will outline surveillance and monitoring requirements and action levels.

Recommendation 9

NRCan recommends the Proponent provide information about the open pit slope stability analysis.

Response

See attached (Appendix II) memorandum "Fortune Minerals – Summary Report on Geotechnical Studies for the Open Pit and Underground Mine Designs for the NICO Project" dated December 9, 2011.

The NICO open pit will expose good quality intrusive and metasedimetary rock masses. The proposed open pit will be of modest overall depth of approximately 250 m where overall slope is expected to be controlled by the stability of individual benches and the need to optimize bench geometry to minimize waste stripping.

Due to the combination of moderate overall slope height and competent rock mass, inter-ramp and overall slope stability are not significant concerns. As the pit will be excavated within a hill, the base of the pit will be only about 120m below the nearby lowland ground surface.

The open pit will eventually mine through the underground workings that will be excavated during the first years of production. Stability assessments of pit-underground interactions have been carried out to confirm that the proposed mine plan is safe and reasonable from a geotechnical perspective.

Recommendation 10

For the CDF slope stability modelling, NRCan recommends that the Proponent clarify how the 22° friction angle was derived for the glacio-lacustrine unit.

Response

The occurrence and thickness of glacio-lacustrine clays encountered in the previous site investigations were relatively limited, No undisturbed samples were obtained that were suitable for shear strength testing. Subsequent geotechnical investigations will carry out index, strength and consolidation tests on this unit. The feasibility design was based on assumed shear strength parameters. From our experience, the peak effective angle of friction of glacio-lacustrine clays is typically in the range of 20 to 25°. A phi parameter of 22 degrees is considered to be conservative given the moderate plasticity of the clay.

Recommendation 11

NRCan recommends that the Proponent provide further information to justify the use of a 22° friction angle for the glacio-lacustrine material and the use of circular slip surface in a cross-section in which a weak foundation layer exists.

Response

The use of an effective angle of internal friction of 22 degrees for the glacio-lacustrine clay unit was justified in the previous response. The slope stability analysis will be redone once new geotechnical information is obtained from future investigations. The analysis will include searches for the minimum factor of safety, considering both circular and viable composite failure surfaces. If extensive weak deposits were to be identified in the area of the toe of the CDF, then appropriate design measures would be incorporated (e.g. toe berms or shear keys).

Recommendation 12

NRCan recommends that, if Figure 13.2-4a and Figure 13.2.2 (DAR: 13 SON Terrain and Soils, Section 13.2) are to be used in the future for regulatory or other applications, that the following inconsistencies be corrected:

a) Figure 13.2.4a and Figure 13.2.2 should use the same terrain units

Response

The same terrain units are used in both figures. The reason they appear different, is they have been identified as complex map units based on the scale and resolution of the imagery used for mapping. Simple map units are used to describe areas where only one terrain type is represented. Complex map units are used to describe areas where a dominant, co-dominant, and/or subdominant terrain type occurs.

The basic terrain map units are as follows:

1) Fg – Glaciofluvial (this one contains 2 variants: 1 = gravels and 2 = sands)
2) M – morainal/till
3) N – fen (organic)
4) O –frozen organic (potential permafrost)
5) B – bog (organic)
6) R - rock
7) Disturbance
8) Unclassified
9) water

Terrain units were determined from the ELC mapping. For the regional study area, the ELC map developed from Landsat imagery was used as a basis for producing the regional scale terrain maps. Vegetation classification and mapping were completed in several steps. A preliminary ELC map was developed for the vegetation RSA using Landsat Thematic Mapper satellite imagery (28.5 x 28.5 m resolution) that was captured on 24 July 2001. An aerial reconnaissance survey completed in September 2003 was used to

verify a draft land cover classification. This initial classification was updated and finalized using field data collected during vegetation and wildlife surveys carried out at 132 sites between 2003 and 2006.

For the local study area, the ELC map developed from IKONOS imagery was used as a basis for producing the terrain maps. For the local study area, a preliminary ELC map was developed for the vegetation LSA using IKONOS satellite imagery (0.8 m panchromatic resolution) captured on 5 August and 21 August 2006, as this higher resolution imagery was deemed more suitable for mapping at the local scale (the higher resolution imagery was not available for the entire regional study area). An aerial reconnaissance survey completed in July 2006 was used to verify the draft ELC within the LSA. This initial classification was updated and finalized using field data collected during vegetation and wildlife surveys carried out at 132 sites between 2003 and 2006. In the summer of 2008, a wildfire burned a portion of the LSA and RSA. To update the ELC, a Landsat 7 image captured on 8 August 2008 was obtained. The burned area was classified and isolated from the rest of the imagery. The resulting burn polygon was used to update the ELC maps.

The ELC vegetation units were then used as part of the mapping process to derive correlations between field observations, terrain features, and the ELC vegetation types. Due to the resolution of the ELC data, many terrain map units were presented as complexes to capture the range of terrain types on the landscape. Minor components of a terrain unit (i.e., less than 20% representation within a map unit) were not mapped. The terrain map unit delineations were largely inferred from the ELC units, as well as the interpretation of landscape features (i.e., elevation contours and landform), and then correlated to field survey results. Thus, the terrain map should be viewed as a predictive model of terrain distribution. The information should not be applied for predicting site-specific characteristics without collecting additional field information.

The regional scale map is a broader estimation of terrain distribution across the landscape. The local scale map is a more detailed estimation of terrain distribution across the landscape.

b) Figure 3.2-1 should make use of other sources of data to complete "unclassified" regions

Unclassified areas are portions of the LSA for which an ELC vegetation class could not be assigned due to satellite interference (i.e., cloud, haze, and shadow). Because the terrain map unit delineations are largely inferred from the ELC vegetation classes, as well as the interpretation of landscape features (i.e., elevation contours and landform), and correlated to field survey results, areas without an ELC vegetation class could not be assigned a terrain map unit. Terrain map units for the unclassified areas cannot be identified without follow-up programs.

c) *glacio-lacustrine deposits/soils and till exposed on hillsides and elsewhere should appear on terrain maps*.

Any glaciolacustrine materials that may be present are associated with lakes and/or areas of frozen organic, bogs, and fens. Therefore these terrain units can be used to make an inference on the location of these materials. Till exposed on hillsides would not show up on these maps, as they have been produced at a scale too coarse to delineated these features. Additional information from follow-up programs could be used to identify these features, as well as to modify the terrain map.

Closure

We trust the information contained in this letter satisfies the issues discussed during the conference call of 26 July 2012. If any additional information is required, please contact the undersigned.

GOLDER ASSOCIATES LTD.

Matthew Bowman. B.Sc.
Junior Groundwater Specialist

Marc Rougier, P.Eng.
Principal

Ken Bocking, M.Sc., P.Eng.
Principal

JG//MR/KB/jg

Attachments: Appendix I – Response 2c Supporting Documents
Appendix II – Response 9 Supporting Document

c:\users\jgibson\documents\sharepoint drafts\responses to nrcan technical recommendations.docx

APPENDIX I
Response 2c Supporting Documents

PROCEEDINGS OF THE CONFERENCE ON FRACTURED AND JOINTED ROCK MASSES
LAKE TAHOE/CALIFORNIA/USA/3-5 JUNE 1992

Fractured and Jointed Rock Masses

Edited by
L.R.MYER & C.-F.TSANG
Lawrence Berkeley Laboratory, California, USA
N.G.W.COOK & R.E.GOODMAN
University of California, Berkeley, USA

A.A.BALKEMA/ROTTERDAM/BROOKFIELD/1995

Fractured and Jointed Rock Masses, Myer, Cook, Goodman & Tsang (eds) © 1995 Balkema, Rotterdam. ISBN 90 5410 591 7

Interpretation and synthesis of discrete fracture orientation, size, shape, spatial structure and hydrologic data by forward modelling

W. Dershowitz
Golder Associates Inc., Redmond, Wash., USA

Abstract

This paper describes the use of principles of forward modelling to develop a consistent set of tools for the interpretation of geometric and hydrologic discrete fracture properties. These procedures simulate the data collection process to obtain synthetic samples which can be compared directly to in situ measurements.

I. INTRODUCTION

Although fracture geometric information is frequently collected from boreholes and geologic mapping, it is difficult to derive in situ fracture geometry, due to well documented problems of bias, censoring, and truncation ([1] Baecher, Lanney and Einstein, 1977; [2] Terzaghi, 1964; [3] Warburton, 1980).

This paper describes a consistent set of procedures for interpretation of fracture geometric and hydrologic data, and development of realistic three dimensional discrete fracture conceptual models using the technique of "forward modelling" (Figure 1). In the usage of this paper, the term forward modelling refers to the derivation of parameters by simulation of the data collection process using assumed in situ conditions, in contrast to "inverse modelling", in which model parameters (as opposed to physical properties) are adjusted to match observed behavior. In the approach developed here, a statistical description of fracture orientation, size, shape, and spatial distribution is assumed based upon coarse analysis of the data. The process used to collect the available data is then simulated, including processes of bias, censoring, and truncation. This produces a simulated set of field data, which can then be compared to field measurements. Based upon this comparison, the assumed statistical description can then be modified, and the process repeated until a statistical description is found which is consistent with observations. The goodness of fit between measured and simulated field measurements can be evaluated visually, by statistical comparison, and by use of statistical tests such as the χ^2 and Kolmogorov Smirnov test.

Forward modelling has several advantages over mathematical approaches such as those developed by [3] Warburton (1980). The most important of these is the ability to directly account for known bias, censoring, and truncation processes. The forward modelling approach directly simulates the process used for data collection, and therefore automatically accounts for these processes. In addition, forward modelling offers greater flexibility than mathematical approaches. Thus, in this simulation approach, fracture size can be derived for generalized fracture shapes defined by polygons. In contrast, mathematical approaches are limited to circular and rectangular fracture shape assumptions.

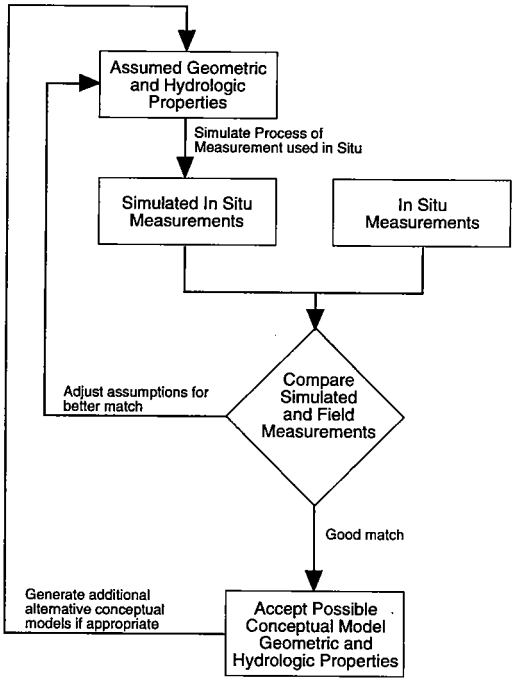

Figure 1. Forward Modelling Approach

II. FRACTURE SIZE

Fracture size is one of the most critical geometric properties for discrete fracture analyses for rock strength, stability, and hydrologic properties. However, no general mathematical procedures have been developed for derivation of fracture size

from surface mapping "trace" data. The forward modelling approach for derivation of fracture size is implemented as follows:

- make reasonable assumptions for fracture size distributions, orientation distributions, spatial distribution

- define the sampling plan carried out to collect the data to be analyzed. The sampling plan includes the type of survey (line, area, circle), the sampling window size, shape and orientation, as well as truncation limits on size such as minimum mapped fracture

- define the bias, censoring, and truncation processes in the field program used to collect data. **Biases** will include, for example, a tendency for field geologists to sample larger fractures more frequently, and the higher frequency of intersections between mapping surfaces for larger fractures perpendicular to the mapping surface. **Censoring** and **truncation** will include, for example, the limitations imposed by the size of the mapping surface, and the decision to map fractures only greater than a certain length.

- Define rules to describe bias, censoring, and truncation processes. [4] Geier et al. (1992), for example, defined a rule in which the probability of mapping a fracture given an intersection with a mapping surface was defined by an equation of the form,

$$P[L|L_{min},c_L] = \left\{ \begin{array}{ll} 0, & L < L_{min} \\ \dfrac{L|L_{min} - 1}{c_L - 1}, & L_{min} \le L \le c_L L_{min} \\ 1, & L > c_L L_{min} \end{array} \right\} \quad (1)$$

L_{min} = smallest recorded trace length [L]

c_L = censoring parameter [-]

In other words, the probability of observing an existing trace smaller than L_{min} is taken to be zero. This probability increases linearly between L_{min} and $c_L L_{min}$. It is assumed that traces larger than $c_L L_{min}$ are always mapped. For a given mapping scale, L_{min} is the smallest trace length in the dataset. The most appropriate value of c_L might vary with the mapping scale and methodology, but a constant c_L was assumed for all scales, to limit the number of parameters.

- Simulate the process of sampling using the defined sampling rules and assumed fracture geometry, producing a simulated trace length distribution. These simulations are carried out by generating stochastic realizations of fractures with these assumed distributions of properties, and calculating the intersections between those fractures and the defined sampling plan. The effect of geometric bias is accounted for in the process of intersection between sampling surface and fractures. The effect of other biases are accounted for using rules relating fracture intersections to recorded fracture intersections using equation 1 above.

- Compare the simulated trace length distribution against the field measurements, and adjust assumptions until appropriate assumptions are found. The match between simulated and field trace lengths can be evaluated visually, and using tests such as the χ^2 and Kolmogorov Smirnov tests.

Figure 2 presents the results of analysis of fracture trace length analyzed in terms of a lognormal distribution.

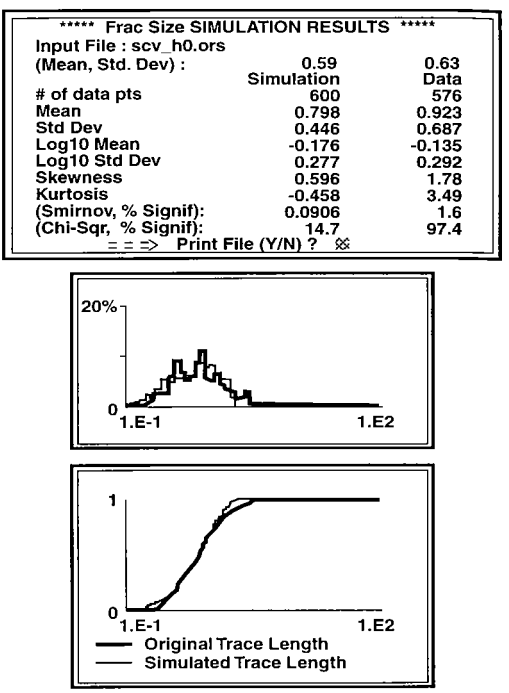

Fracture Zone H
[13] Based on data from Bursey, Gale, and Maclead, (1991) Stripa TR91-19

Figure 2. Forward Modelling of Fracture Radius

Geier et al. (1991) [5] analyzed fracture data at the Finnsjön, Sweden site, and found that the data could be analyzed by this method using a single power law distribution at scales from 1 to 103 meters. The form of the power law distribution is,

$$f_r(r_e) = \frac{b_r - 1}{r_{min}} \left(\frac{r_{min}}{r_e} \right)^{b_r}, \quad r_e \ge r_{min} \quad (2)$$

where r_{min} is an arbitrary lower limit (to avoid singularity in the distribution) set smaller than the smallest semi-tracelength measured, and b_r is the power law exponent. This form was used because it is implied by the observed power law distribution for tracelength.

Figure 3 shows the Kolmogorov Smirnov statistic KS (comparing simulated and observed trace length L) as a function of b_r and c_L. Estimated confidence intervals are given by curves of constant KS_r. KS_r is fairly insensitive to variation of c_L in the range 2 to 6, for values of b_r close to 3.1, so this is a good estimate of b_r even if the form of the bias probability differs from the model in Equation 1.

III. ORIENTATION

The bias in measured orientation is well documented ([2] Terzaghi, 1964, [6] Einstein et al, 1980). Measured orientations are biased due to the relative orientations of fractures and sampling lines and planes, and due to the relative size of

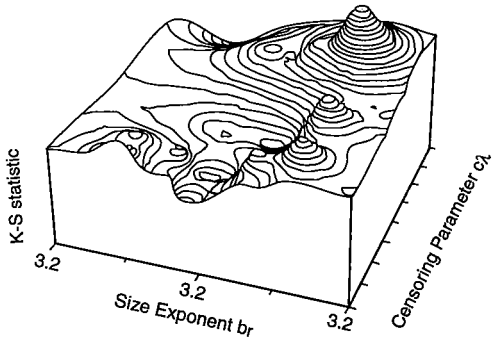

Figure 3. Optimal solution for Power Law Fracture Simulation Orientation

fractures with different orientations. Unfortunately, when all available corrections for bias in orientation measurements are applied, the result can be reduced to a uniform distribution ([7] Dershowitz, 1979).

The forward modelling approach implemented in the "Interactive Set Identification System" (ISIS) algorithm accounts for the bias in orientation data, without losing the data itself through multiple correction factors. In this approach, the analysis begins with an assumption that all of the measured fractures can be corrected to in situ orientations using a modified [2] Terzaghi (1964) correction. This correction is applied by adding fractures to the observed fractures in proportion to their probability of being omitted due to sampling bias. A set of simulated measurements are then obtained from boreholes and trace planes through this orientation distribution, and compared to the measurements. The correction is then modified until simulated measurements are obtained which correspond well to field measurements. Figure 4 illustrates a comparison of measured and simulated orientations as measured on a fracture trace plane, using a bootstrap resampling approach for fracture generation ([8] Dershowitz et al, 1991).

This approach has been implemented utilizing a unique set identification algorithm based upon pattern recognition. This algorithm recognizes that fracture sets should be defined by similarity in all of their properties, not just on orientation. The user therefore defines the properties to be used in defining sets (e.g., orientation distribution, mineralization, size, foliation, striation). The user then examines the available data and defines

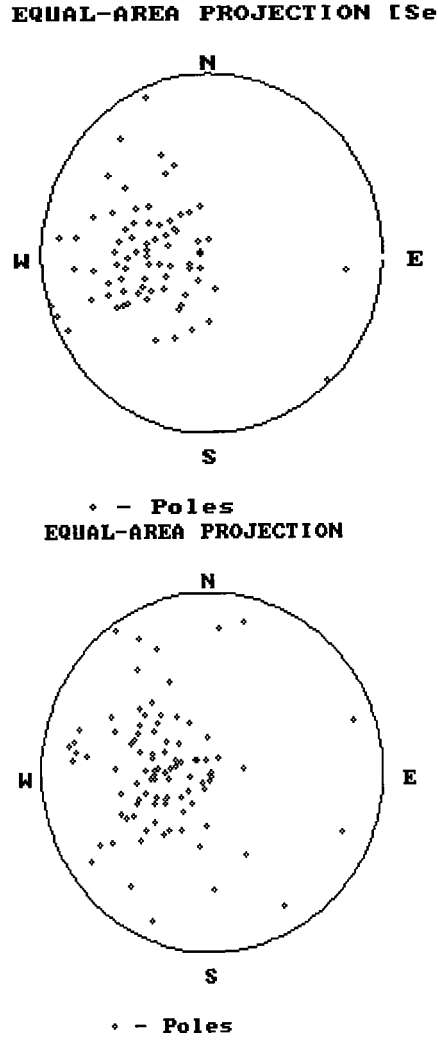

Figure 4. Comparison of Measured and Bootstrap Simulation Orientation

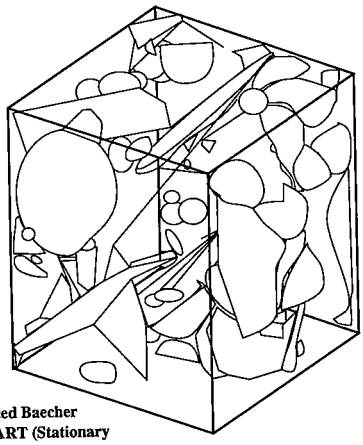

a) Enhanced Baecher Model, BART (Stationary Poisson Point Process)

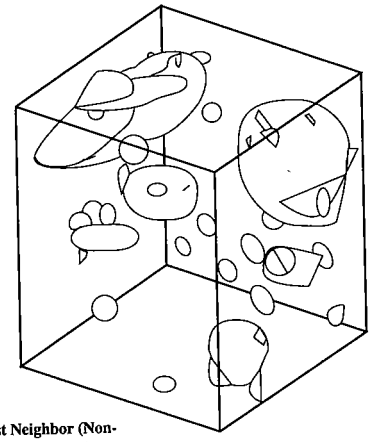

b) Nearest Neighbor (Non-Stationary Poisson Point Process)

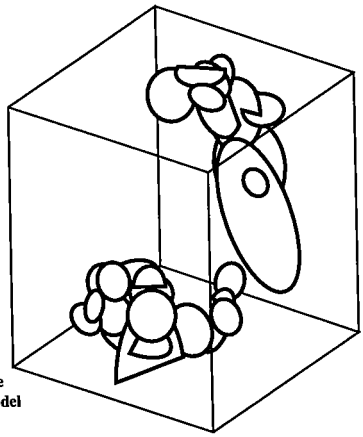

c) Levy-Lee Fractal Model

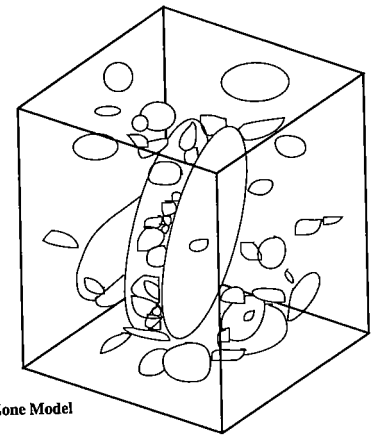

d) War Zone Model

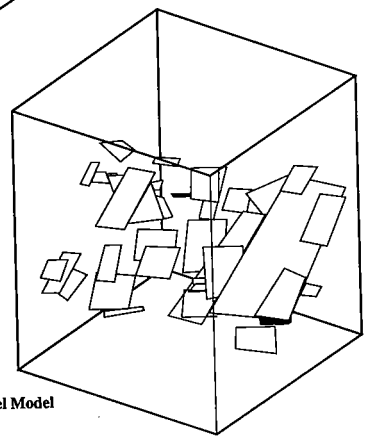

e) Poisson Rectangel Model

Figure 5.Discrete Fracture Conceptual Models

the number of sets which should be considered based on the available data, and the statistical properties of each set. The algorithm then cycles through the available fracture data, and assigns fractures to sets using a probability proportional to the statistical similarity of the fracture to the properties defined for each set. Once all fractures have been assigned to sets, the properties of the sets are recalculated based upon the fractures assigned, and the assignment process is repeated.

This approach is particularly robust, and is able to assign fractures to sets even when those fractures are part of the cluster overlap often seen in stereographic projections. Since the user can assign weights of importance to each of the properties to be considered, the user can define sets which satisfy the specific engineering problems. While hydrologic analysis may require sets defined with a high weighting on mineralization, rock bolt analysis may require sets defined based upon size and orientation.

IV. SPATIAL STRUCTURE

Fracture spatial structure is derived by assuming a conceptual model for fracture location and termination, and generating stochastic realizations of that conceptual model using fitted distributions of fracture orientation and size, together with measured parameters for fracture termination and other properties. Conceptual models evaluated include the Poisson process, compound and non stationary Poisson process (enhanced Baecher, BART, and nearest neighbor models), fractal models (Levy Lee fractal model), and empirical/geostatistical models (war zone model) ([8] Dershowitz et al, 1991), Figure 5. Three dimensional stochastic realizations are then sampled using the same types and orientations of trace plane used to collect field data, and the measured and simulated trace planes are compared. The assumed conceptual models can then be adjusted as necessary to obtain a good match. Figure 6 presents a comparison of stochastically generated trace maps and field measurements for a drift at the Stripa, Sweden experimental mine.

V. HYDROLOGIC PROPERTIES

The forward modelling analysis technique for fracture hydrologic properties is illustrated in Figure 7. In this approach, the significant fracture hydrologic properties are assumed to be the conductive fracture frequency λ_c and transmissivity T_f

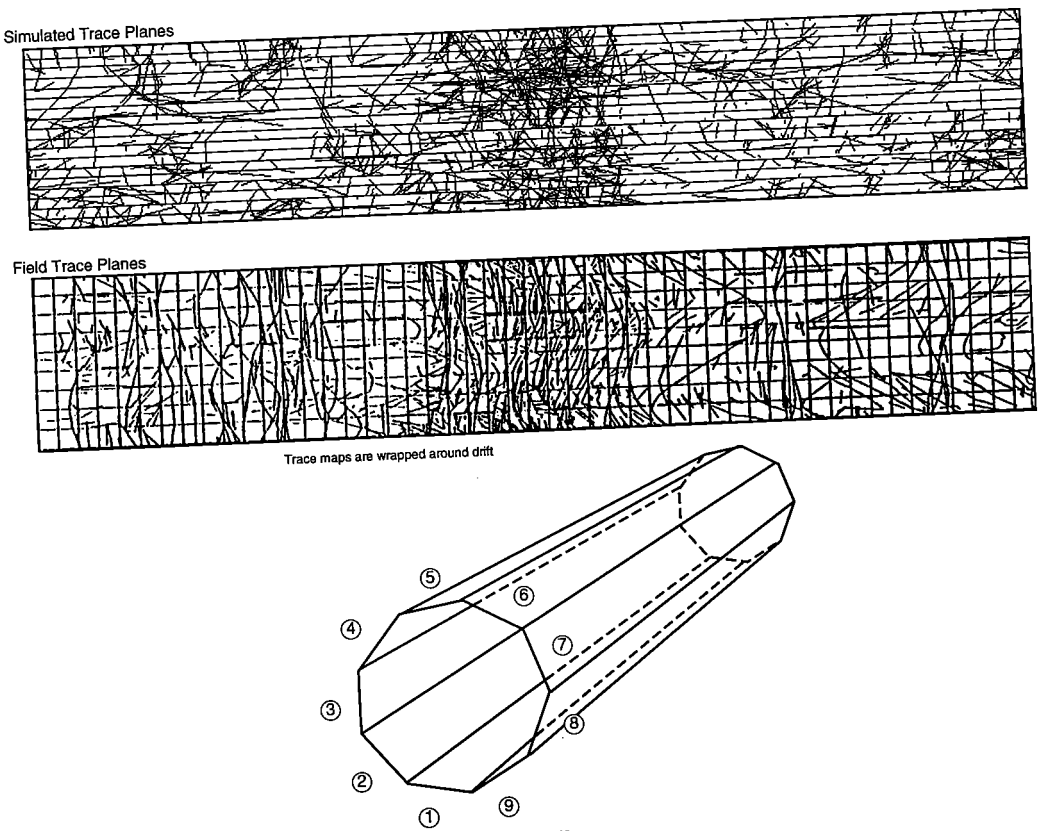

Figure 6. Simulated and Mapped Fracture Traces from Stripa Validation Drift

distribution. The data which is commonly available is the transmissivity T_i of packer intervals as measured using constant flow or constant head packer tests.

The approach developed for derivation of the fracture transmissivity distribution and conductive fractures intensity from packer test data is an extension of the analytical approach of [9] Osnes et al. (1988).

The method assumes that the net transmissivity of a test zone is equal to the sum of the transmissivities of the conductive fractures that intersect that test zone (Figure 7):

$$T_i = \sum_{j=1}^{n_i} T_{ij} \qquad (3)$$

Where T_{ij} is the apparent transmissivity of the ith packer interval, n_i is the number of conductive fractures in the ith interval, and T_{ij} is the transmissivity of the jth conductive fracture within the ith interval. Within any given interval, the number of conductive fractures, n_i is assumed to be a random number defined by a the spatial distribution of fracture locations. For a range of stationary and non stationary distributions for fracture locations, the Poisson distribution ([10] Benjamin and Cornell, 1970) can be used to describe the distribution of the number of fractures in a packer interval.

$$f_n(n) = \frac{\bar{n}^n e^{\bar{n}}}{n!} \qquad (4)$$

Where $\bar{n}$ is the Poisson process rate, which is equal to the expected value of n. The conductive fracture frequency is given by $f_c = \bar{n}/L_i$, where L_i = the length of the test zone. For non stationary fracture patterns (such as patterns which increase in fracture density with depth), the intensity f_c can be defined as a function of the spatial coordinates.

The distribution of fracture transmissivities is assumed to be independent within each packer interval, with a given distributional form, with parameters defined, for example, by a mean and standard deviation. The distribution of T_i is the sum of a random number of random events, and is therefore a compound process ([11] Feller, 1971).

For any given set of parameters describing the distribution of fracture

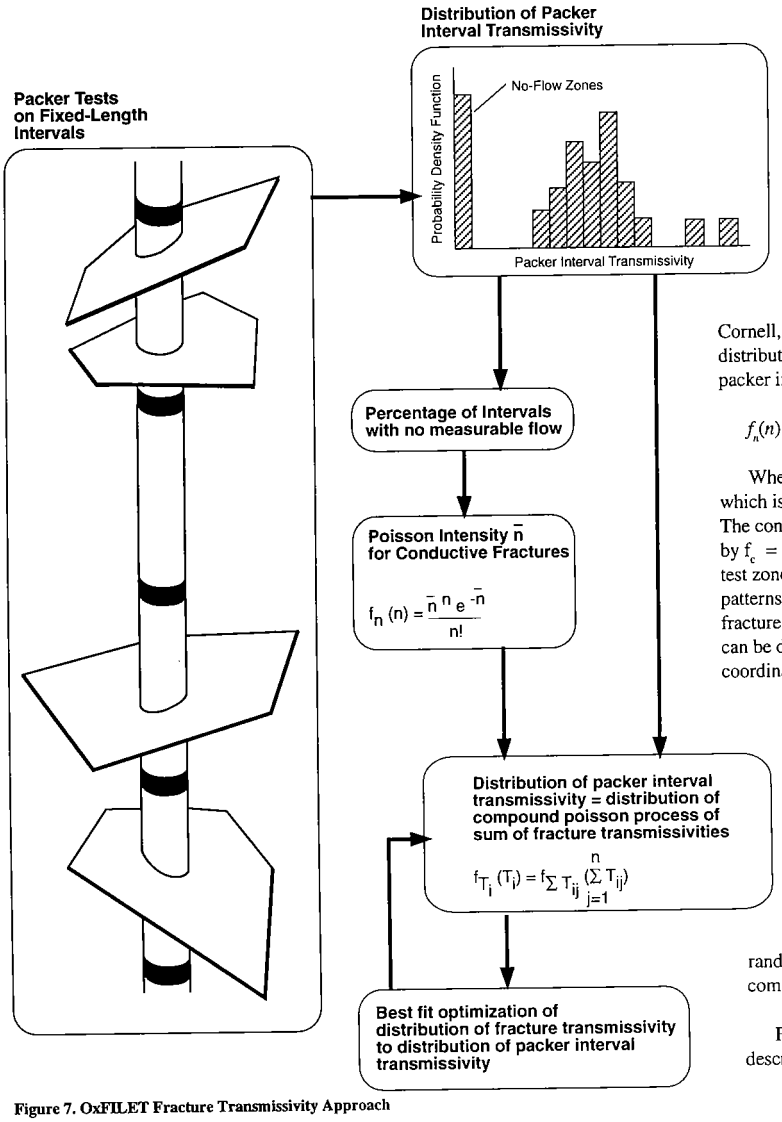

Figure 7. OxFILET Fracture Transmissivity Approach

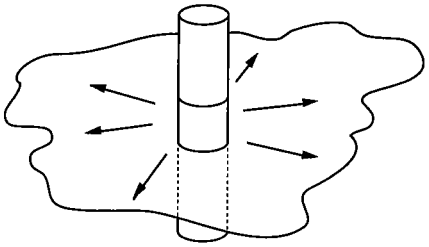

a) Packer Test Controlled by Single Fracture

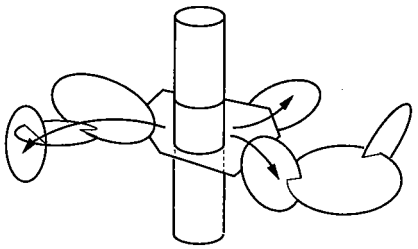

b) Packer Test Controlled by Fracture Network

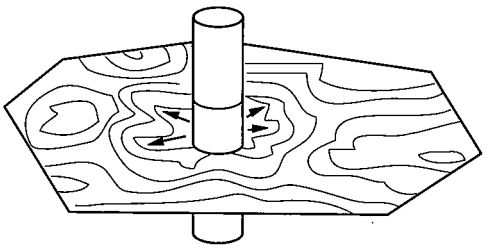

a) Packer Test Controlled by Local Fracture Roughness

Figure 8. Alternative Interpretations of Packer Interval Transmissivity

transmissivity $f(T_{ij})$ and conductive fracture frequency f_c the distribution of packer interval transmissivities $f(T_i)$ were found by Monte Carlo simulation, with the best fit value found by a simulated annealing search routine. Simulated intervals that contain no conductive fractures, or that have values of T_i less than $T_{threshold}$ the lowest threshold transmissivity that could be reliably measured in the field, are assigned a transmissivity equal to $T_{threshold}$.

The intensity and transmissivity distributions for the conductive fractures are then estimated by finding the best match between the observed distribution of packer interval transmissivities $f(T_i)$ and the distribution of test zone transmissivities found by simulation for given fracture frequency and single fracture transmissivity distributions. This match is found both visually and by comparison of Kolmogorov Smirnov (K-S) or Chi Squared statistics (χ^2). The values of $\bar{n}$, μ_{logT} and σ_{logT} that provided the best K-S or χ^2 minimize D are taken to be the best estimates of those parameters.

Flow and transport simulations frequently require that the fracture transmissivity used be the effective transmissivity through a fracture between the fractures intersecting the fracture ("cross-fracture transmissivity", T_{fi}). Three alternative interpretations are possible for the relationship between T_{fi} and T_{ij}, the transmissivity seen in the fixed interval packer test (Figure 8).

- The packer test influences one fracture at a time, such that the transmissivity seen for each fracture T_{ij} is equal to the cross fracture transmissivity, T_{fi}.

- The packer test is strongly influenced by the local fracture aperture near the borehole. In this case the transmissivity seen by the packer test is a small scale ("at borehole") transmissivity, and the cross fracture transmissivity T_{if} must be found using a correlation of the form,

$$T_{ij} = B_f T_{fi} \tag{5}$$

The proportionality constant B_f is described as a normally distributed random variable with mean and standard deviation provided by the user. An example of the relationship between T_{fi} and T_{ij} from numerical simulation is shown in [12] Geier et al. (1992) in this volume.

- The packer test influences a network with a number of interconnected fractures. In this case, the transmissivity seen by the packer test, T_{ij}, is a network transmissivity related to the cross-fracture transmissivity of a number of fractures. Assuming series flow through the n fractures influenced by the packer test, the relationship between T_{ij} and T_{fi} could be given approximately by,

$$T_{ij} = \frac{\bar{m}}{\sum_{i=1}^{\bar{m}} \frac{1}{T_{fi}}} \tag{6}$$

For this approach, an additional parameter $\bar{m}$ the mean number of fracture per network seen by packer tests must be specified. The distribution of $\bar{m}$ is assumed to be Poisson.

VI. CONCLUSIONS

The approach presented here provides procedures for derivation of the hydrologic and geometric properties necessary for discrete fracture analyses. This approach has been applied extensively at sites in Sweden [4], [14], and Japan [15]. These applications have demonstrated that the approach has several significant advantages: it allows identification of not just a single "best" description of in situ fracture geometry and properties, but any number of alternative field conditions consistent with observations; it fully and explicitly corrects for bias, censoring and truncation due to the process of data collection; and it allows the development of all the properties necessary for three dimensional discrete fracture modelling.

VII. ACKNOWLEDGMENTS

The technology described in this paper was initially developed at the Massachusetts Institute of Technology, under the guidance of Prof. H. Einstein, and at the University of California

at Berkeley, under the guidance of Charles Wilson and Tom Doe. These approaches have been developed further by Golder Associates, with support from nuclear waste management authorities in the US (DOE), Sweden (SKB), Switzerland (Nagra), the European Community (CEC) and OECD/NEA. The author would like to thank his colleagues at Golder Associates offices in Seattle, Uppsala, Nottingham, and Tokyo for their contributions to the development of the forward modelling and discrete feature analysis methodologies.

VIII. REFERENCES

[1] Baecher, G. B., N. A. Lanney, and H. H. Einstein. Statistical Description of Rock Properties and Sampling, Proceedings of the 18th U.S. Symposium on Rock Mechanics, American Institute of Mining Engineers, pp. 5C1-8, 1977.

[2] Terzaghi, R. Sources of error in joint surveys, Geotechnique, Vol. 15, pp. 287-304, 1964.

[3] Warburton, P. A Stereological Interpretation of Joint Trace Data. International Journal of Rock Mechanics, Mining Sciences, and Geomechanics Abstracts, Vol. 17, pp. 63-66, 1980.

[4] Geier, J., C L. Axelsson, L. Hssler, and A. Benabderrahmane. Discrete Fracture Modelling of the Finnsjön Rock Mass. SKB Technical Report, SKB, Stockholm, 1992.

[5] Geier, J. and C L. Axelsson and W. Dershowitz. Discrete Fracture Modelling of the Finnsjön Rock Mass: Phase 1 Feasibility Study. SKB Technical Report, SKB, Stockholm, 1991.

[6] Einstein, H., Baecher, G., D. Veneziano, W. Dershowitz et al. Risk Analysis for Rock Slopes in Open Pit Mines. Publication R80-17, Order No. 669, Department of Civil Engineering, Massachusetts Institute of Technology, Cambridge MA, 1980.

[7] Dershowitz, W. S. A Probabilistic Model for the Deformability of Jointed Rock Masses, M.S. Thesis, Massachusetts Institute of Technology, Cambridge, MA, 1979.

[8] Dershowitz, W. G. Lee, and J. Geier. FracMan Version 2.3 User Documentation: Interactive Discrete Feature Data Analysis, Geometric Modelling, and Exploration Simulation. Golder Associates Inc., Seattle WA, 1991

[9] Osnes, J.D., A. Winberg, and J. Andersson. Analysis of Well Test Data Application of Probabilistic Models to Infer Hydraulic Properties of Fractures, Topical Report RSI 0338, RE/SPEC Inc., Rapid City, South Dakota, 1988.

[10] Benjamin, J.R. and C.A. Cornell. Probability, Statistics, and Decision for Civil Engineers. McGraw Hill Book Company, New York, 1970.

[11] Feller, W. An Introduction to Probability Theory and Its Applications. John Wiley and Sons, New York, 1971.

[12] Geier, J., W. Dershowitz, P. Wallmann, and T. Doe. Discrete Fracture Modeling of In Situ Hydrologic and Tracer Experiments. Proceedings, Fracture and Jointed Rock Masses, Taho, NV, June, 1992.

[13] G. G. Bursey, J. E. Gale, and R. Maclead, Fractlow Consultants Inc., St. John's, Newfoundland, Canada A. Strahle, and S. Tiren, Swedish Geological Co., Uppsala, Sweden, August, 1991

[14] Dershowitz, W., P. Wallmann, and S. Kindred. Discrete Fracture Modelling for the Stripa Site Characterization and Validation Drift Inflow Predictions. SKB Stripa Technical Report TR-91-16. SKB, Stockholm. 140p, 1991.

[15] Uchida, M., T.W. Doe, W. Dershowitz, and P. Wallmann. Simulation of Fracture Flow at the Kamaishi Validation Drift. Proceedings, Fourth Annual International Conference on High Level Radioactive Waste Management, Las Vegas. American Society of Civil Engineers, NY, 1993.

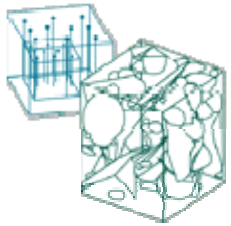

FRACMAN®
TECHNOLOGY GROUP

12 November, 2010

Nico – Derivation of Rock Mass Porosity from Packer Tests on Fractured Rock

Doo-Hyun Lim, Bill Dershowitz

Golder Associates

Analysis Strategy

- Packer tests provide packer interval transmissivity, not an equivalent rock mass hydraulic conductivity
- Assume that this packer interval transmissivity is directly related to the sum of the transmissivities of fractures intersecting that well interval
- Carry out a deconvolution from the distribution of packer interval transmissivities to the fracture conductive intensity and transmissivity.
- This analysis is implemented in FracMan as OxFilet ("**O**snes E**x**traction from **F**ixed-**I**nterval-**L**ength **E**ffective **T**ransmissivities") adapted from Osnes et al (1988).

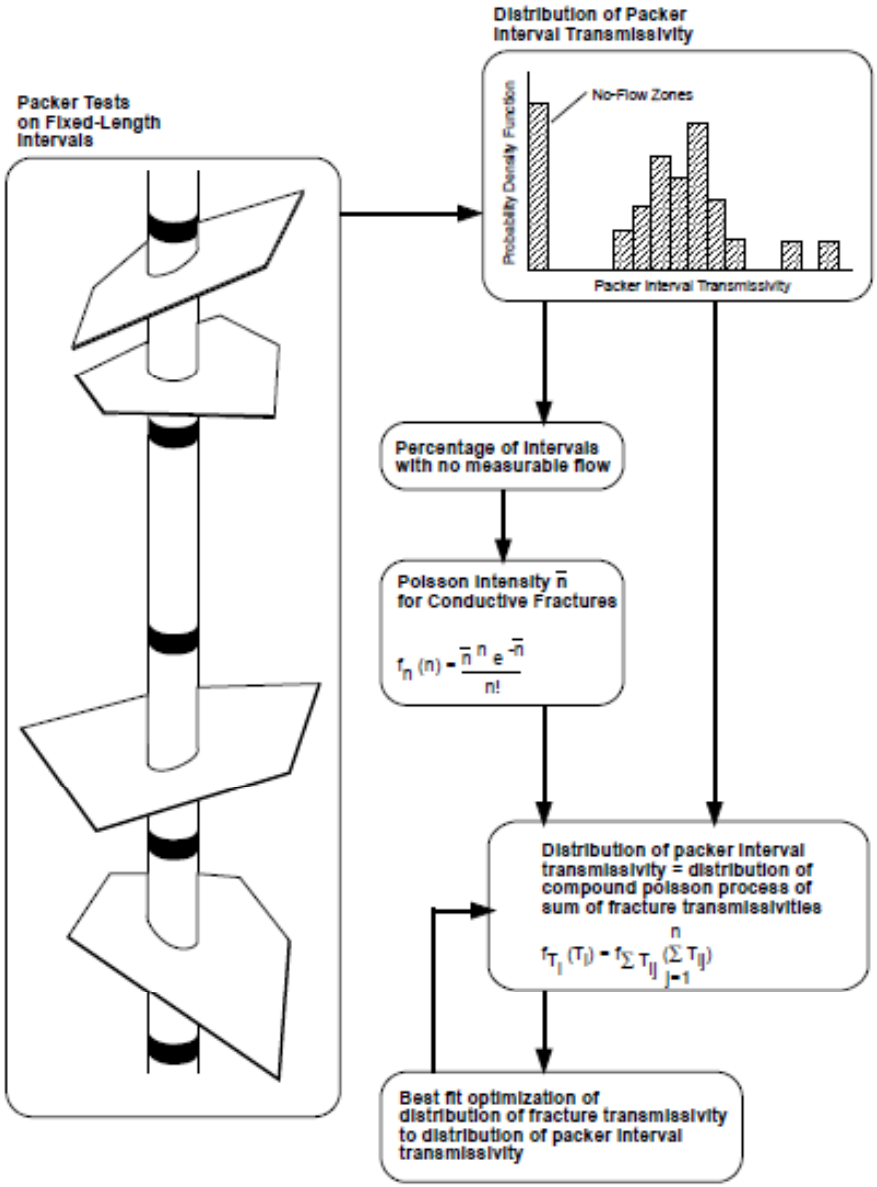

Nico-03-281 Packer Test Result

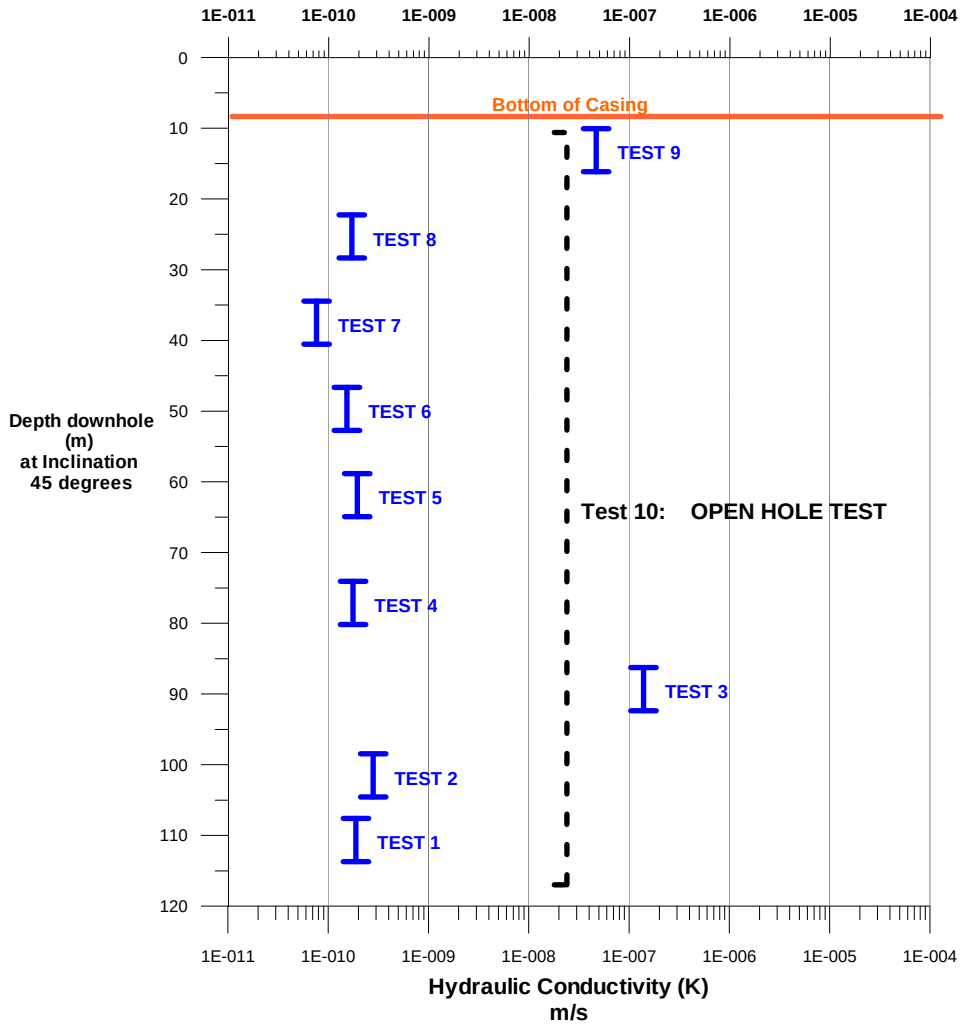

LEGEND

Discrete 20 ft (6.10m) packered interval tested using the Constant Head method

Open Hole test using a single Packer set just below the casing, tested using the Constant Head method.

NOTES:

1. Measurable flows were observed only during tests 10, 9 and 3. Remaining test intervals each had NIL flows despite pressures of up to 180 psi for 10 minutes.
2. Hydraulic conductivity values at test intervals 1-2 and 4-8 were estimated assuming a flow of 0.05 Litres and the maximum test pressure and time period attempted on the interval. See appended test data sheets for details.

Nico-03-282 Packer Test Result

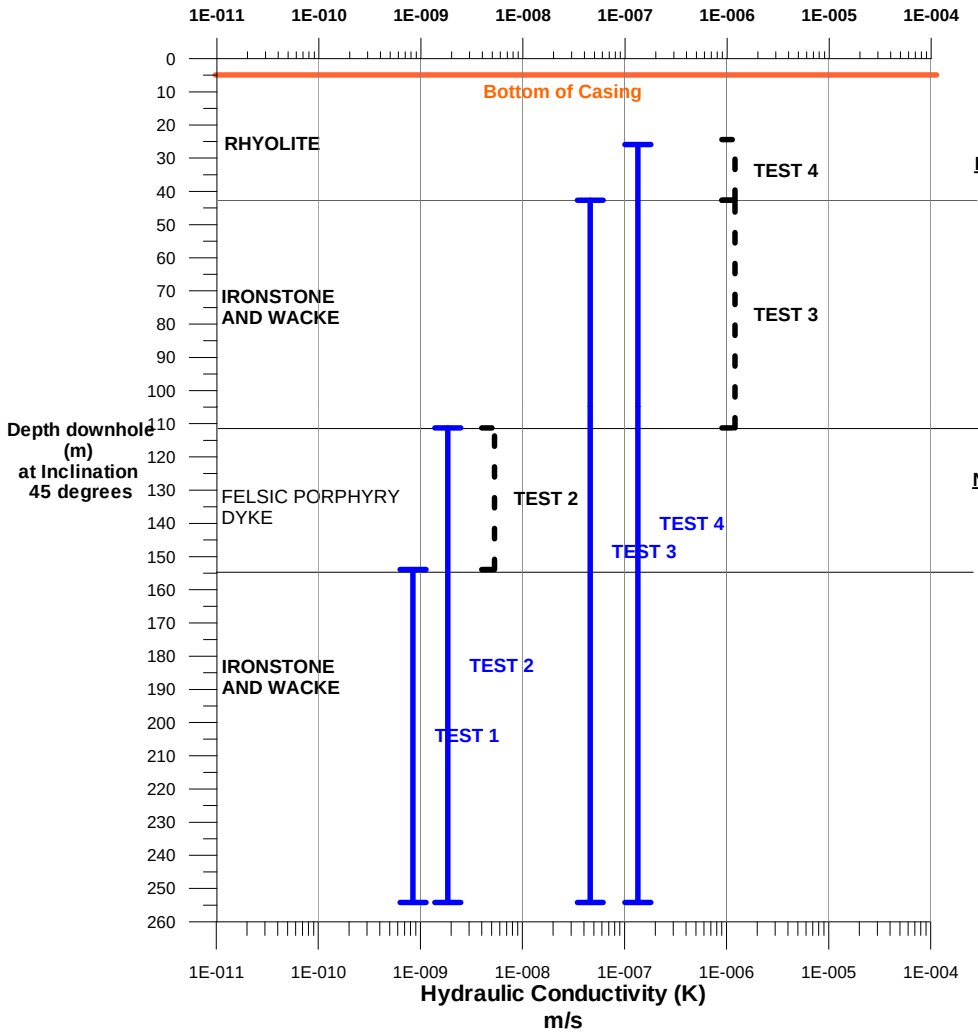

LEGEND

Upstaged test intervals packer tested using the Constant Head Method. Intervals selected based on major geological contacts.

Inferred Hydraulic conductivity for overlapping intervals based on upstage test results.

NOTES:

1. Measurable flows were observed during all four tests.

Nico-03-283 Packer Test Result

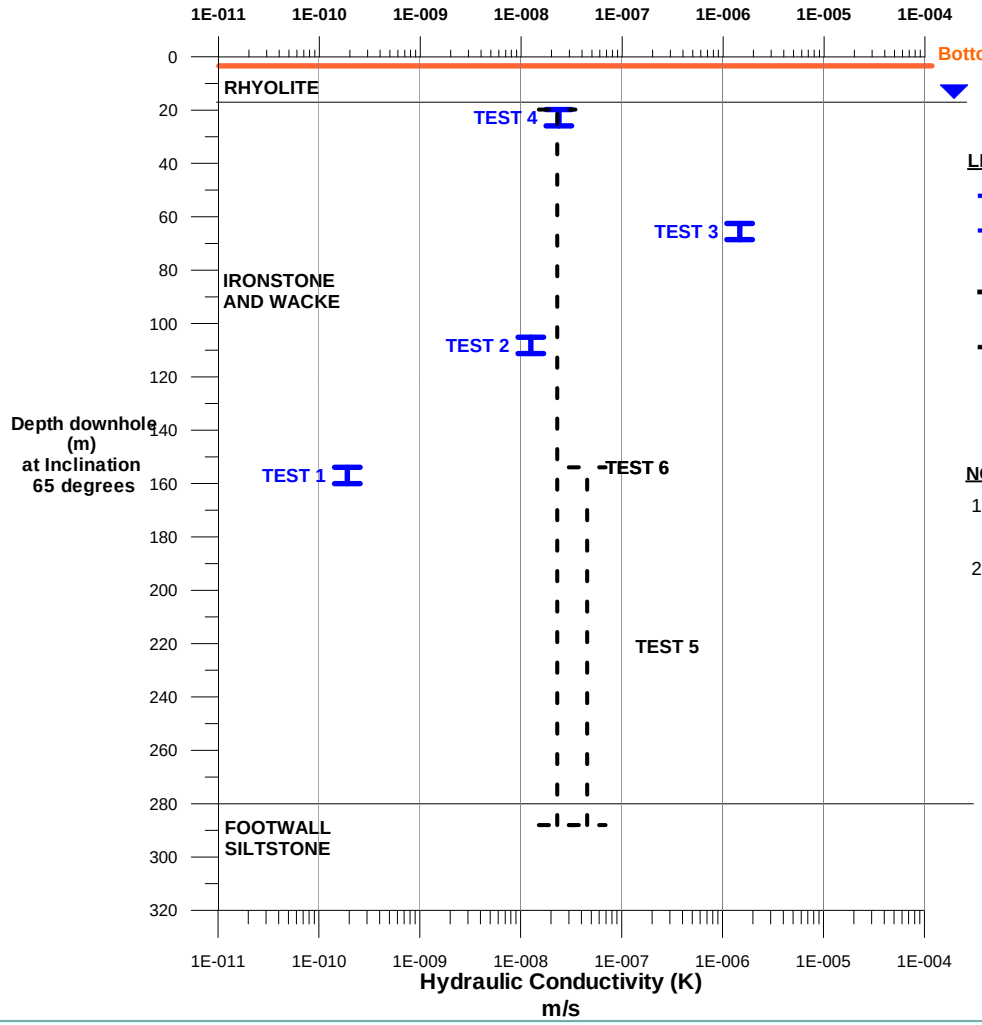

LEGEND

Discrete (6.10m) intervals tested using the Constant Head Method.

Upstage interval tested using single packer and the Constant Head Method.

NOTES:

1. Measurable flows were observed during all but the first test.
2. Hydraulic conductivity value at test interval 1 was estimated assuming a flow of 0.05 Litres and the maximum test pressure and time period attempted on the interval. See appended test data sheets for details.

Packer Test Result: Provided From Client

Hole	Test	From	To	k	Rock Type
		m	m	m/s	
03-281	Test 10 (2)	10.67	117.04	2.6287E-08	Open Hole, both rock types
03-281	Test 9	10.06	16.15	5.38539E-08	Ironstone
03-281	TEST 8	22.25	28.35	1.9749E-10	Ironstone
03-281	TEST 7	34.44	40.54	8.80629E-11	Ironstone
03-281	TEST 6	46.63	52.73	1.7657E-10	Ironstone
03-281	TEST 5	58.82	64.92	2.24032E-10	Ironstone
03-281	TEST 4	74.06	80.16	2.03518E-10	Ironstone
03-281	TEST 3	86.25	92.35	1.5984E-07	Ironstone
03-281	TEST 3a	10.06	117.04	1.39734E-08	***Ignore***
03-281	TEST 2	98.45	104.54	3.21885E-10	ironstone
03-281	TEST 1	107.59	113.68	2.16749E-10	Siltstone

Exclude due to overlapped test 10(2)

Siltstone

Hole	Test	From	To	k	COMMENT
		m	m	m/s	
03-282	TEST 4 (Isolated)	24.38	42.67	1.20935E-06	Rhyolite
03-282	TEST 3 (Isolated)	42.67	111.25	1.20935E-06	Ironstone
03-282	TEST 2 (Isolated)	111.25	153.92	5.32439E-09	Dyke
03-282	TEST 1	153.92	254.19	8.46829E-10	Ironstone

Single Data for Rhyolite

Single Data for Dyke

Hole	Test	From	To	k	Rock Type
		m	m	m/s	
03-283	TEST 1	153.92	160.01	1.91546E-10	Ironstone
03-283	TEST 2	105.15	111.25	1.26144E-08	Ironstone
03-283	TEST 3	62.48	68.58	1.48169E-06	Ironstone
03-283	TEST 4	19.81	25.91	2.38942E-08	Ironstone
03-283	TEST 5	153.92	288.02	4.56043E-08	Ironstone
03-283	TEST 6	19.81	288.02	2.29796E-08	Ironstone

Ironstone: yellow colored

Depths are downhole

Data: For B Dersh.xlsx

Ironstone Packer Interval Transmissivity Data

T=kh

Hole	Test	From	To	k	COMMENT	T	h
		m	m	m/s		m2/s	m
03-281	Test 9	10.06	16.15	5.385E-08	Ironstone	3.28E-07	6.10
03-281	TEST 8	22.25	28.35	1.975E-10	Ironstone	1.20E-09	6.10
03-281	TEST 7	34.44	40.54	8.806E-11	Ironstone	5.37E-10	6.10
03-281	TEST 6	46.63	52.73	1.766E-10	Ironstone	1.08E-09	6.10
03-281	TEST 5	58.82	64.92	2.240E-10	Ironstone	1.37E-09	6.10
03-281	TEST 4	74.06	80.16	2.035E-10	Ironstone	1.24E-09	6.10
03-281	TEST 3	86.25	92.35	1.598E-07	Ironstone	9.74E-07	6.10
03-281	TEST 2	98.45	104.54	3.219E-10	ironstone	1.96E-09	6.10
03-282	TEST 3 (Isolated)	42.67	111.25	1.209E-06	Ironstone	8.29E-05	68.6
03-282	TEST 1	153.92	254.19	8.468E-10	Ironstone	8.49E-08	100.0
03-283	TEST 1	153.92	160.01	1.915E-10	Ironstone	1.17E-09	6.10
03-283	TEST 2	105.15	111.25	1.261E-08	Ironstone	7.69E-08	6.10
03-283	TEST 3	62.48	68.58	1.482E-06	Ironstone	9.03E-06	6.10
03-283	TEST 4	19.81	25.91	2.389E-08	Ironstone	1.46E-07	6.10
03-281	Test 10 (2)	10.67	117.04	2.629E-08	Open Hole, both rock types	2.80E-06	106.0
03-283	TEST 5	153.92	288.02	4.560E-08	Ironstone	6.12E-06	134.0
03-283	TEST 6	19.81	288.02	2.298E-08	Ironstone	6.16E-06	268.0

Oxfilet Input

OxFilet Deconvolution of Fracture Transmissivity - Ironstone

CELEBRATING 50 YEARS in 2010

```
**** OXFIL SIMULATION RESULTS ****

 Input File : airons~1.fil
 Fracture Network [Const]:     m=   1
 Min. Transmissivity:          1e-007
 Distribution option : LogNormal
Arith.(Mean,Dev): 6.79e-007  1.8e-005
Log10 (Mean,Dev):     -7.59      1.11
(# Frac/m, Length):  0.187       44.2

-------------------------------------

                  Simulation  FIL Data

# of Intervals           17         17
Mean               7.81e-006  6.43e-006
Std Dev            1.84e-005  1.99e-005
Log10 Mean             -6.23      -6.32
Log10 Std Dev           1.03      0.943
Skewness                2.61       3.32
Kurtosis                6.19       9.84
% Nonconductive         52.9       52.9

-------------------------------------

(Smirnov, % signif): 0.118        100
(Chi-Sqr, % signif):  8.39       59.1
```

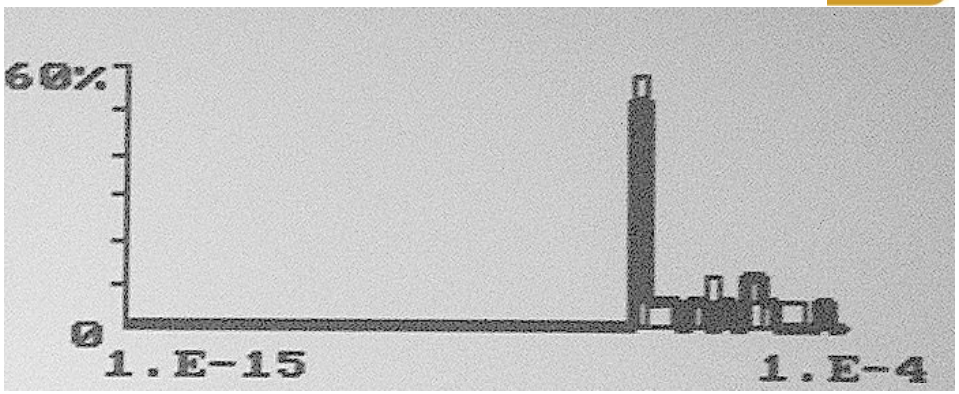

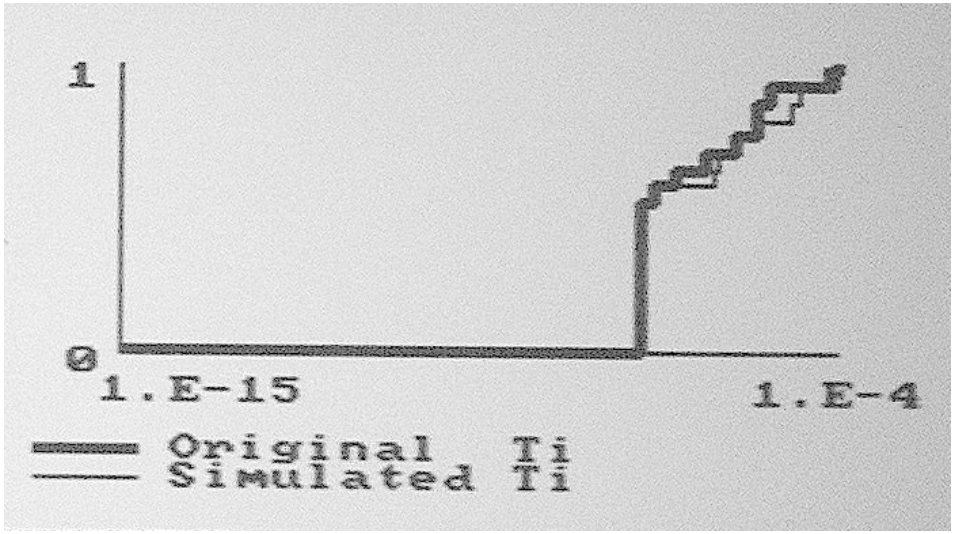

Avg P10 for Ironstone: 0.35

Golder Associates

Cubic Law vs Doe Law

- Confined Aquifer:
  Transmissivity $T = K\,e = c\,e^{1}$

  K – Hydraulic Conductivity m/s

  aperture e

- Real Rough Fracture with heterogeneous infilling "Doe Law" $T = c\,e^{2}$

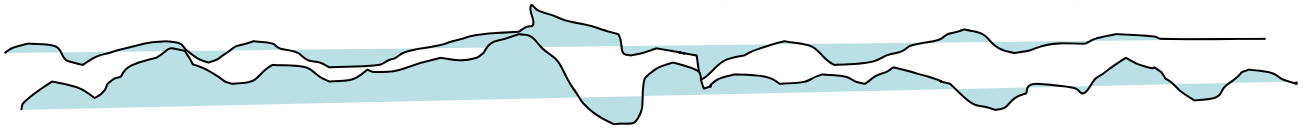

  aperture e

- Parallel Plates = Cubic Law $T = c\,e^{3}$, *c ≈ 1.e-6*

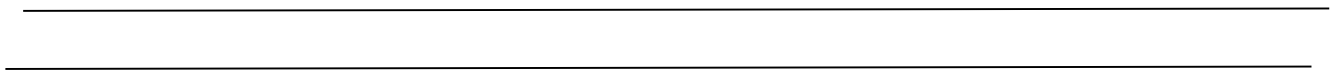

  aperture e

Correlations for
Transmissivity (T), Storativity (S), Aperture (e)

- $T=a_L \cdot L^{b_L}$ (1)

  where L(frac size) [m]=r$\sqrt{\pi}$, r is equivalent fracture radius

  a_L=5e-10, b_L=1.4

- $e=a \cdot T^{b}$ (2)

  where *a*=0.5, *b*=0.5 for TRUE block experiment "Doe Law"

- $S= a_s \cdot T^{b_s}$ (3)

  where a_s=0.46, b_s=0.5

From Dershowitz et al., 2003, "Correlations between Fracture Size, Transmissivity, and Aperture", in Soil and Rock America, Conference Proceedings, pp 887-891.

Evaluation of Equivalent Porosity

- **Evaluation of Transmissivity distribution and intensity P10c by OxFilet**
  - LogNormal (6.79e-7 m^2/s, 1.8e-5 m^2/s), T_{min}=1e-7 m^2/s
  - Total P10c=0.187 [1/m]
  - P10c with T_{min}=1e-7 m^2/s: P10c=0.056 [1/m]
- **Size – T correlation => Size Distribution is obtained from T distribution**
  - LogNormal (156m, 484m) , r_{min}=25m
- **Aperture and Storativity Correlation**
- **DFN Generation (without truncation for porosity evaluation)**
  - Intensity: P10c=0.187 [1/m] without truncation
  - Size: LogNormal (156m, 484m) without truncation
  - Orientation: Bootstrap with K=50
  - Frac Size => T => Aperture & Storativity (correlation equations are shown in previous slides)
- **Upscaling: Oda Tensors**

Discrete Fracture Network (DFN) Simulation for Upscaling (P_{10c})

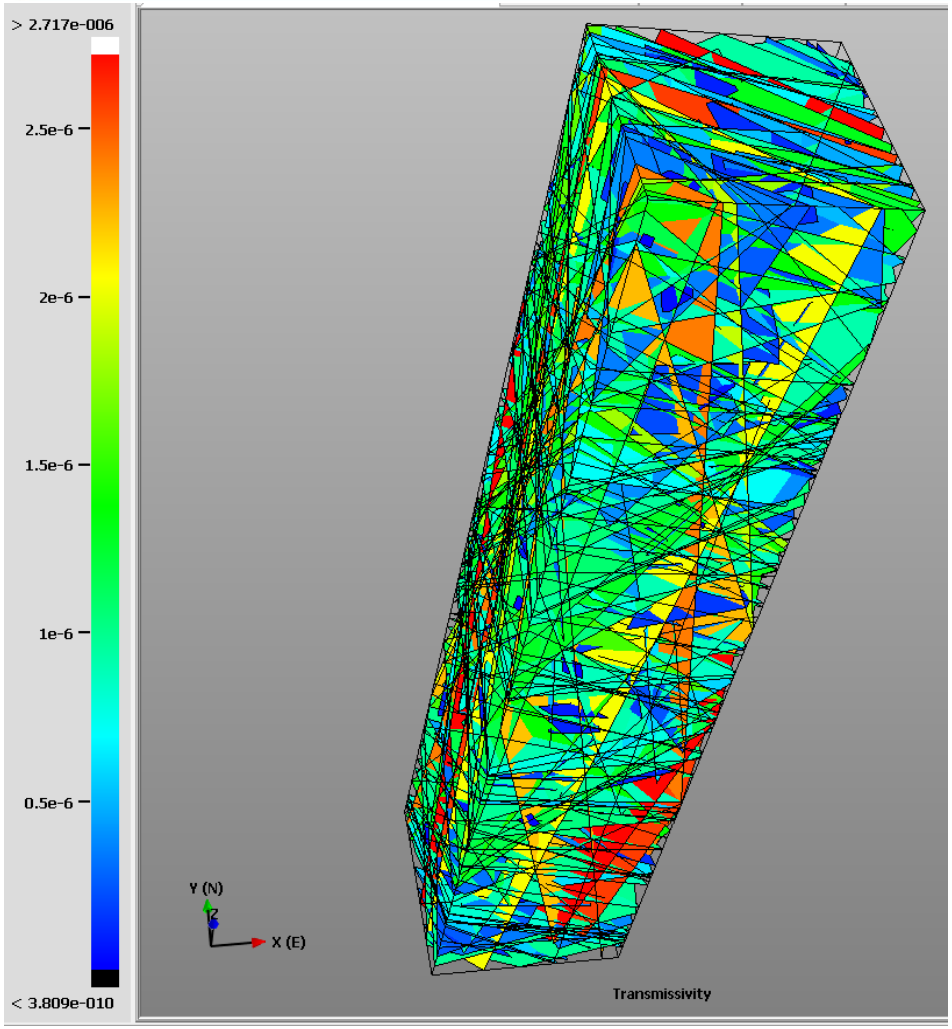

DFN Parameters

- Intensity: P10c=0.187 [1/m]
- Size: LogNormal (156m, 484m) without truncation
- Orientation: Bootstrap with K=50
- Frac Size => T => Aperture & Storativity (correlation equations are shown in previous slides)

Generation Region: 200mx200mx1000m

Orientation Comparison of Data & Simulation

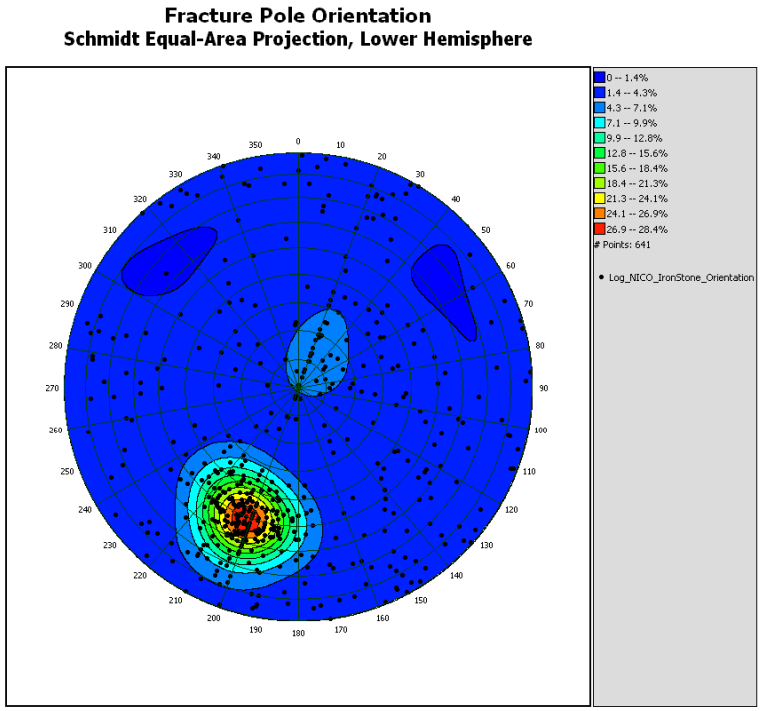

Data

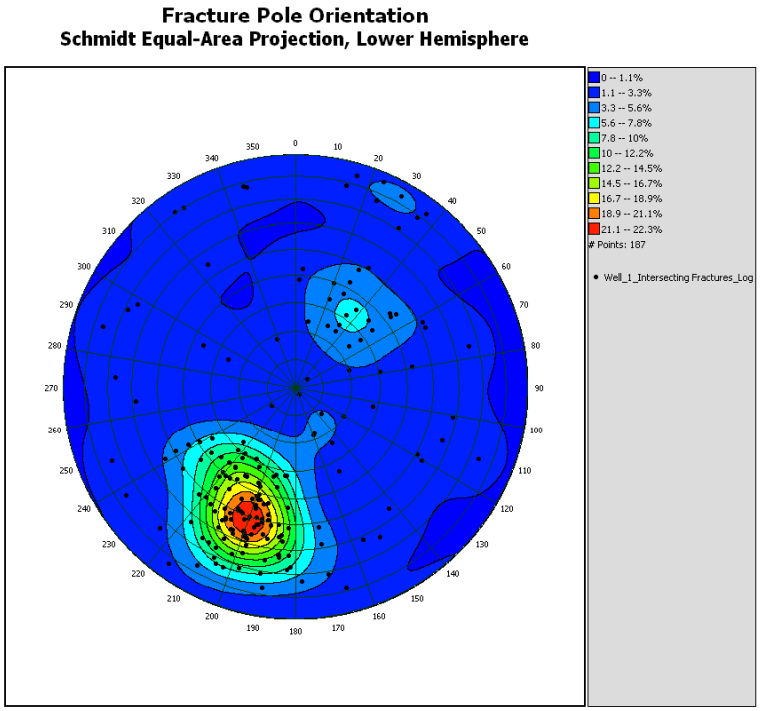

Simulation

Generated DFN Statistics

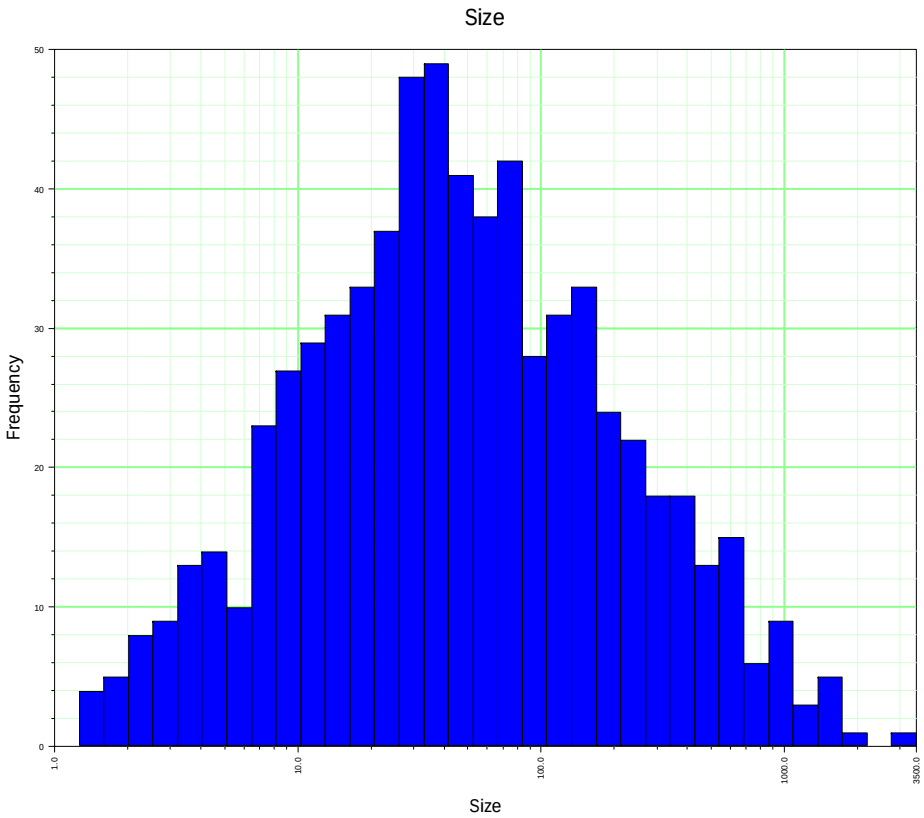

Equivalent Radius mean	133.46306
Equivalent Radius std dev	261.43793
Equivalent Radius min	0.46456005
Equivalent Radius max	3193.5467

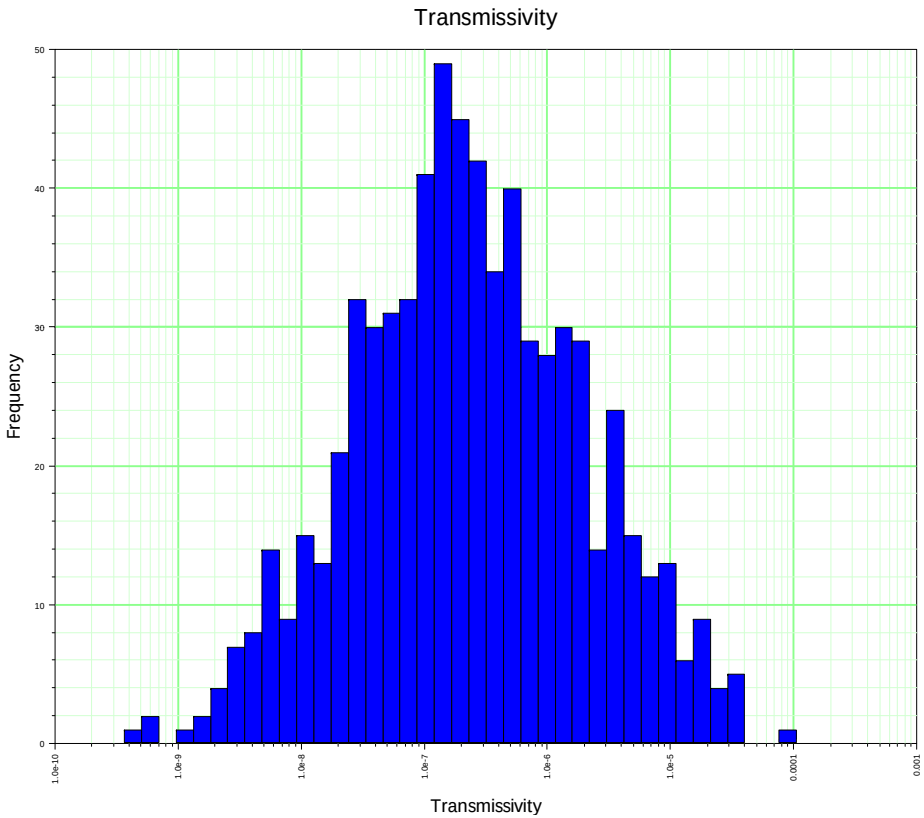

Transmissivity, mean	1.735345e-006
Transmissivity, std dev	5.4940567e-006
Transmissivity, min	3.809186e-010
Transmissivity, max	8.9733825e-005

Generated DFN Statistics

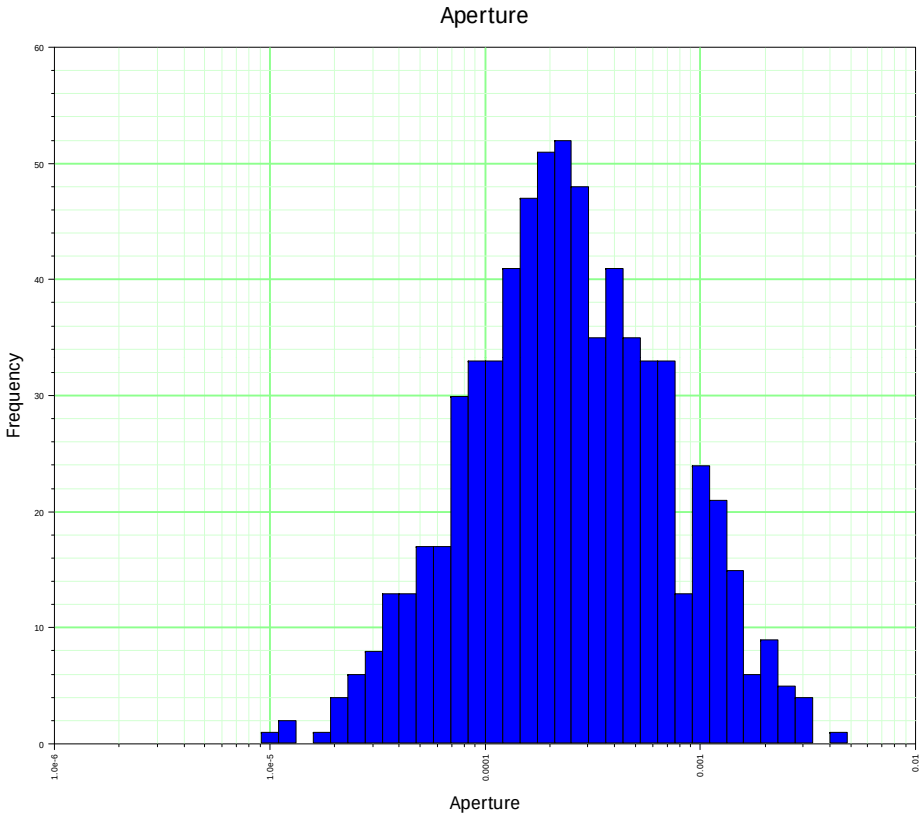

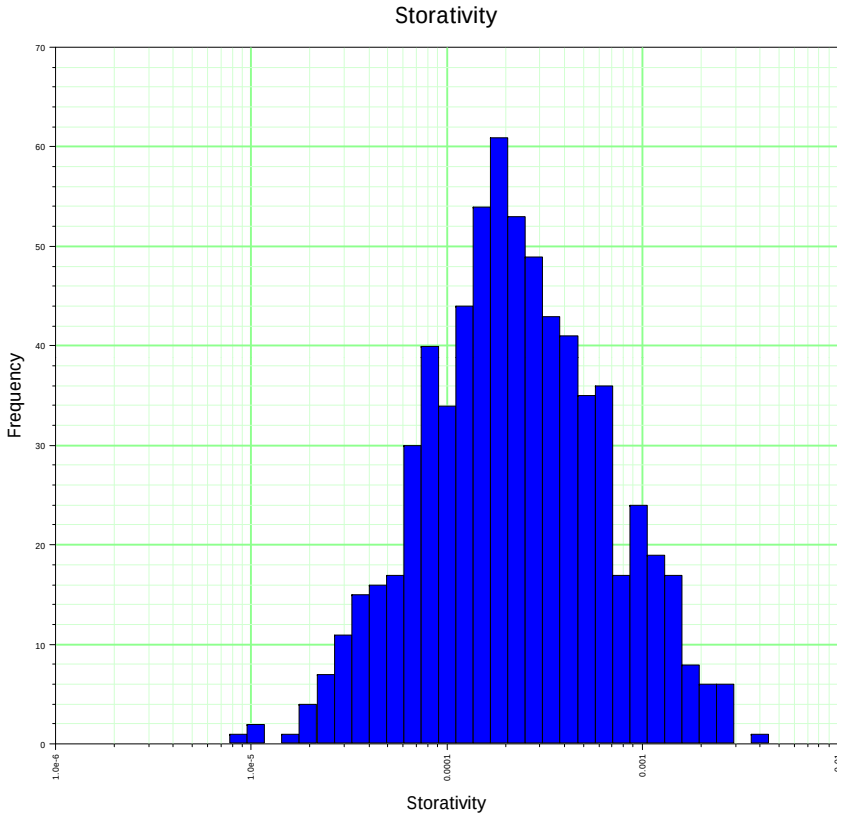

Aperture, mean	0.00041455455	Storativity, mean	0.00038139018
Aperture, std dev	0.00051221081	Storativity, std dev	0.00047123394
Aperture, min	9.758568e-006	Storativity, min	8.9778823e-006
Aperture, max	0.0047363969	Storativity, max	0.0043574851

Equivalent Porosity by P_{10c} without Truncation

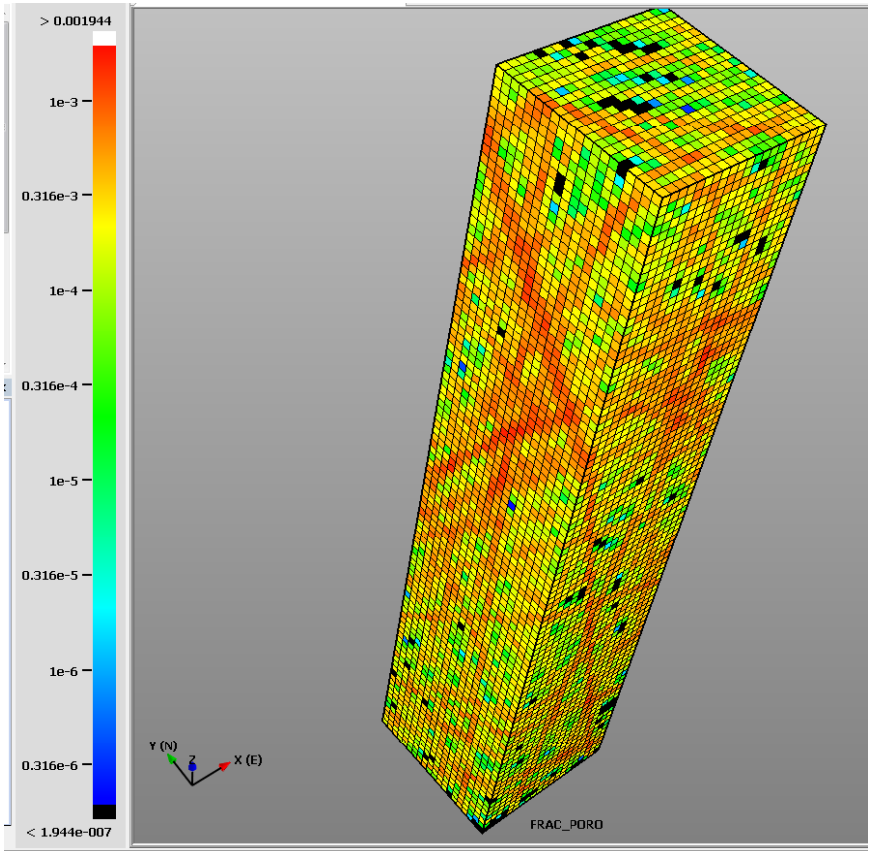

Max Porosity = 0.2%
Mean Porosity = 0.034%
SD Porosity = 0.024%

Questions on Formation Depths

Depth x Cos (65)

Depth given in Excel

Type	Depth	65 incline
Rhyolite	34	14
Rhyolite	47	20
Wacke&Schist	55	23
Wacke&Schist	895	378
Siltstone	898	380
Siltstone	944	399

282 proc.xls

Not Matched (similar for 281 and 283 wells)

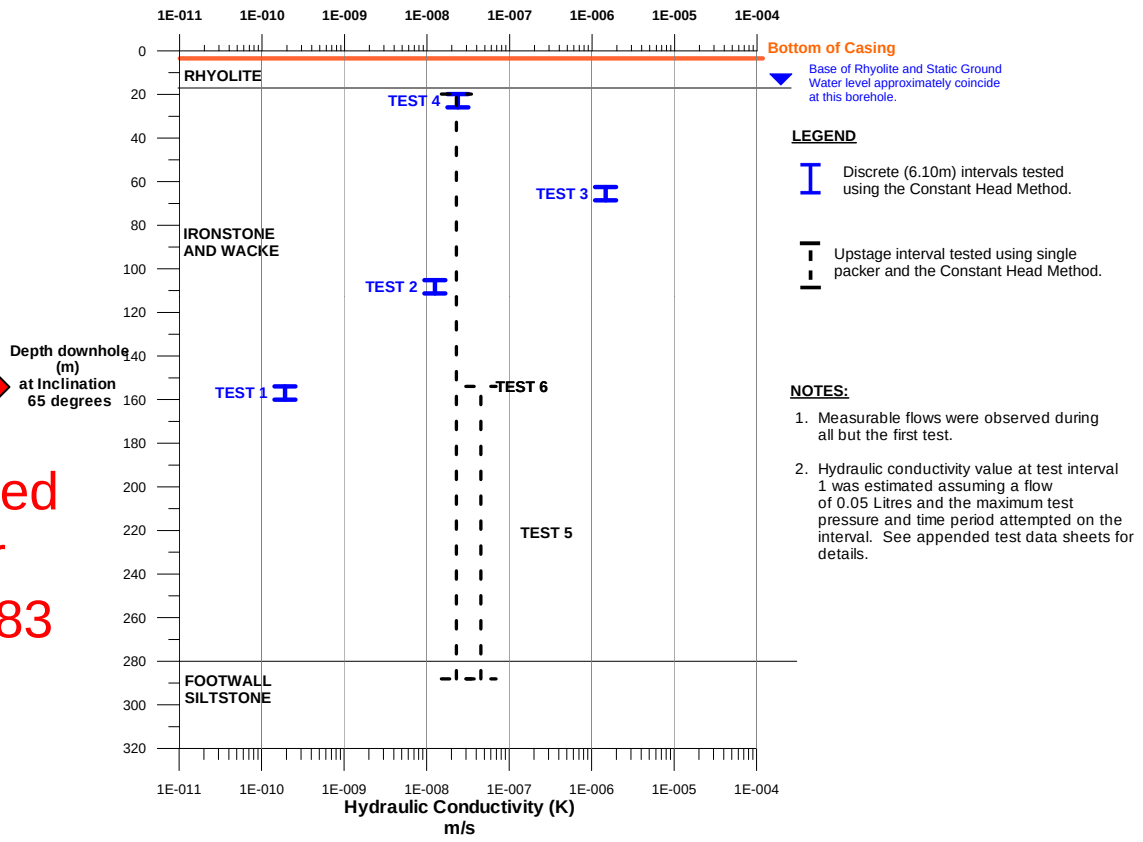

APPENDIX II
Response 9 Supporting Documents

DATE December 09, 2011 **PROJECT NO.** 11-1118-0066 (6000-TM-DOC009)

TO Tom Rinaldi / Chris Sharpe / Mike DeCarlo
Fortune Minerals Limited

CC Eugene Puritch, P.Eng. (P&E Mining Consultants Inc.)

FROM Luiz Castro / Marc Rougier / Chuck Steed **EMAIL** lcastro@golder.com, csteed@golder.com

FORTUNE MINERALS – SUMMARY REPORT ON GEOTECHNICAL STUDIES FOR THE OPEN PIT AND UNDERGROUND MINE DESIGNS FOR THE NICO PROJECT

This memorandum provides a summary of geotechnical stability analyses for the most recent geometries of the NICO project open pit and underground workings. It is intended as a support document to a NI43-101 Mining Report that P & E Mining Consultants Inc shall prepare by providing the results of analyses to November 2011.

This version, Revision A is provided to Chris Sharpe at Fortune Minerals for initial review.

Rev. No.	Date	Description	Prepared by	Reviewed by	
Rev. A	9 December 2011	Summary of Rock Engineering Stability Assessments	Luiz Castro	Marc Rougier	

1.0 INTRODUCTION

Fortune Minerals Limited (Fortune) retained Golder Associates Ltd. (Golder) to provide geotechnical support for the open pit and underground designs, NICO Project, a cobalt-gold-bismuth project in the Northwest Territories (NWT). Golder has provided ongoing support since 2003.

Through 2010 and to November 2011 Fortune Minerals and P & E Mining Consultants have been carrying out detailed design work to optimize location, number and size of the proposed underground workings relative to the ultimate pit shell and its intermediate phases, which had been finalized previously, in 2009. The updates in this document pertain specifically to the geotechnical analyses to support this mine design work, and can be found in Sections 7 to 9.

For completeness, in the Sections 2 to 6 of this memorandum summarize the geotechnical studies that have been carried out from 2003 to present that are pertinent to this update. .

2.0 MINE PLAN SUMMARY

Mining of the NICO ore zone will commence by extracting the richer ore zones using underground mining techniques during the first two to three years (year 3) of operations, followed by advancing an open pit to year 19. Starting in about mind-way through the mine life the pit will cross the existing underground openings.

The open pit is planned to be developed in three phases, identified as Phases 1 to 3, with Phase 1 sub-divided into Phases 1A and 1B, as illustrated on Plate 1 . The underground component will consist of mining stopes,

using upper blastholes and without backfill. As the open pit advances towards these open stopes, they will be backfilled with broken rock from the pit floor via drop raises or as they are exposed.

The ultimate open pit (Phase 3) will be about 1215 m long by 500 m wide and progress down to a maximum depth of about 240 m (pit floor at Elev. 240 m). Review of the slope geometries indicates that the maximum inter-ramp slope angles conform with the recommendations provided in the Golder 2004 Technical Memorandum on slope design. Review of the pit shell Phases 1 to 3 indicates maximum inter-ramp slope angles of 50˚.

The engineering geology investigations include: i) outcrop mapping by Fortune in 1998-2000, ii) geotechnical logging and rock strength testing of exploration core in 1998, iii) geotechnical logging of exploration core in 2003, iv) geotechnical logging and core orientation of holes oriented for slope design in 2003, and v) additional laboratory rock strength testing from definition drilling core obtained in 2010.

The pit slope designs indicated competent rock masses for which overall slope stability would not be a control on slope design for the anticipated slope heights. Consequently, pit slope designs were based on kinematic assessments, with assumed achievable bench geometries controlling slope the inter-ramp angle.

Underground geometries were based on the same engineering geology model. Analyses included i) semi-empirical stope design and ii) three-dimensional numerical modeling for evaluating the interaction of the open pit and underground openings.

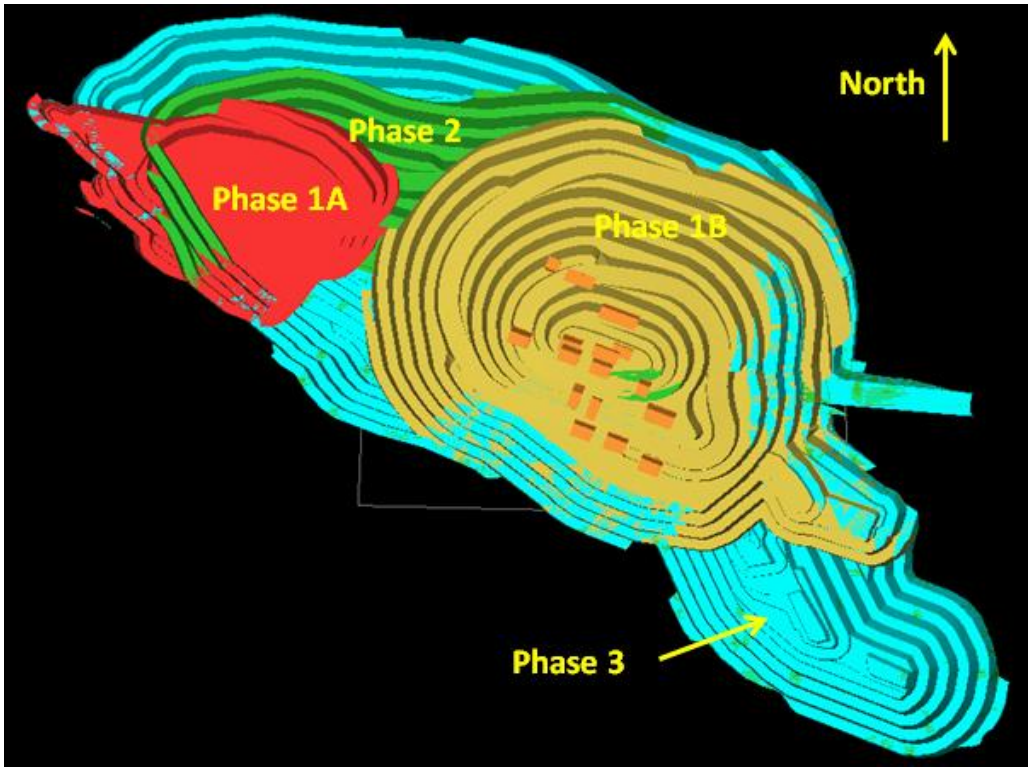

Plate 1: Schematic Representation of the phase pit shells and the 2011 planned underground stopes.

3.0 BACKGROUND

3.1 Geology

The NICO deposit is located in the southern part of the Great Bear magmatic zone, comprising Paleoproterozoic volcanic and plutonic rocks exposed from the Great Slave Lake in the south to Great Bear Lake in the north (Golder, 2004).

The oldest exposed rocks in the area are meta-sedimentary rocks. The NICO deposit is hosted in Snare Group sedimentary rocks that comprise a 3 to 5 km wide succession of siltstone, impure dolomite, subarkosic wacke and arenite (Goad et al., 1998).

Nico mine will be developed within the Black Rock Ironstone formation. This is a formation of meta-sedimentary rock with mineralization consisting of several closely stacked, stratabound, irregular, mineralized bearing lenses in altered siltstone and subarkosic wacke units. The formation dips at approximately 50° towards 030° (North-North East). The major mineralized zones to be mined in this formation consist of two sub-parallel lenses, approximately 40 m apart.

3.2 Discontinuous Permafrost Conditions

3.2.1 Regional

The NICO Project is located within the zone of discontinuous permafrost (Brown, et al, 2001). Within the discontinuous zone, permafrost occurs together with unfrozen ground. The permafrost zones are quite patchy depending on certain types of terrain, mainly peat lands. The annual thaw may reach a depth of 3 m and lenses of permafrost may form or disappear, depending on local short-term influences.

3.2.2 Local

EBA (EBA, 2005b) described the permafrost conditions specific to the area located south of the current proposed plant site location and west of the current proposed polishing pond location as follows (area referred as “South Basin” at that time):

> “The project site is located within a zone of discontinuous permafrost. Ice-rich organic soils were encountered overlying ice-rich perennially frozen glaciolacustrine and lacustrine clays and silts. Preliminary ground temperatures measured after thermistor installation suggests that the valley slopes of the proposed tailings dam abutments may be unfrozen.
>
> Valley bottoms and depressions are underlain by frozen deposits of glacial and post-glacial origin, and also contain meta-sedimentary rocks. The predominant vegetation along the valley floor consists of a thick *Sphagnum* moss cover with relatively dense stands of black spruce forest, with some stunted trees leaning in random directions as a result the cyclical frost heave that occurs in fine-grained perennially frozen soils.
>
> Unfrozen igneous rocks, predominantly volcanic in origin, comprise the surrounding hills and ridges, which overlie and intrude the meta-sedimentary rocks. The valley slopes, bedrock hills and ridges are sparsely vegetated with lodgepole pine, white spruce, white birch, and aspen. The hills and ridges exhibit well developed cryoplanation terraces (i.e. step-like features formed on exposed bedrock slopes due to intense frost wedging from snow banks) on their sides. Unconsolidated rock debris, boulders, and soil are found on the terraces and lower portions of the bedrock slopes.”

3.3 In Situ Stresses

There are no in-situ stress measurements for the NICO project. The *in situ* stress state was assumed to be represented by the following relationships (common regional properties within the Canadian Shield):

$\sigma_{H1} = 1.8 \times \sigma_v$ Azimuth: 025°

$\sigma_{H2} = 1.3 \times \sigma_v$ Azimuth: 115°

$\sigma_{v3} = 0.027 \times depth\ (m)$ Vertical

These gravitational in situ stresses were based off a datum (surface) elevation of 305 m. The major in-situ stress is assumed to be horizontal and acting along azimuth 025°, approximately normal to the strike of the orebody. The intermediate horizontal in-situ stress acts along azimuth 115°. The minor in-situ stress is equal to the vertical stress and increases with depth.

4.0 DRILLHOLE LOCATIONS MAP

The following is a brief summary of subsurface investigations at the NICO site, including selected drillholes for features other than the open pit and underground investigations, with notes on thermistor and piezometer installations, for completeness. The locations of these boreholes are shown on Figure 1:

- Golder 2003: Pit and underground geotechnical inclined diamond drilling investigations with stand pipe and thermistor completions.
- EBA 2004, Golder 2006 and Golder 2010: Shallow geotechnical investigations to determine overburden and top of bedrock conditions. Standpipe, vibrating wire piezometer and thermistor completions as noted.
- Fortune Minerals 2010: Condemnation drill holes, geotechnically logged, Co-Disposal facility area.
- Fortune Minerals 2010: Definition drillhole, geotechnically sampled for laboratory strength testing. This hole is sub-vertical and located adjacent to 03-281.

Additional 2010 drill holes, by EBA for in the area labeled Plant Site, for investigation of foundation conditions are not shown.

5.0 ENGINEERING GEOLOGY

The NICO site is located below the tree line in hilly, woody and muskeg terrain. Outcrop exposures on hills are common. Discontinuous permafrost has been found in low-lying and wetland areas.

The mineralized rock (black rock altered ironstone), the footwall rock (metamorphosed siltstones), hanging wall/cap rock (potassium-feldspar altered rhyolite) and feldspar dykes are all strong to very strong rocks with good to excellent RQD.

Both the black rock and the meta-siltstone have a low hydraulic conductivity, less than 10^{-8} m/s and less that 10^{-9}m/s with depth. The dykes and volcanic cap rocks have higher hydraulic conductivity, attributed to the greater degree of fracturing observed in these rocks.

Static groundwater levels within the proposed open pit and underground mine workings footprint follow topography. On the hills it is within 20 m of ground surface. At lower elevations it discharges, such as in the

"Bowl Zone" valley on the northwest end of the proposed site. This discharge feeds the Grid Stream and the Grid Ponds, and is naturally elevated in some metals, such as arsenic, due to the geochemistry of the bedrock.

The main rock type to be exposed in ultimate pit slopes (hanging wall and footwall) and in stopes will be the black rock ironstone. Review of surface mapping and oriented core data suggests that there is a consistent structural fabric within this unit, characterized by moderate to widely spaced joints dipping parallel to the 40° - 45° northeast dipping siltstone / black rock ironstone contact.

The meta-sedimentary rocks and the black rock ironstone unit are banded, and the peak orientation of discontinuities associated with the banding (foliation joints) is slightly steeper, dip 50°, than the contact dip between the footwall siltstone and the black rock ironstone. The spacing with which these banding / strata sub-parallel joints occur is moderate to wide (e.g. 0.5 m to 1.0m) in the oriented core; at drillhole 03-282, about 50 features with this orientation were intercepted over a borehole length of over about 210 metres. Similarly, at drillhole 03-283, about 190 features were intercepted over about 270 metres. The structural fabric within the siltstone and greywacke meta-sedimentary rocks is consistent with that in the black rock ironstone.

The structural fabric within the volcanic (altered rhyolite) cap rock, which will have limited exposures on upper benches of the ultimate pit slopes (no more than 20m vertically) is distinct from the underlying meta-sedimentary rocks. The volcanic rocks are blocky, with sub-vertical and sub-horizontal joint sets. They lack the footwall parallel bedding / foliation set prevalent in the meta-sedimentary rocks.

The four main geotechnical rock types at the Fortune site are described in Table 1.

Table 1: Geotechnical Units (after Golder, 2005a)

Rock Type (from oldest to youngest)	Typical Rock Strength	Typical Number of Joint Sets	Significant Exposures in Proposed Mine Workings
Footwall Siltstone ▪ Light grey, fresh, fine grained ▪ Bedded ▪ Dip 40-50 ° to the NE	R5 Very strong rock Average UCS = 97.5 ± 39 MPa	2 to 3 smooth to rough, planar	Non-mineralized. ▪ Host rock for bulk sample portal and decline (underground ramp). ▪ Footwall on a limited number of underground panels. ▪ Limited exposure on proposed Ultimate Slopes
Black Rock Ironstone (meta-sedimentary rock) ▪ Dip 40-50 ° to the NE ▪ Banded *Note that this unit is also referred to as Schist in previous reports.*	R3-R4 Medium strong to strong rock Average UCS = 109 ± 43.8 MPa	2 to 3 smooth to rough, planar	Mineralized (including sulphides and magnetite). Significantly heavier than other rock types. Arsenopyrite banding prevalent. ▪ Footwall and hanging wall for most ultimate pit slopes. ▪ Footwall, hanging wall, roof and backs of most underground panels.
Greywacke (meta-sedimentary rock) ▪ Dip 40-50 ° to the NE ▪ Bedded	R5-R6 Very strong to Extremely strong rock	2 to 3 smooth and planar	Non-mineralized. ▪ Overlies the black rock altered ironstone (schist) ▪ Also occurs as un-mineralized zones within the ironstone
Volcanics Rhyolite that is highly potassium feldspar altered, which colours the rock red.	R5 Very strong rock	3-4 smooth to rough, planar	Mineralized (but not economic). ▪ Overlies the greywacke as a discontinuous cap. ▪ Will be exposed on some open pit slopes,

Rock Type (from oldest to youngest)	Typical Rock Strength	Typical Number of Joint Sets	Significant Exposures in Proposed Mine Workings
These rocks form the hanging wall	Average UCS = 147 ± 73 MPa		mainly upper benches of the hanging wall ▪ Observed to be highly fractured at surface.
Dykes	R5-R6 Extremely strong rock Average UCS = 155 ± 46 MPa	3-4 smooth to rough, planar	Sub-vertical intrusions that cross-cut the host rocks. ▪ Potential exposures both on proposed ultimate pits and underground openings

Note that while the black rock ironstone is termed a schist in exploration and geological logs, in geotechnical terms the unit does not have a strong, closely spaced foliation that behaves as a preferred plane of weakness. Rather the unit is massive, with distinctive bands of arsenopyrite mineralization within the host black rock meta-sedimentary rock. Field observations and review of the failures from uniaxial strength testing indicate that the banding alignment (foliation) is not a preferred plane of weakness.

6.0 OPEN PIT DESIGN

Pit slope design recommendations were provided for the Feasibility Study in the Golder (2004) technical memorandum. The next paragraphs summarize the structural fabric assessment and rock slope stability analysis results and recommended bench configurations that were provided to the project.

6.1 Structural Data

Surface fault traces were mapped by Fortune geologists from the exposed outcrops and their locations were presented on Figures 1 and 2 of Golder November 2004 Technical Memorandum. Faults are typically healed to slightly broken at surface. Fault zones interpreted at depth are based on displaced geological or mineralization features. While some zones of broken core / low RQD are reported, these do not necessarily correspond to the locations of inferred faults in the borehole records. Most faults are considered healed based on this information.

Structural fabric data were obtained from nine oriented core holes (six drillholes logged by Golder-trained Fortune geologists, three logged by Golder in 2003) and from surface mapping carried out by Fortune in 1996-1997 and 1997-1998. The results of the detailed review of lower hemisphere, equal area projections of discontinuity populations obtained from both oriented core and surface mapping are summarized below.

6.1.1 Meta-sedimentary Rocks

The three (3) oriented core holes and surface mapping data indicate similar and consistent discontinuity population sets within the siltstone, the black rock altered ironstone and greywacke meta-sedimentary rocks, as shown in
Table **2**.

Peak orientations that parallel the footwall strike or the faults mapped by Fortune (Golder 2004 Technical Memorandum) and are considered most likely to be potentially continuous at the bench to multi-bench scale are labelled F1 to F3. The remaining peaks, considered more likely to be discontinuous at the bench to multi-bench scale are labelled J1 to J4. Potentially continuous discontinuities are of most concern with respect to control of multi-bench scale slope stability.

Orientation Bias

All core orientation data were obtained from geotechnically logged exploration or in-fill definition drillholes with southwest azimuths and, as such, have potentially not intercepted possible discontinuity sets dipping to the southwest (parallel to the drillholes). Those discontinuities, if they exist and were continuous and persistent, would control the slope configurations on the hanging wall of the open pit or could combine to form underground wedges. This ***possible*** footwall perpendicular "cross-joint" set is labeled J4 for purpose of these discussions.

The surface mapping data collected by Fortune in 1996 and 1997 agrees with the oriented core data, in that it captures the same set distributions as the oriented core, but also suggests, by the limited number of poles intercepted, that the J4 is set poorly developed and discontinuous. Additional surface mapping collected by Fortune in 1998 generated a similar distribution of peak orientations.

Table 2: Peak Orientations of Discontinuity Populations in the Meta-sedimentary Rocks (after Golder, 2005)

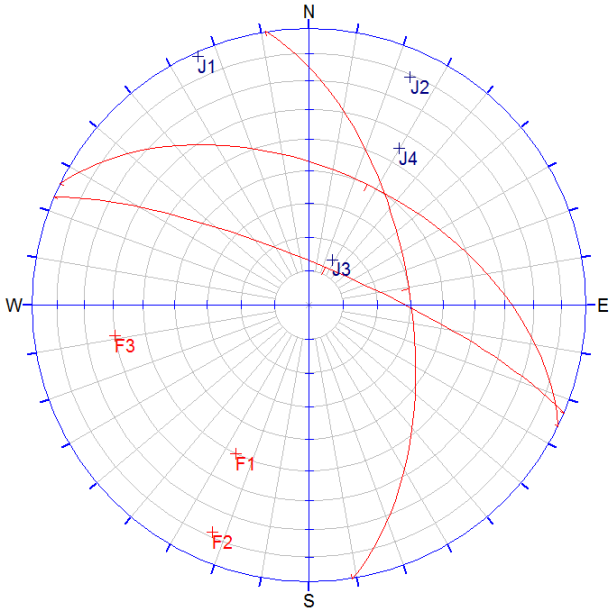

Set ID	Dip / Dip Direction (°)	Joint Set Description	% / Number
F1	50 / 026	parallel to sub-parallel to footwall	5.8 / 16
F2	78 / 023	sub-vertical sets striking parallel to the footwall,	2.2 / 6
F3	60 / 081	sub-vertical set striking perpendicular to the footwall.	2.2 / 6
J4	55 / 210	set dipping into footwall ***(based on surface mapping only)***	1.5 / 2
J3	15 / 207	Prevalent sub-horizontal set	3.4 / 10
J2	79 / 204	Minor joint set	2.2 / 6
J1	88 / 156	Minor joint set	2.2 / 6

Notes:

1. Sets in bold, **F1 to F3**, are considered most likely to be potentially continuous.

2. Because of the uniformity of oriented core hole azimuths and consistency of data in core holes and surface mapping, the peak orientations above were selected from a single borehole, 03-282, which was considered representative of the meta-sedimentary rock structural fabric for purposes of this assessment. Set J4, based on surface mapping, was added for completeness.

3. %/ Number generally refers to the pole concentration at the peak orientation of the set based on a 1% counting circle on a lower hemisphere equal area stereonet. For Set J4, this is based on a surface mapping database of 87 poles from 1997. For the remaining sets, the percent and number are based on O3-282 data, which had 284 poles.

6.1.2 Volcanics

The altered rhyolite cap rock and the intrusive dykes have a different structural fabric than the metasediments, as showin in

Table 3. Jointing in these rocks is characterized by steep sub-vertical sets and orthogonal, sub-horizontal sets, and the absence of the footwall parallel discontinuity set (i.e., F1 set) observed in the metasediments.

Table 3: Peak Orientations of Discontinuity Populations in the Volcanic Cap Rock (Potassium Feldspar Altered Rhyolite) (after Golder, 2005)

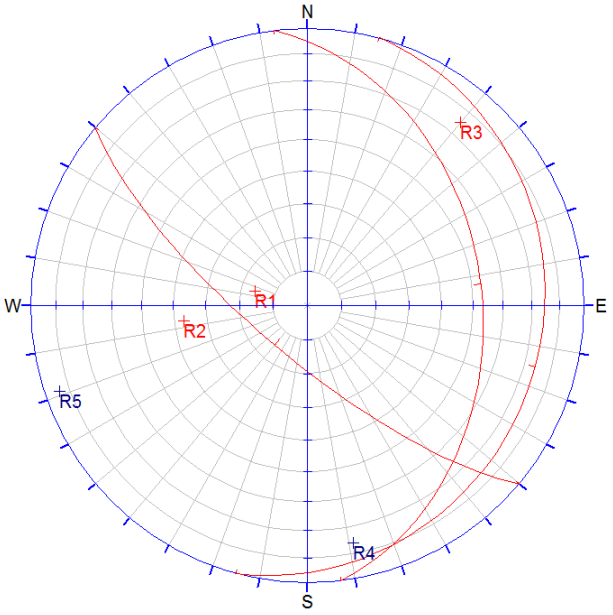

Set ID	Dip / Dip Direction (°)	Set Description	% / Number
R1	16 / 105	Peak orientations of lat Sets (dips < 38 degrees)	8.0 / 4
R2	37 / 083		8.0 / 4
R3	75 / 220	Steep set with strike sub-parallel to Footwall	3.4 / 2
R4	76 / 349	Sets R4 and R5 are orthogonal.	5.8 / 3
R5	84 / 071		4.6 / 3

Notes:

1. Sets in bold, R1 to R3, are considered most likely to be potentially continuous based on prevalence and / or fault and contact trends.

2. Because of the uniformity of oriented core hole azimuths and consistency of data in coreholes and surface mapping, the peak orientations above were selected from a single borehole, 03-282, which was considered representative of the cap rock structural fabric for purposes of this assessment

3. %/ Number refers to the pole concentration at the peak orientation of the set based on a 1% counting circle on a lower hemisphere equal area stereonet.

6.2 Slope Design Definitions

A pit slope has three major components: bench configuration, inter-ramp slope and overall slope, as illustrated on Plate 2. The bench configuration is defined by vertical bench separation (or bench height), catch berm width (or berm width) and bench face angle (or batter). The inter-ramp slope is formed by a series of uninterrupted benches and the overall slope is formed by a series of inter-ramp slopes separated by haul roads.

The inter-ramp angle (IRA) corresponds to the angle subtended by a line joining the toes of the benches on the wall and the horizontal. The overall slope angle corresponds to the angle formed by the line joining the toe of the lowest bench with the pit crest and the horizontal. Therefore, the incorporation of ramps onto a wall will result in a slope that has a shallower overall slope angle than the inter-ramp angle.

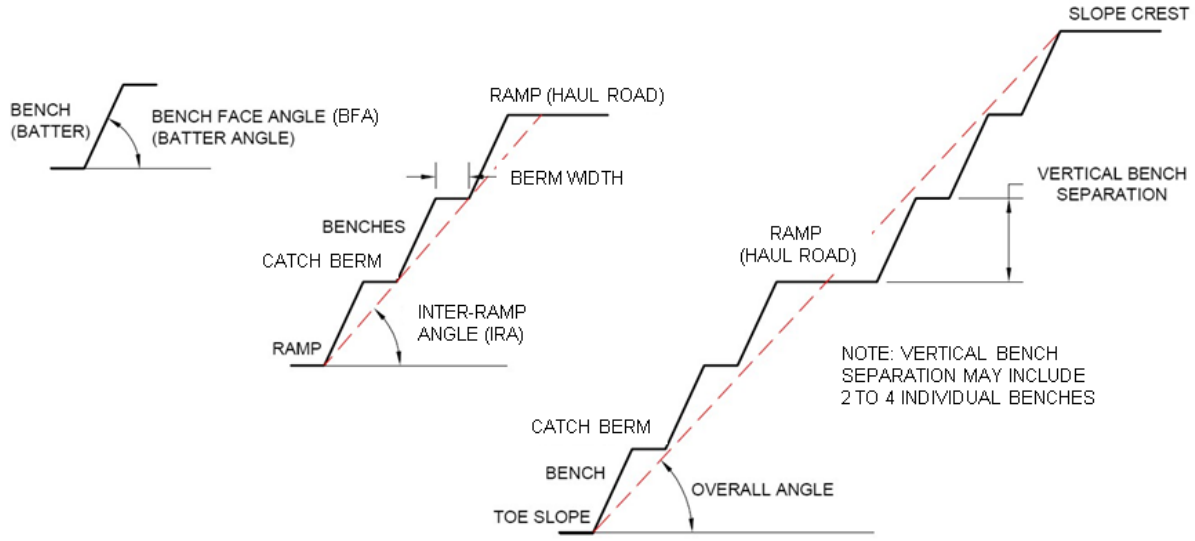

Plate 2: Schematic Representation of Bench Face Angle (BFA) and Inter-Ramp Angle (IRA) and Overall Slope Angle (OSA)

6.3 Kinematic assessment

The kinematic assessments indicate that bench configurations on some wall orientations will be controlled by potential planes and wedges involving structures assumed to be potentially continuous because they parallel the regional interpreted fault trends. For purposes of this assessment, a shear strength of phi=30 ° and cohesion of c=0 was assigned to all discontinuities. This strength is considered conservative given the variability of joint surface character. Joint surfaces showed minimal surface alteration.

Results of the kinematic assessment are summarized in the Golder 2004 Technical Memorandum. Plate 3 exemplifies the kinematic analysis for the footwall slopes considering the rock mass fabric for the meta-sedimentary rocks.

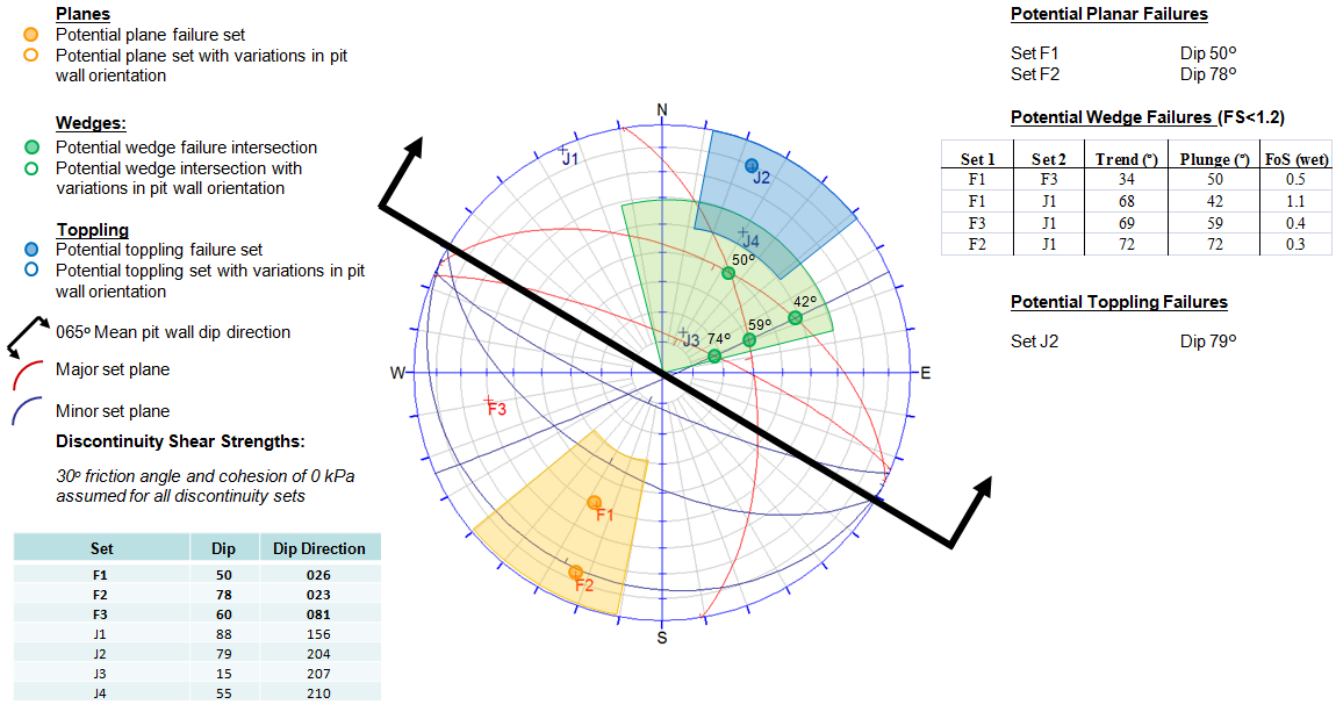

Plate 3: Example of kinematic analyses for the FW wall (slope dip direction of 30°), considering the rock mass fabric for the meta-sedimentary rocks.

6.4 Slope Design Recommendations

The following are the slope design recommendations for ultimate pit slopes in rock, presented by wall dip direction for the three design sectors.

Bench geometries were developed assuming adequate dewatering of the rock slopes will have been achieved due to exposure and blasting. Horizontal drains (e.g., 50 mm to 76 mm diameter, open holes, drilled at approximately 10° upwards and to a about 50 m depth into the walls) may be required in localized areas if persistent seepage is noted during pit operations or if adequate pore water depressurization is not achieved. If necessary, these holes can be lined with 25 mm perforated/slotted PVC pipe to maintain open drillholes and free draining conditions.

Recognizing the extreme cold temperature at the NICO site, water flowing from these drainholes should be manifolded into pipes to the sumps, in order to prevent face freeze-up in the winter months. The drainholes will also help reduce icing up of the slope face in the winter, which could lead to ice-falls.

Implementation of proper controlled blasting techniques on all benches will improve the probability of success in achieving the recommended bench scale and inter-ramp design parameters.

Table 4: NICO Open Pit Slope Design Recommendations (after Golder, 2004)

Slope Dip Direction	Rock Type	Maximum Vertical Bench Separation (m)	Bench Face (or Batter) Angle (°)	Minimum Berm Width (m)	Maximum Inter-ramp Angle (°)
020° to 030° FOOTWALL	Meta-sedimentary Rock	15m	75	8.5	**50°** [1,2]
	Volcanic Cap Rock[3]	15m	75	8.5	**50°**
200° to 210° HANGINGWALL	Meta-sedimentary Rock	15m 20m	75 75	8.0 9.0	**51°** [4,5] to **54°** [4,5]
	Volcanic Cap Rock[3]	15m	75	8.0	**51°**
ENDWALLS	All rock types	15m	75	8..5	**50**[6]

Notes:

1. Actual Inter-ramp and overall slopes on the footwall slope will most often be less than 50 degrees, controlled by the local dip of the stratabound mineralization zones (see cross-sections) and placement of ramps.
2. Bench face angle controlled by set potential for planar failures involving set F2, dip 78°, inter-ramp slope angle controlled by set F1 (foliation), mean dip 50°.
3. Some slopes will expose significant amounts of volcanic rocks on upper benches. While the kinematics indicate that the structural fabric in the volcanic rocks is more favourable and that steeper slopes could be achieved, surface exposures are blocky and broken, and ravelling can be expected on excavated slopes. For this reason a steeper design for slopes in volcanics is not presented. Initial operating experience with volcanic slopes will determine whether ravelling will require modified blasting practices or shallower inter-ramp angle.
4. Bench face angle on the hanging wall will controlled by potential for planar failures involving set J2 (dip 79°). Inter-ramp angle on the hanging wall controlled by potential for planar instability involving set J4 (dip 55°). Should the F2-J2 wedge be prevalent (plunge 51°) the inter-ramp angle will require flattening from 54° to 51°.
5. The hanging wall slope design is considered aggressive. It is recommended that in order to optimize the hanging wall design, ramps be placed on the footwall, which will be mined at the flatter angles conforming to the dip of the stratabound mineralization zones.
6. Potential for toppling failure, particularly on the hanging wall, is not considered a control on bench design given the moderate to wide spacing of joints. Localized toppling instabilities may still occur. Should toppling failure be problematic, a mid-bench catch-berm may be required.
7. Potential wedge F1-F3, plunge 50° will control slope design on southeast dipping end walls. Northwest dipping end walls have been assigned the same recommended configuration for consistency.
8. Where the open pit slope is greater than 90m to 120m high without being crossed by a ramp or wider berm, it is recommended that extra wide (allow 12m to 15m) geotechnical bench be placed on the slope as a conservative measure. This bench is intended to provide additional catchment against potential rock fall hazard. The width has not been designed, the 12m to 15m is recommended based on experience.

6.5 Pit and Underground Seepage Estimates

Open pit operations may only begin after several years of underground mining development which will significantly dewater the open pit zone. Groundwater seepage into the open pit is expected to be very low, as a result. Combined pit and underground seepage is estimated to be on the order of 100 m^3/day throughout the life of mine. This will be verified as excavation and initial mining occurs. These estimates are based on in-situ measurements of hydraulic conductivity, observed seepage into the decline and closed form and numerical modeling. These investigations are summarized in Golder 2010c..

7.0 UNDERGROUND MINE

The stope design and the interaction of the open pit and underground stopes were discussed in the Golder (2005) and Golder (2010a and b) technical memoranda and through exchange of emails with the P& E project team.

Through these interactions, the planning for the underground mine has changed. Recognizing that the major mineralized zones consisted of two sub-parallel lenses, which were approximately 40 m apart, the initial mine planning considered the excavation of sub-parallel series of transverse stopes that would be located near the hanging wall (labeled as the MZ stopes) and in the footwall (labeled as LZ stopes). The stopes would not be backfilled during the underground mining and would be separated by sill and rib pillars, which would be recovered later on during the open pit mining.

As described in Section 1.0, the plan has always being to backfill the stopes with broken rock from the pit floor via drop raises or as they become exposed, with the progressing on the open pit excavations through the ore body.

Subsequently in 2011, the number of stopes has been substantially reduced, now accounting for only 315,000 tons The current plan is to mine selected longitudinal and transverse stopes and minimize their potential impacts on the future open pit mining.

Since these stopes will not be backfilled during the underground mining, they were designed to be mined with dimensions that would ensure stability while they remained open.

The next sub-sections present the steps for the stope design used for the NICO project.

7.1 Semi-Empirical Open Stope Stability Analyses

An assessment of potential stoping dimensions has been carried out using the Mathews/Potvin stability method (Mathews et al., 1981; Potvin, 1988) for open stope stability. Input requirements for the method include assessment of rock mass quality for the various walls of the stope, assessment of the stress concentration within the excavated stope walls and assessment of the orientation of typical joint sets within the rock mass.

The following assumptions have been applied to this assessment (Golder 2005 Technical Memorandum):

- The ore body has a strike length of approximately 1200 m (based on current ore body interpretation) and dips at approximately 50°. A median ore body width of 25 m in the transverse direction has been considered and it is assumed that any stoping will be carried out in this direction.
- Consideration was given to physical limitations such as equipment size and drilling accuracy (drillhole deviance). As a result the excavation dimensions considered initially a strike span of 15 m to provide enough room for equipment movement and a sublevel height of 25 m to minimize drillhole deviance.
- Rock mass qualities are based on the summary results from the 1998 and 2003 core logging and strength testing exercises. The metasediments identified at the deposit will comprise the back, sidewalls, and hanging wall of all stopes.
- The quality of rock masses can be classified as fair ($3 \leq Q' \leq 10$) for the -1 std case and good ($10 \leq Q' \leq 40$) for the mean and +1 std case. As the major controlling factor within the ratings for the rock mass classification is the strength of the rock unit, the metasediments can be generally simplified as strong

(50MPa < UCS < 100 MPa) with an assumed uniaxial compressive strength of 75 MPa, to take into account some of the variation in the rock strength (note that the average UCS = 109 ± 43.8 MPa).

- Rock mass for the Black Rock Ironstone was assessed as having on average good quality (10 ≤ Q' ≤ 40) with an average Q' of 14.9 (Golder, 2005). Considering a standard deviation of ±1, the Q' values equate to an approximate GSI range of 64 to 72, with an average of 68.
- The assumed in-situ stress conditions are provided in Section 3.3. Three-dimensional numerical modeling was carried out using the MAP3D© program to estimate the induced stresses in the induced stresses were calculated at the mid points of the back, the side wall, and the hanging wall. For the stability assessment the stopes were grouped as being located at depths above and below a depth of 150 m, which was used for general reference.
- Critical discontinuity set orientations were extracted from the summary stereonets produced from the oriented core and surface mapping program (see Tables 2 and 3).

In the Mathews/Potvin stability graph, rock quality (reflected by the modified stability number N') is related to stope geometry (reflected by the hydraulic radius, HR). Several curves are included in this graph to divide the chart into different zones, referred to as stable, transitional and caving zones for unsupported and supported stope walls, as depicted on Plate 4.

The stope hydraulic radius HR corresponds to the area divided by the perimeter of the exposed stope surface analyzed, as follows:

$$HR = \frac{wxh}{2(w+h)}$$

Where w and h refer to the width and height of the stope wall.

The N' stability number is assessed as follows:

$$N' = Q' \times A \times B \times C$$

Where Q' is the rock mass quality, and A, B, and C are adjustment factors based on the stress conditions, orientation of structures, and most likely mode of failure respectively.

The intersection of the stability number (N') with the stable zone / unsupported transition zone curve, corresponding to the maximum sized unsupported opening considered to be "stable" (i.e., minimum dilution). The hydraulic radius (HR) corresponding to this stable zone / unsupported transition zone curve was recommended for the design of the stopes, recognizing that they will be developed by using upper blastholes and without the possibility of installing ground support on the back or sidewalls.

The mid point within the unsupported transition zone of the Mathews chart corresponds to the average maximum sized opening that lies in the transition between no support required and support required. The HR for this mid-point has also presented for comparison purposes.

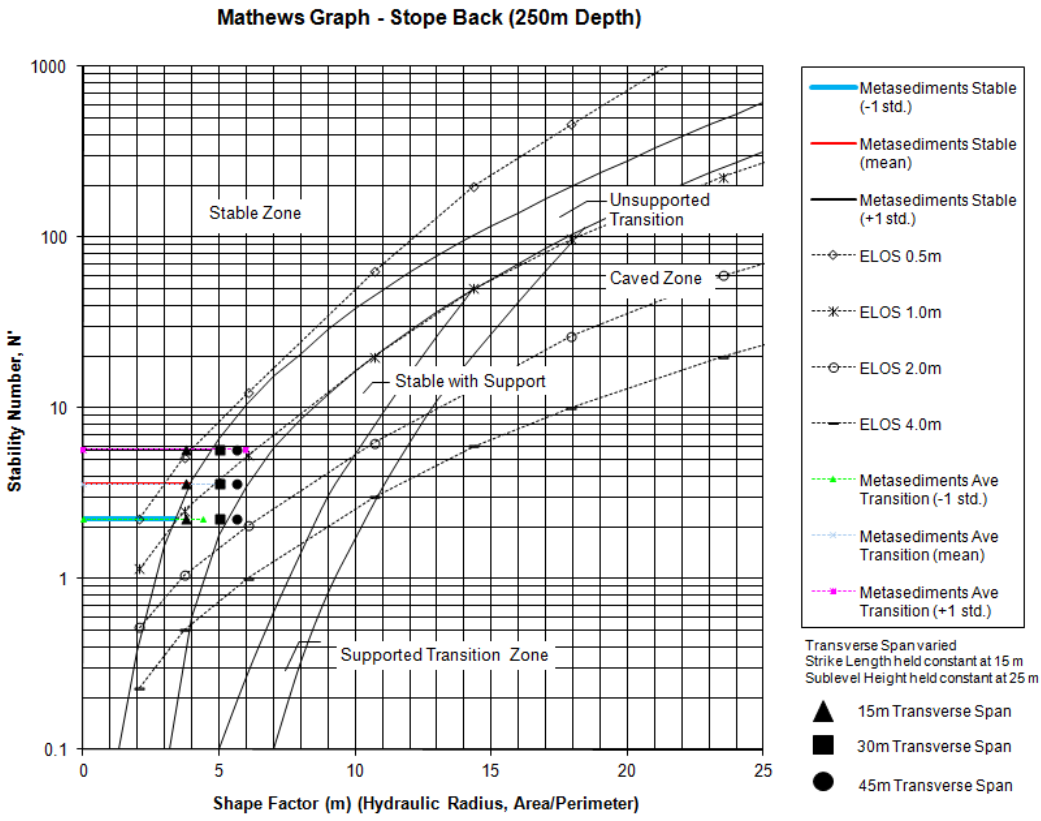

Plate 4: Application of the Mathews/Potvin open stope stability graph to the back of a stope located at a depth of 250 m.

7.1.1 2005 Stope Stability Assessment

A preliminary stope stability assessment was carried out using Mathews/Potvin Stability Graph and the results were presented in the Golder (2005) Technical Memorandum. This initial assessment estimated the following:

Table 5: Preliminary Values of Maximum Hydraulic Radius (HR) for Unsupported Walls

DEPTH (m)	HR BACK (m)	HR FOR THE HW (m)	HR FOR THE SIDEWALLS (m)
100	4.3	7.5	6.8
250	3.9	7.5	5.4

Based on these hydraulic radius, HR values and considering that the stopes would not be supported, for the Scoping Level Study, it was recommended for the Scoping Level Study that the stopes have a strike length of 12 m, stope height of 25 m and stope length (in the transverse direction) of 30 m to 35 m, creating HR values for back = 4.3 to 4.5 m, HR for HW = 4.1 m, and HR for sidewalls = 6.8 m to 7.3 m. In addition, 12 m wide sill and rib pillars were recommended to be used between the LZ (footwall) and MZ (hanging wall) series of stopes.

7.1.2 2010 Stope Stability Assessment

For the Feasibility Study, additional stability analyses were carried out to assess the induced stresses generated as a result of interaction of the underground and open pit excavation. Three-dimensional numerical modeling was carried out using the boundary element code MAP3D©. Based on the numerical results, Table 6

Table 6 provides the revised values of hydraulic radius recommended for the stope design (i.e., see values highlighted in grey).

Values of hydraulic radius were calculated for the geometries of the stopes provided by P & E. The calculated HR values were then compared to those shown in Table 6. The stope geometries that initially exceeded the recommended HR values were highlighted and re-designed in order not to exceed the 'maximum stable unsupported' value of HR.

Table 6 and Table 7 contain the 2011 planned stope dimensions and the calculated HR values for the back and walls, respectively. As observed, these stope dimensions (i.e., back and hanging walls) are within the recommended HR values and systematic ground support (e.g., cable-bolts) is not anticipated to be required.

Table 6: Revised Values of Maximum Hydraulic Radius (HR) for Unsupported Walls

Rock Type	Q'	A	B	C	Calculated N'	HYDRAULIC RADIUS [1]	
						MAXIMUM STABLE UNSUPPORTED (m)	AVERAGE UNSUPPORTED TRANSITION (m)
Depth < 150 m							
BACK STABILITY							
Metasediments (-1 std.)	**9.3**	0.90	0.5	2	8.4	5.1	6.8
Metasediments Stable (mean)	**14.9**	0.90	0.5	2.0	13.4	6.1	7.9
Metasediments Stable (+1 std.)	**24.0**	0.90	0.5	2.0	21.6	7.3	9.2
HW STABILITY							
Metasediments (-1 std.)	**9.3**	1.00	0.2	4	7.45	4.9	6.5
Metasediments Stable (mean)	**14.9**	1.00	0.2	4	11.94	5.9	7.6
Metasediments Stable (+1 std.)	**24.0**	1.00	0.2	4	19.16	7.0	8.9
SIDEWALL STABILITY							
Metasediments (-1 std.)	**9.3**	0.55	0.5	4.0	10.2	5.5	7.2
Metasediments Stable (mean)	**14.9**	0.55	0.5	4.0	16.4	6.6	8.4
Metasediments Stable (+1 std.)	**24.0**	0.55	0.5	4.0	26.3	7.9	9.8
		Depth > 150 m					
BACK STABILITY							
Metasediments (-1 std.)	**9.3**	0.45	0.5	2.0	4.2	4.0	5.4
Metasediments Stable (mean)	**14.9**	0.45	0.5	2.0	6.7	4.7	6.3
Metasediments Stable (+1 std.)	**24.0**	0.45	0.5	2.0	10.8	5.6	7.3
HW STABILITY							
Metasediments (-1 std.)	**9.3**	0.50	0.2	4.0	3.7	3.8	5.2
Metasediments Stable (mean)	**14.9**	0.50	0.2	4.0	6.0	4.5	6.1
Metasediments Stable (+1 std.)	**24.0**	0.50	0.2	4.0	9.6	5.4	7.1
SIDEWALL STABILITY							
Metasediments (-1 std.)	**9.3**	0.30	0.5	4.0	5.6	4.4	5.9
Metasediments Stable (mean)	**14.9**	0.30	0.5	4.0	9.0	5.3	6.9
Metasediments Stable (+1 std.)	**24.0**	0.30	0.5	4.0	14.4	6.3	8.1

[1] Recommended range of HR values are highlighted in grey.

Table 7: Hydraulic Radius Values for 2011 Planned Stopes – Back Dimensions

Stope #	Tonnes	Depth (m)	Back Strike Length (m)	Width (m)	Area (m^2)	Perimeter (m)	Hydraulic Radius, HR (m)	Target HR
Stope 1	16,637	124	35	15	525	100	5.3	6.1
Stope 2	7,222	124	15	15	225	60	3.8	6.1
Stope 3	14,459	90	30	15	450	90	5.0	6.1
Stope 4	21,166	110	45	15	675	120	5.6	6.1
Stope 5	17260	170	25	15	375	80	4.7	4.7
Stope 6	17,517	150	25	15	375	80	4.7	4.7
Stope 7	9,035	185	20	15	300	70	4.3	4.7
Stope 8	14,040	>150	45	10	450	110	4.1	4.7
Stope 9	5,909	>150	20	10	200	60	3.3	4.7
Stope 10	17,347	>150	25	15	375	80	4.7	4.7
Stope 11	9,575	>150	15	15	225	60	3.8	4.7
Stope 12	16,149	>150	25	15	375	80	4.7	4.7
Stope 13	16,498	>150	25	15	375	80	4.7	4.7
Stope 14	16,173	>150	25	15	375	80	4.7	4.7
Stope 15	22,765	<150	35	15	525	100	5.3	6.1
Stope 16 (RL190S2)	13,938	<150	24	12	288	72	4.0	6.1
Stope 17 (RL190S1)	13,382	<150	20	12	240	64	3.8	6.1
Stope 18	20,800	<150	25	15	375	80	4.7	6.1
Stope 19	15,133	<150	25	15	375	80	4.7	6.1
Stope 20	15,271	<150	25	15	375	80	4.7	6.1
Stope 21	14,674	<150	25	15	375	80	4.7	6.1

Table 8: Hydraulic Radius Values for 2011 Planned Stopes – Sidewall Dimensions

Stope #	Tonnes	Depth (m)	Stope Height (m)	Width (m)	Area (m2)	Perimeter (m)	Hydraulic Radius, HR (m)	Target HR
Stope 1	16,637	124	11	35	385	92	4.2	5.9
Stope 2	7,222	124	10	15	150	50	3.0	5.9
Stope 3	14,459	90	12	30	360	84	4.3	5.9
Stope 4	21,166	110	15	45	675	120	5.6	5.9
Stope 5	17260	170	17	25	425	84	5.1	5.3
Stope 6	17,517	150	17	25	425	84	5.1	5.3

Stope #	Tonnes	Depth (m)	Stope Height (m)	Width (m)	Area (m2)	Perimeter (m)	Hydraulic Radius, HR (m)	Target HR
Stope 7	9,035	185	15	20	300	70	4.3	5.3
Stope 8	14,040	>150	11	45	495	112	4.4	5.3
Stope 9	5,909	>150	13	20	260	66	3.9	5.3
Stope 10	17,347	>150	18	25	450	86	5.2	5.3
Stope 11	9,575	>150	18	15	270	66	4.1	5.3
Stope 12	16,149	>150	18	25	450	86	5.2	5.3
Stope 13	16,498	>150	18	25	450	86	5.2	5.3
Stope 14	16,173	>150	18	25	450	86	5.2	5.3
Stope 15	22,765	<150	18	35	630	106	5.9	5.9
Stope 16 (RL190S2)	13,938	<150	20	12	240	64	3.8	5.9
Stope 17 (RL190S1)	13,382	<150	20	12	240	64	3.8	5.9
Stope 18	20,800	<150	22	25	550	94	5.9	5.9
Stope 19	15,133	<150	16	25	400	82	4.9	5.9
Stope 20	15,271	<150	16	25	400	82	4.9	5.9
Stope 21	14,674	<150	16	25	400	82	4.9	5.9

7.2 Stope Backfilling

Various options of backfilling for the underground stopes were discussed in detail during design meetings. Stopes beneath the direct excavation of the pit are required to be backfilled as the pit floor approaches them, in order to provide a secure working floor. As the plan is to develop stopes that will be stable, initial backfilling from underground will only be carried out on the proposed stopes.

It is anticipated that as the footprint of the pit floor will be bigger than that of the underground stopes sufficient backfilling material should be available. To supplement backfilling if required, low grade waste rock from surface operations can be used.

Stopes located immediately underneath the planned pit ramp must be fully backfilled prior to advancing the ramp. These stopes will likely require drop raises to be drilled from the surface for placement of muck, and the stopes would be tightly filled prior to advancing the ramp over them. Fill utilized for tight filling the tops of these stopes could consist of a slurry muck (or cemented rock fill) or lean mix concrete. Such mixes have been used for stope backfill in other similar projects utilizing a mix design as shown below in Table 9.

Table 9: Example of Slurry and Lean Mix Concrete Design

Type of Mix	Water (kg/m^3)	Cement (kg/m^3)	Coarse Aggregate (kg/m^3)	Fine Aggregate (kg/m^3)	Slump (mm)	28-Day Compressive Strength (MPa)
Slurry Muck	114	132	1650	412 (20%)	40 ± 10	15
Lean Mix Concrete	210	100	1040	1130	170 ± 20	1

8.0 INTERACTION OF OPEN PIT AND UNDERGROUND OPENINGS

A 3-D numerical model of the underground and surface mine workings was constructed and used to determine the magnitude of the induced stresses during the staged mining of the underground and open pit. Map3D©, a boundary element analysis code, was used for the stress analyses. Results were presented in the Golder (2010a and b) Technical Memoranda.

The model considered an average GSI of 68 (see Section 7.0) and a uniaxial compressive strength (UCS) of 75 MPa. All rock mass properties were modelled assuming elastic conditions.

The geometries of the MZ and LZ stopes and Phase 3 pit shell were supplied in 2010 by P&E as AutoCAD drawings, as illustrated on Plates 5 and 6.

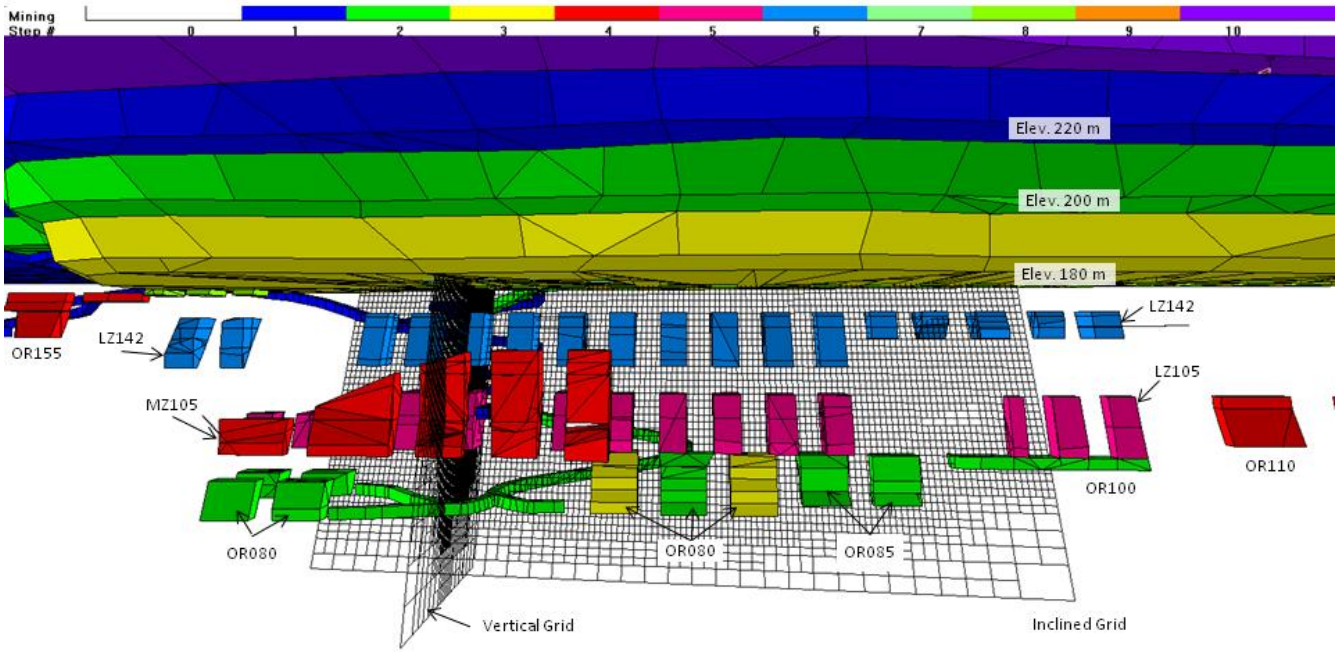

Plate 5: Map3D Model - southwest perspective, including the initial open pit excavation.

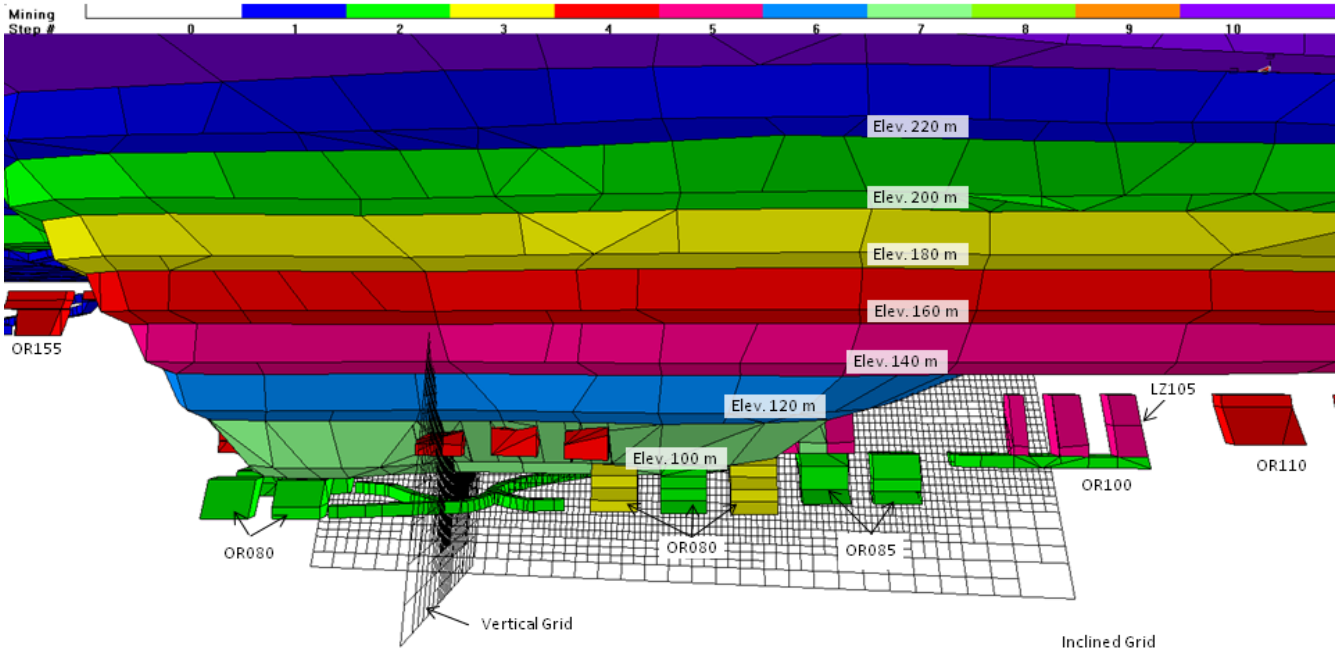

Plate 6: Map3D Model - southwest perspective, including the pit excavation to Elev. 100 m.

8.1 Stresses on Rib Pillars

The mining layout was prepared considering 12 m and 10 m wide rib pillars between the stopes above Elev. 105 m (i.e., MZ and LZ stopes) and below Elev. 105 m (i.e., between stopes OR080 and OR0805), respectively, as depicted on Plate 7. In addition, 12 m thick sill pillars were planned between the LZ stopes.

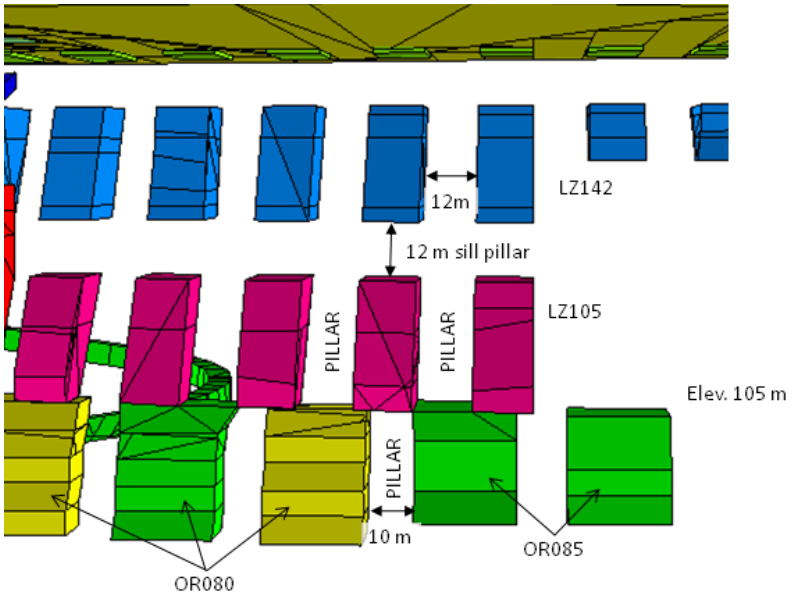

Plate 7: Detail of the pillars that will be formed between the LZ 105, OR080 and OR085 stopes.

For the LZ (footwall) stopes, the rib pillars were aligned in the same direction; however, for the OR stopes, the rib pillars were off-set in relation to the above pillars, as also shown on Plate 7. This plate also shows that no sill pillar would be left between the LZ 105 and OR08/085 stopes.

Several grid planes were used in the model to extract the induced stresses in the sills and rib pillars during the simulation of the mining sequence. Some of the relevant results are also presented on Plates 8 to 10. Plate 8 indicates that the σ_1 stresses in the rib pillars at the end of UG mining will increase to 14 MPa and 18 MPa between the stopes LZ105 and OR080/OR085, respectively. These stresses, normal to the pillar section, corresponds to about 18% and 24% of the uniaxial compressive strength (UCS) of the intact ore zone rock (i.e., assumed to be 75 MPa).

As the open pit is excavated, the stresses in the rib pillars at the LZ105 and OR080/085 levels will increase to > 20 MPa (Plate 9) and 26 MPa (Plate 10), when the pit floor is at Elev. 120 m and 100m, respectively. Under these higher σ_1 stresses, it is likely that these pillars will show rock mass damage and potentially fail. The higher rib stresses between stopes OR080 and 085 should not be too great of concern, assuming that the stopes will be backfilled. Since the plan is to blast the sill and rib pillars from an upper elevation and fill the adjacent stopes, these highly stressed pillars should not affect the stability of the excavations. However, mining from the Elev. 120 m to 100 m could present some additional production challenges due to these highly stressed pillars, such as when drilling the blastholes.

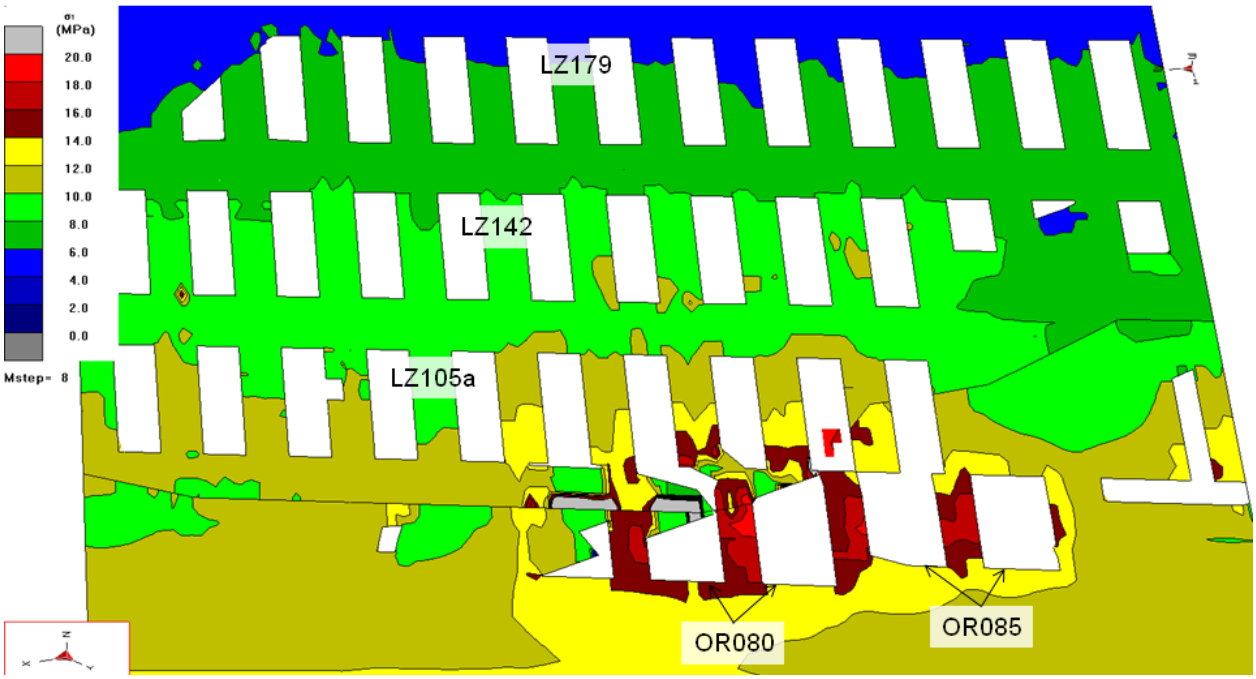

Plate 8: Step 8 – Major principal induced stress (σ_1) contours after the underground mine is complete. Note that the σ_1 increases to about 18 MPa for the pillars located between the OR080 and OR085 stopes.

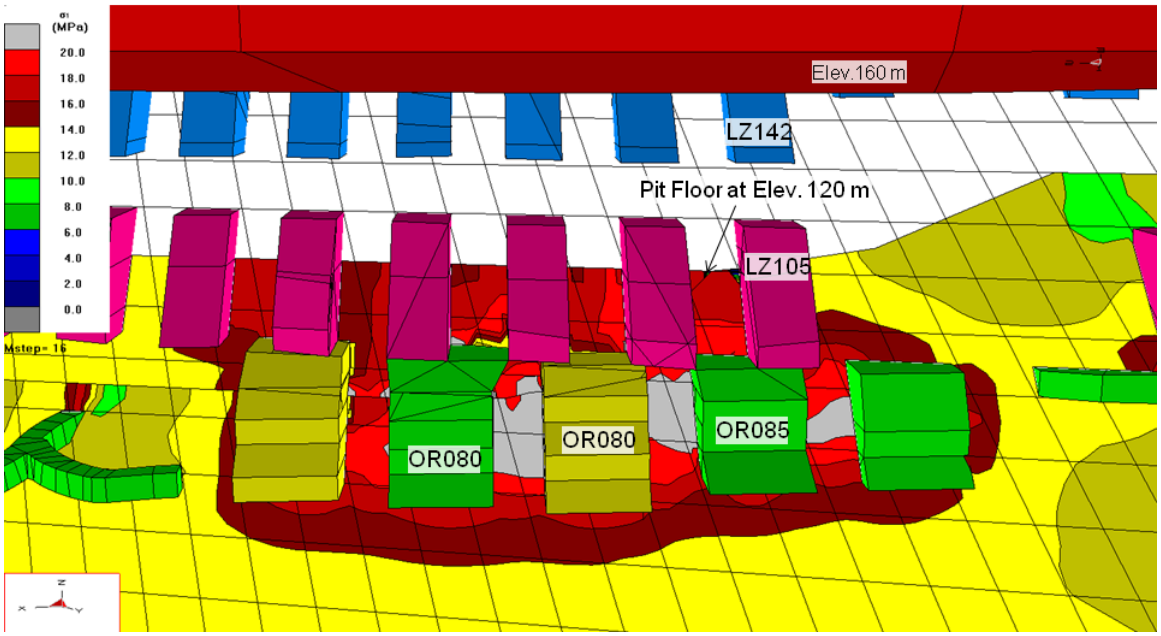

Plate 9: Step 16 – Major principal induced stress (σ_1) contours as the open pit advances to Elev. 120 m. Note that the σ_1 increases to > 20 MPa for the pillars located between the OR080 and OR085 stopes.

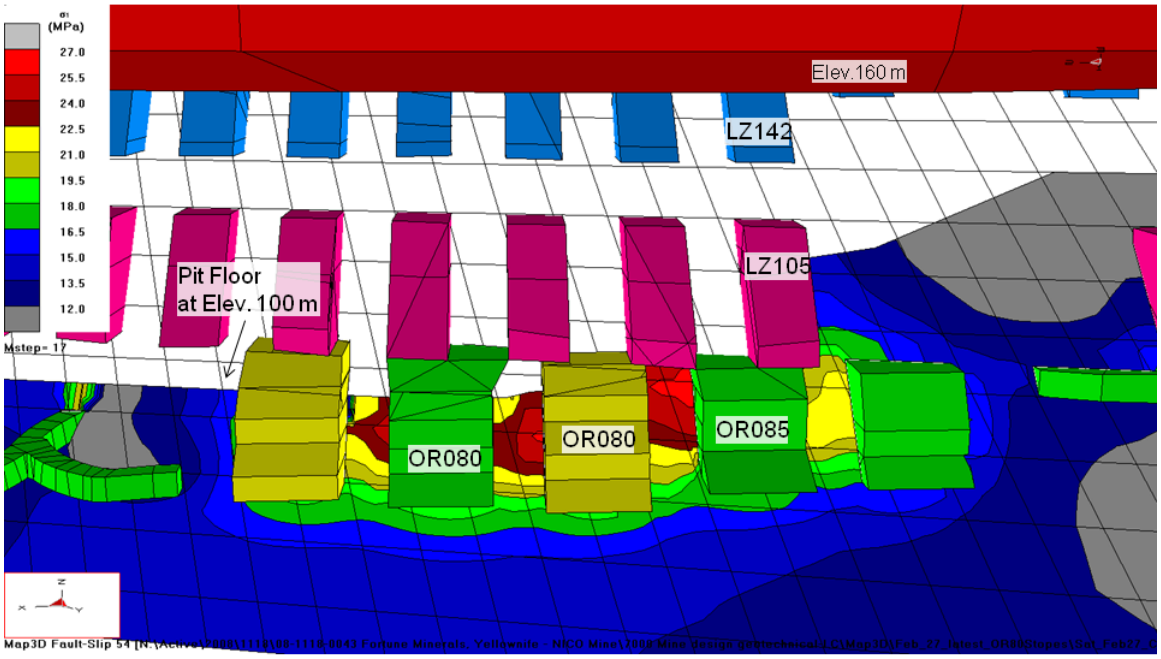

Plate 10: Step 17 – Major principal induced stress (σ_1) contours as the open pit advances to Elev 100 m. Note that the σ_1 increases to 26 MPa for the pillars located between the OR080 and OR085 stopes.

Plates 11 to 14 show the contours of the minor principal induced stresses (or confining pressure, σ_3). From the start of the excavation of the underground stopes, σ_3 in the sill pillars decreases from initially 5 MPa to 0 MPa. As the underground mining is completed (shown on Plate 11 in Mining Stage 8), σ_3 reduces and even becomes negative (or in tension) in some of the rib pillars located between the stopes, indicating rock mass relaxation

(i.e., see bluish and greyish contour areas). It should be noted that there will also be rock mass relaxation within the sill pillars as the open pit advances, even though σ_3 does not go into tension. As a result, it was recommended that cable bolts be installed from the back of the stopes and into the sill pillars to maintain the stability of these pillars not only during the underground mining, but also for support as the open pit is excavated.

Plates 12 and 14 highlight that the excavation of the open pit causes further rock mass relaxation. This occurs not only for the rib pillars, but also on the sill pillars, for the areas closer to the excavated pit boundaries.

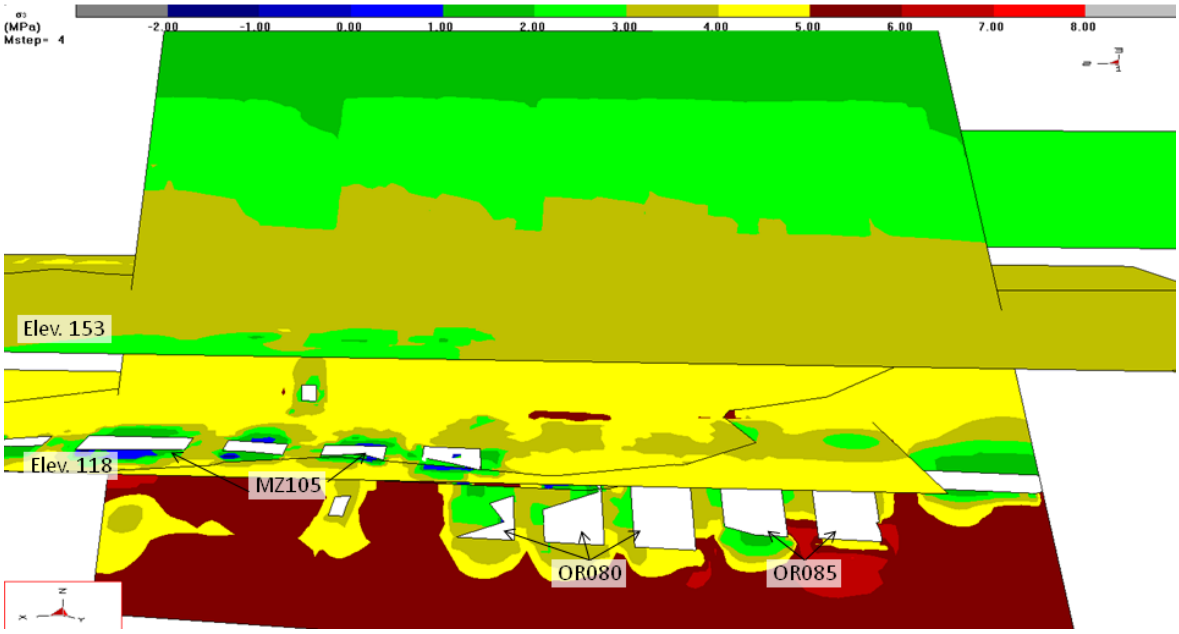

Plate 11: Sigma 3 – Mining Stage 4.

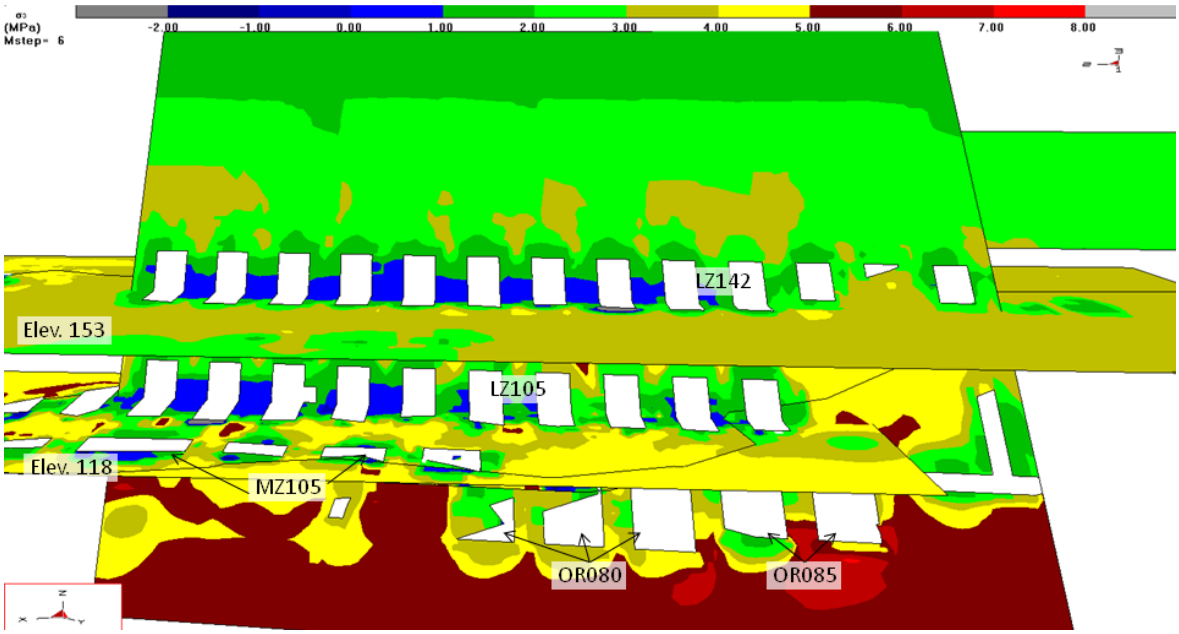

Plate 12: Sigma 3 – Mining Stage 6.

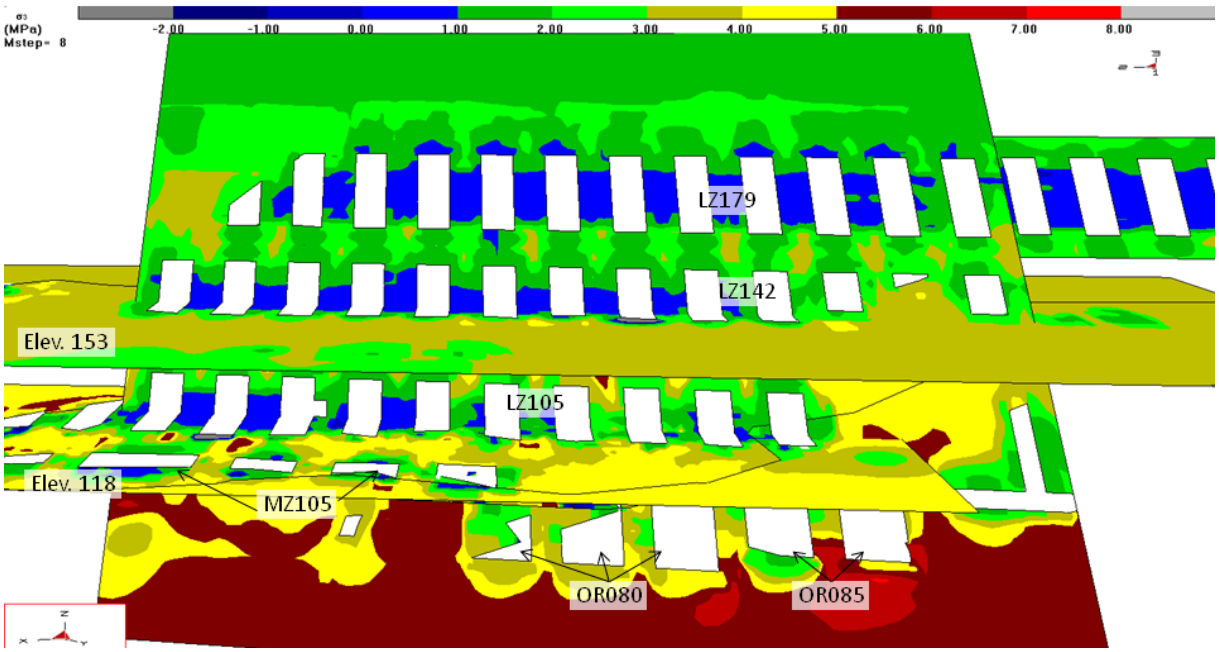

Plate 13: Sigma 3 – Mining Stage 8, corresponding to the completion of the U/G mining excavation.

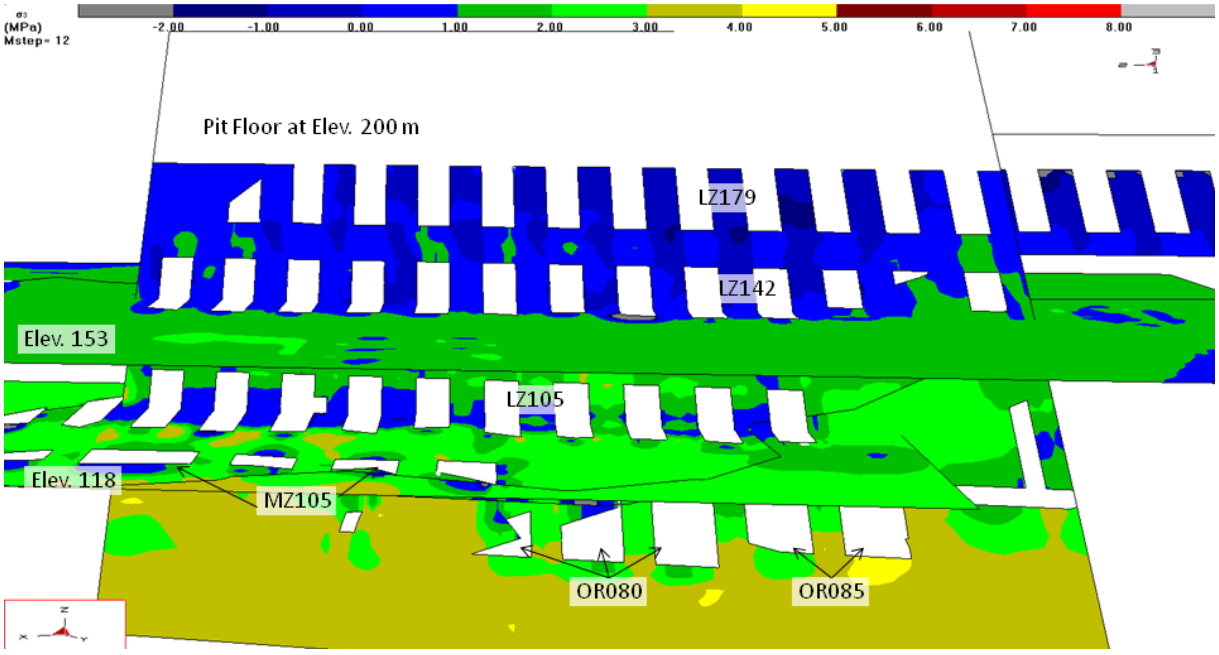

Plate 14: Sigma 3 – Mining Stage 12, as the open pit is excavated to Elev. 200 m.

9.0 2011 PLANNED STOPES

Most of the discussions presented in Section 8.0 were re-evaluated by Fortune and P&E and a decision was made to:

- Use stope dimensions that would minimize the potential for dilution;
- Not carry out any backfill during the underground mine; and
- Minimize as much as practically possible the interaction of the stopes with the open pit.

Plates 15 to 17 show the revised 2011 stopes and the Phases 1B, 2 and 3 pit shells, respectively. There will be minimum interaction of the stopes and the Phase 1B pit shell (Plate 15). In places where the stopes will intercept the wall, the berm was considered wide enough to accommodate any local sloughing from the stope. By the time the Phases 2 and 3 are excavated, almost all the stopes would be located inside the pitm as depicted on Plates 16 and 17.

Based on the 2011 mine planning, as illustrated on Plates 15 to 17, it was decided that it would not be necessary to do additional three-dimensional numerical modeling.

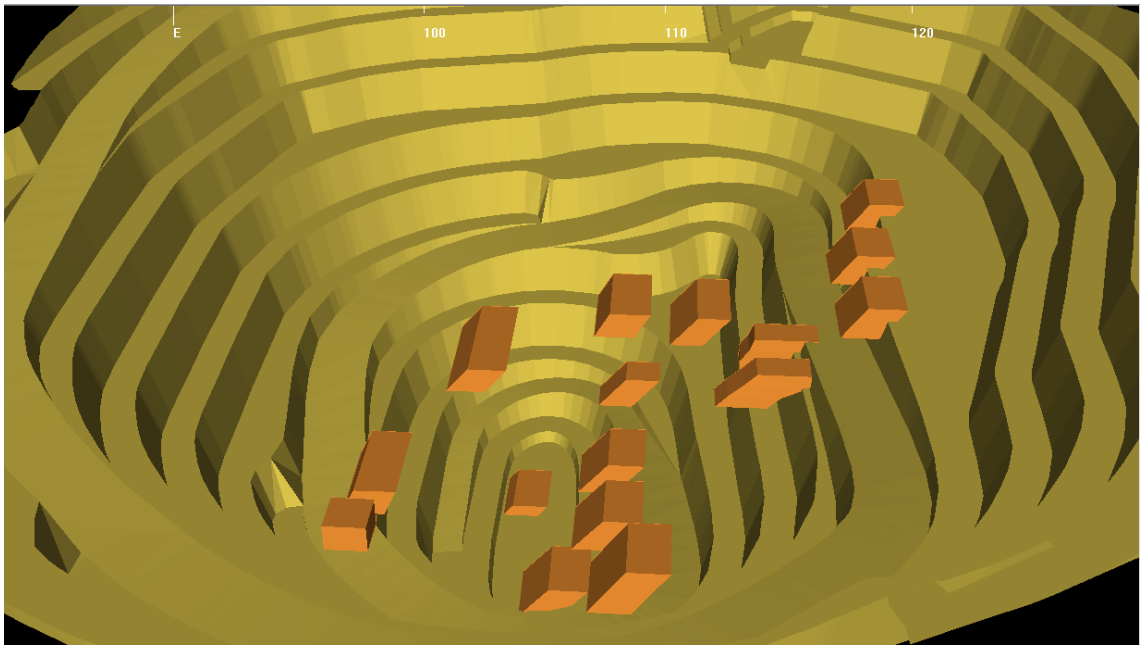

Plate 15: Phase 1B and 2011 Planned Underground Stopes.

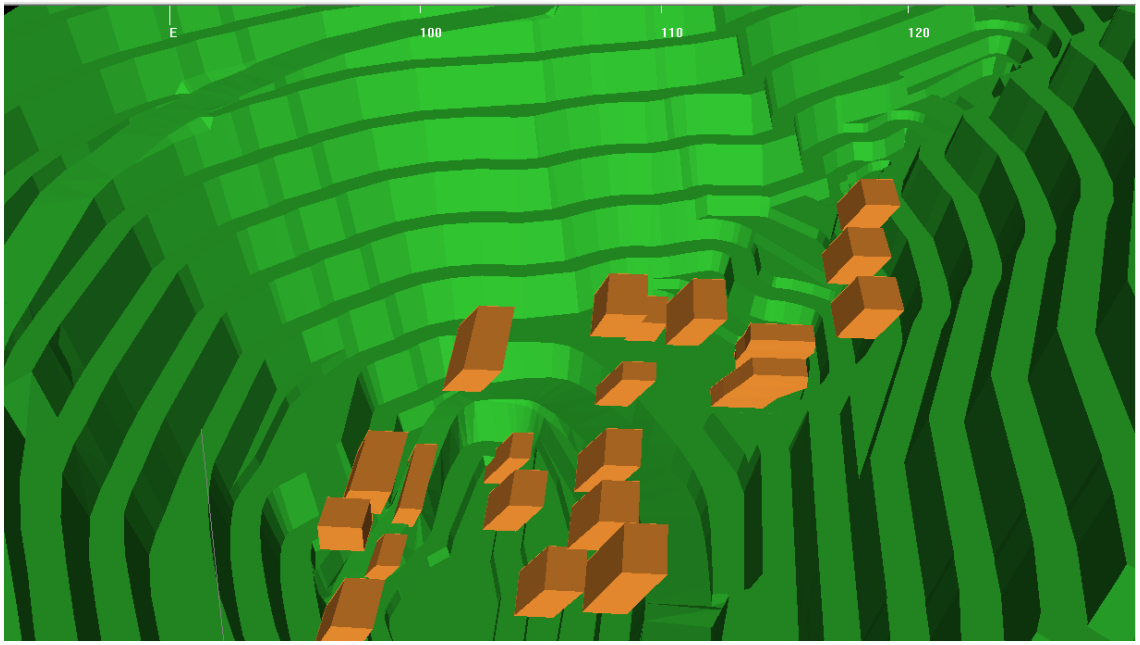

Plate 16: Phase 2 and Planned Underground Stopes.

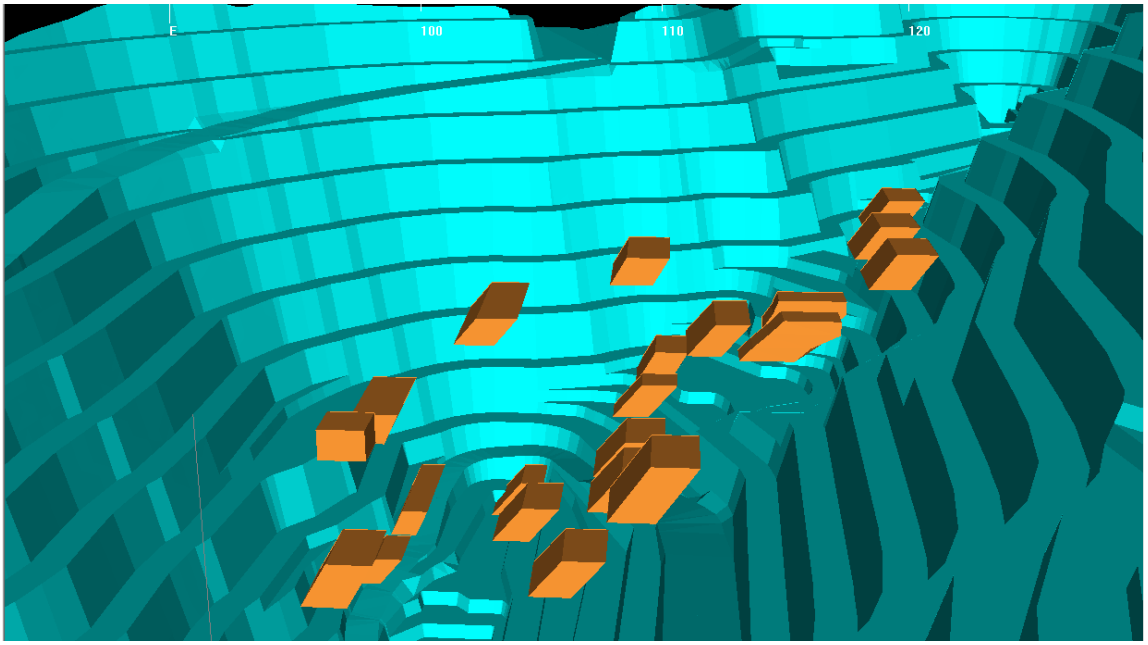

Plate 17: Phase 3 and 2011 Planned Underground Stopes.

10.0 FINAL REMARKS

This technical memorandum summarizes the work completed to November 2011 for the Nico Mine geotechnical design. Please note that the analyses have been carried out based solely on results of previous investigation drilling and summaries. It is recommended that a geotechnical assessment of the exposed development ramp and drifts is carried out as they are excavated in order to confirm the rock mass parameters used in these geotechnical studies.

We trust that the scope and effort presented meet your expectations.

GOLDER ASSOCIATES LTD.

Draft

Marc Rougier, P. Eng.

Associate

Draft

Luiz Castro, P.Eng.
Principal

Draft

Chuck Steed, P.Eng.
Principal

MS/LC/CS/MR/ms

n:\active\2011\1118\11-1118-0066 fortune mineral-nico-yellowknife\6000 ad-hoc engineering support\doc009_geotech investigation plan tech memo_09dec11\dec_2011_version a to csharpe.docx

REFERENCES

Brown, J., O.J. Ferrians, Jr., J.A. Heginbottom, and E.S. Melnikov. 1998, revised February 2001. Circum-arctic map of permafrost and ground ice conditions. Boulder, CO: National Snow and Ice Data Center/World Data Center for Glaciology. Digital media.

EBA Engineering Consultants Ltd., 2005a. NICO Mine Access Route Evaluation, Final Report, March 2005. Report submitted to Fortune Minerals Ltd., London, Ontario.

EBA Engineering Consultants Ltd., 2005b. NICO Tailings Dam and Process Plant Facilities 2004 Geotechnical Site Investigation, Final Report, April 2005. Report submitted to Fortune Minerals Ltd., London, Ontario.

Goad, et al, 1998. The NICO and Sue-Dianne Proterozoic, Iron Oxide-hosted, Polymetallic Deposits, Northwest Territories: Application of the Olympic Dam Model in Exploration.

Golder Associates Ltd., 1999. A Review of Geotechnical Data and Recommendations for Pit Slope Design Configurations, NICO Deposit. July 19, 1999. Project 982-1426.

Golder Associates Ltd., 2003. Factual Report on Geotechnical and Hydrogeological Investigations for the Proposed Open Pit and Underground Mine Workings. Nico Deposit – Northwest Territories. Project # 03-1117029.

Golder Associates Ltd., 2004. Technical Memorandum – Open Pit Slope Design Recommendations for Nico Project. Memorandum submitted to Fortune Minerals Ltd. on November 3, 2004.

Golder Associates Ltd., 2005a. Factual Report on Geotechnical and Hydrogeological Investigations (2003) for the Proposed Open Pit and Underground Workings, NICO Deposit, Northwest Territories.

Golder Associates Ltd., 2005b. Technical Memorandum – Stoping Dimensions Based on Mathews/Potvin Stability Graph Analysis. Memorandum submitted to Robin Goad and Gene Puritch on January 25, 2005. Proejct # 05-1117032.

Golder Associates Ltd., 2007. Report on NICO Tailings Dams and Process Plant Facilities 2006 Geotechnical Site Investigation. Submitted to Fortune Minerals Limited. April 2007.

Golder Associates Ltd., 2010a. Technical memorandum on Geotechnical Underground Design for the Nico Project. Document DOC093 submitted to P & E Mining Consultants Inc. on February 18, 2010. Project # 08-11180043.

Golder Associates Ltd., 2010b. Technical memorandum on Geotechnical Underground Design for the Nico Project, including stopes OR080 and OR085. Document DOC0101 submitted to P & E Mining Consultants Inc. on April 23, 2010. Project # 08-11180043.

Golder Associates Ltd., 2010c. NICO Fortune Minerals Groundwater Modeling - Technical Supporting Document for the NICO Project EIA. February 2011. Project # 10-11180046.

Herget, G. Rock stresses and rock stress monitoring in Canada. MRL 90-011(TR) December 1990.

Hoek, E, Kaiser, P.K, and Bawden, W.F. Support of Underground Excavations in Hard Rock, Chapter 14 – The Stability Graph Method. A.A. Balkema, 1995.

Marinelli, F., and W. L. Niccoli. 2000. Simple analytical equations for estimating ground water inflow to a mine pit.

Mathews, K. E., Hoek, E., Wyllie, D.C. and Stewart, S.B.V. (1981). Prediction of Stable Excavations for Mining at Depth below 1000 metres in Hard Rock. CANMET Report DSS Serial No.OSQ80-0081, DSS File No. 17SQ.23440-0-9020, Ottawa: Dept. Energy, Mines and Resources.

Potvin, Y. (1988). Empirical Open Stope Design in Canada, Ph.D. thesis, Dept. Mining and Mineral Processing, Univ. of B. Columbia.

Rock Quality Index Q (Barton et al 1974). "Engineering Classification of Rock Masses for the Design of Tunnel Support". Rock Mechanics, Vol. 6, No. 4, pp. 183-236.

n:\active\2011\1118\11-1118-0066 fortune mineral-nico-yellowknife\6000 ad-hoc engineering support\doc009_geotech investigation plan tech memo_09dec11\dec_2011_version a to csharpe.docx

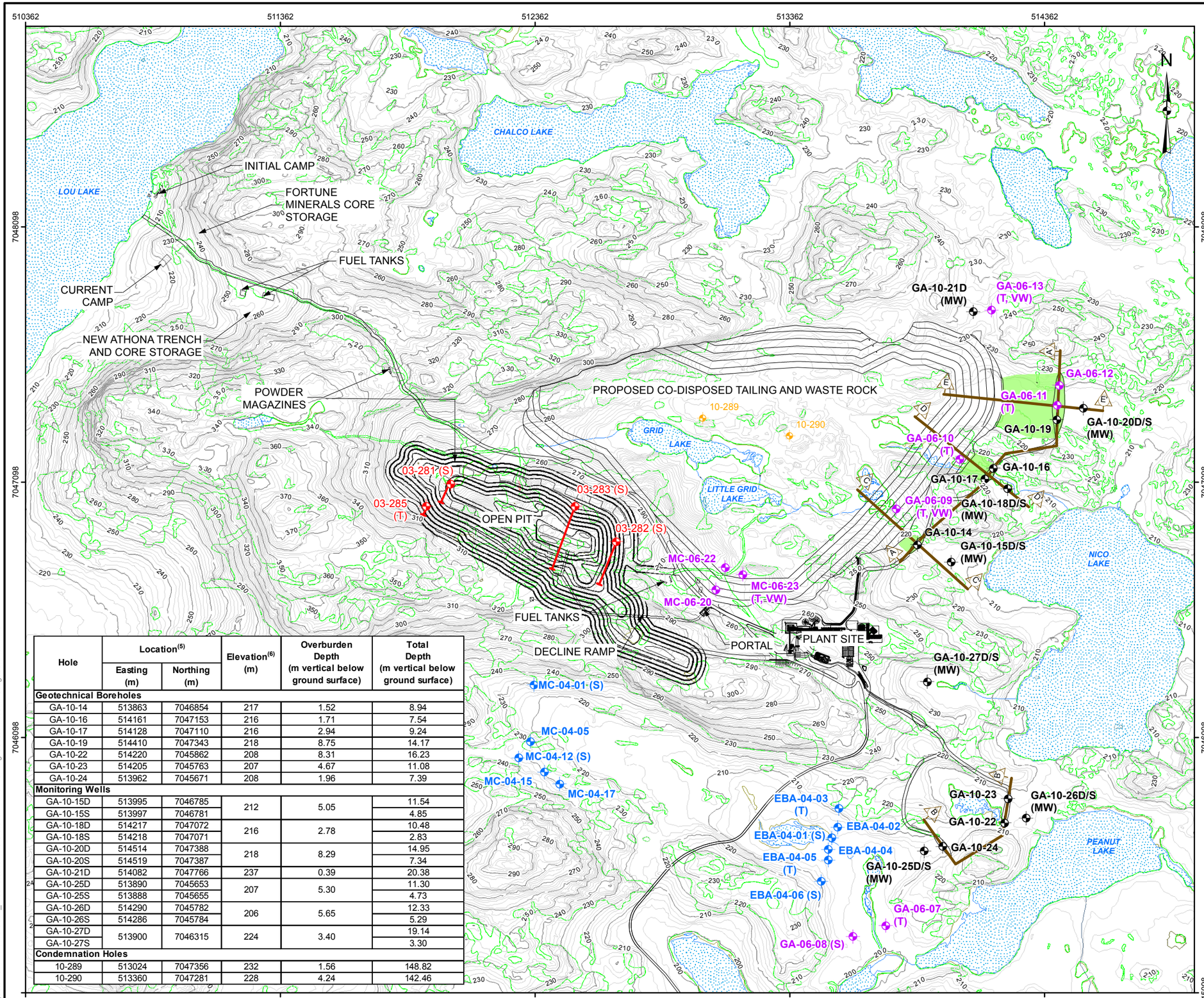

Hole	Location[5] Easting (m)	Location[5] Northing (m)	Elevation[6] (m)	Overburden Depth (m vertical below ground surface)	Total Depth (m vertical below ground surface)
Geotechnical Boreholes					
GA-10-14	513863	7046854	217	1.52	8.94
GA-10-16	514161	7047153	216	1.71	7.54
GA-10-17	514128	7047110	216	2.94	9.24
GA-10-19	514410	7047343	218	8.75	14.17
GA-10-22	514220	7045862	208	8.31	16.23
GA-10-23	514205	7045763	207	4.67	11.08
GA-10-24	513962	7045671	208	1.96	7.39
Monitoring Wells					
GA-10-15D	513995	7046785	212	5.05	11.54
GA-10-15S	513997	7046781			4.85
GA-10-18D	514217	7047072	216	2.78	10.48
GA-10-18S	514218	7047071			2.83
GA-10-20D	514514	7047388	218	8.29	14.95
GA-10-20S	514519	7047387			7.34
GA-10-21D	514082	7047766	237	0.39	20.38
GA-10-25D	513890	7045653	207	5.30	11.30
GA-10-25S	513888	7045655			4.73
GA-10-26D	514290	7045782	206	5.65	12.33
GA-10-26S	514286	7045784			5.29
GA-10-27D	513900	7046315	224	3.40	19.14
GA-10-27S					3.30
Condemnation Holes					
10-289	513024	7047356	232	1.56	148.82
10-290	513360	7047281	228	4.24	142.46

LEGEND

PREVIOUS INVESTIGATION

- 03-382 (S) (NICO 2003/ GOLDER)
- GA-06-10 (GOLDER 2006)
- MC-06-23 (GOLDER 2006)
- MC-04-01 (EBA 2004)
- EBA-04-0 (EBA 2004)

CURRENT INVESTIGATION

- GA-10-25 (GOLDER 2010)
- 10-290 (FORTUNE 2010)
  - (S) - STAND PIPE
  - (T) - THERMISTOR
  - (VW) - VIBRATING WIRE PIEZOMETER
  - (D/S MW) - DEEP OR SHALLOW MONITORING WELL
- RIVER/STREAM
- CONTOUR - *2M INTERVAL*
- CONTOUR - *10M INTERVAL*
- CROSS-SECTION
- EXISTING POND LAKE
- PROPOSED COLLECTION POND AND DAM AREA

NOTE

1. Plant site geotechincal holes not included on this figure.
2. March/April 2010 Drilling Locations were obtained using a handheld GPS Device.
3. - Inclined Borehole

DRAFT

REFERENCE

1. Topographic mapping obtained from Eagle Mapping, Fortune Minerals Limited, 2006 (File: Basemapping (FML, 20060718).dwg)
2. Advanced Exploration Infrastructure - Aker Solutions (File: 0000g001m1a.dwg,, Received - August 19, 2009)
3. Open Pit Configuration - Provided by P & E Engineering (File: Phase 1A, 1 , 2 & Ultimate Pit Polylines.dxf, Recieved October 22, 2009)
4. Co-Disposed Tailing and Waste Rock - Golder Associates (File: alternative3.dwg, October 2009).
5. Projection: UTM Zone11 Datum: NAD 83
6. Ground surface elevation interpreted from topographic ground contours shown on this figure.

500 0 500

SCALE 1:15,000 METRES

PROJECT

FORTUNE MINERALS LIMITED
NICO COBALT-GOLD-BISMUTH-COPPER PROJECT

TITLE

GEOTECHNICAL SITE INVESTIGATION PLAN

Golder Associates
Mississauga, Ontario

Filename: GeotechnicalInvestigationPlan.mxd

PROJECT NO. 11-1118-0066		SCALE AS SHOWN	REV. 0
DESIGN	SC	14 Jan. 2009	FIGURE: 1
GIS	SC	24 Nov. 2011	
CHECK	LC	24 Nov. 2011	
REVIEW	MR	24 Nov. 2011	

G:\Projects\2011\11-1118-0066_NicoFortuneMinerals\GIS\MXDs\Working\GeotechnicalInvestigationPlan.mxd